FLORAL FRAGRANCE PRODUCTION IS A SPECIALIZED PROCESS

By

THOMAS ANGUS COLQUHOUN

A DISSERTATION PRESENTED TO THE GRADUATE SCHOOL OF THE UNIVERSITY OF FLORIDA IN PARTIAL FULFILLMENT OF THE REQUIREMENTS FOR THE DEGREE OF DOCTOR OF PHILOSOPHY

UNIVERSITY OF FLORIDA

2009

To everyone who believed this work possible

ACKNOWLEDGEMENTS

I would like to thank my Ph.D. Committee for their patience and guidance. Special appreciation goes to my advisor, Dr. David Clark, for his ability to see past an occasional display of youthful exuberance. Dr. Harry Klee is recognized for his critical reviews of written work prior to peer-reviewed journal submissions. Additionally, unique gratitude goes to Dr. Kenneth Cline for his interest in and assistance with a particular section of study presented in this work.

TABLE OF CONTENTS

page

LIST OF TABLES

LIST OF FIGURES

Abstract of Dissertation Presented to the Graduate School of the
University of Florida in Partial Fulfillment of the Requirements for
the Degree of Doctor of Philosophy

FLORAL FRAGRANCE PRODUCTION IS A SPECIALIZED PROCESS

By

Thomas Angus Colquhoun

December 2009

Chair: David G. Clark
Major: Plant Molecular and Cellular Biology (PMCB)

Floral fragrance is an integral factor for many angiosperm species interacting with an environment. Individual fragrant flowering species emit specific mixtures and combinations of volatile organic compounds, which can function in various aspects of plant biology. *Petunia x hybrida* cv "Mitchell Diploid" (MD) has large white flowers that emit floral volatile benzenoid/phenylpropanoid (FVBP) compounds in a controlled manner. FVBP emission is confined to the corolla limb tissue, from anthesis to senescence, in a rhythmic pattern where peak FVBP emission is nocturnal. The object of this study was to investigate molecular, biochemical, and metabolic aspects of regulation committed to FVBP production in petunia. Therefore, seven MD genes previously identified as necessary for differential aspects of FVBP production were assayed for coordinate transcriptional regulation. The transcript accumulation assay resulted in similar transcript accumulation profiles for all FVBP genes examined in three out of four categories. Together with previous characterizations, these results indicate that the FVBP genes are a part of a specific group, which is involved in a specific enterprise. Utilizing the transcript accumulation screen and focusing further research on candidate genes whose transcript profiles were similar to known FVBP profiles, *PhCM1* and *PhMYB5d8* were identified. *PhCM1* encodes a plastid localized CHORISMATE MUTASE (CM) isoform that catalyzes the initial committed

step in phenylalanine biosynthesis and is the major CM isoform involved in FVBP production. While characterizing *PhCM1*, PhCM2 was identified as a cytosolic CM isoform, but the transcript accumulation profile was not consistent with FVBP gene profiles and the cytosolic localization separated PhCM2 from pathway proteins and metabolites. Lastly, *PhMYB5d8* encodes an R2R3-MYB transcriptional regulator that contains a C-terminal EAR-domain. A reverse genetic approach suggests that PhMYB5d8 negatively regulates *CINNAMATE-4-HYDROXYLASE* transcript accumulation in the corollas of open petunia flowers.

In short, a simple and cost-effective molecular screen was designed to assay candidate genes for a possible involvement in FVBP production. Two genes were identified and empirically shown to be involved in FVBP production. That is, a biosynthetic enzyme which directs metabolite flux to phenylalanine production and a transcriptional regulator managing transcript levels of a biosynthetic enzyme "downstream" of phenylalanine.

CHAPTER 1
INTRODUCTION AND LITERATURE REVIEW

Introduction

Floral fragrance is a mixture of volatile organic compounds (VOCs) synthesized and emitted by many angiosperm species. The precise composition of volatile compounds emitted is particular to an individual species and is commonly referred to as a scent bouquet. Floral volatile compounds serve multiple roles in the reproductive strategy of many angiosperms. Many fragrant angiosperm species commit to large metabolic expenditures in the production of floral volatile compounds; thus, a specific and complex regulation imparted upon overall volatile production may be common. Therefore, the fundamental goal of this research was to achieve a deeper understanding of the regulation imparted upon the production of FVBPs in order to aid in the successful genetic engineering of a favorable floral fragrance for the commercial market.

Here we examined the detailed transcript accumulation profiles of known petunia floral volatile benzenoid/phenylpropanoid (FVBP) genes, which allowed the grouping of these genes into a floral volatile network based on similar transcript accumulation profiles and related protein functions. For example, the effect of ethylene on transcript accumulation of the FVBP gene network was coordinate and reversible in a time-dependent manner. We then utilized the similar transcript profiles of the FVBP genes to compare and infer possible functions of unknown petunia genes, which resulted in two candidate genes with similar transcript accumulation profiles, *PhCM1* and *PhMYB5d8*. Through molecular, biochemical, and metabolic approaches data was generated that suggest both novel petunia genes are involved in FVBP production. *PhCM1* encodes a plastid localized CHORISMATE MUTASE (CM) isoform that catalyzes the initial committed step in phenylalanine biosynthesis. PhCM1 is the principal CM involved in FVBP synthesis in petunia flowers. *PhMYB5d8* encodes an R2R3-MYB transcriptional regulator

that contains a C-terminal EAR-domain and is highly similar to AtMYB4. PhMYB5d8 negatively regulates *CINNAMATE-4-HYDROXYLASE* transcript abundance and indirectly regulates a subset of FVBP emission in petunia. In conclusion, this study produced a transcript accumulation screen for new petunia genes possibly involved in FVBP synthesis and/or regulation, the identification of two novel genes involved in FVBP production, and numerous insights into FVBP biosynthesis regulation in conjunction with new aspects of regulatory control capable of genetic manipulation.

Floral Fragrance

In a natural environment, all of biology is governed by selective pressures to maximize reproductive successes. Floral VOCs can serve multiple and diverse roles in the reproductive strategy of many angiosperms; such as, antifeedant, antimicrobial, antifungal, and pollinator attraction (reviewed in Dudareva et al., 2006). The latter role (pollinator attraction) can consist of a signal (floral fragrance) and a reward (nectar and/or pollen), and is an attribute of a pollination syndrome. A pollination syndrome is characterized in part by flower morphology, color, fragrance, and nectar production with a result in an increased specialization of the floral phenotype aimed at the attraction of potential pollinators (Fenster et al., 2004). Thus, a mechanism to attract a functional pollinator can equip a sessile plant species with a means to improve the non-self pollen grain to stigma interaction in the appropriate environment. The pollination syndrome does not imply a specific species of pollinator exclusively visits a specific species of plant; instead, pollinators are divided into functional groups or types such as by size, mode of nectar intake, and/or activity. Therefore, the perpetual evolution of the pollination syndrome can be molded by those pollinators that visit the flower most frequently and effectively in a region where the plant is evolving (Fenster et al., 2004).

As a straightforward example, *Petunia axillaris* and *Petunia integrifolia* flower morphology and biochemistry are consistent with a pollination syndrome hypothesis. *P. axillaris* has slender, white flowers and initiates the production of floral VOCs at dusk coinciding with the visitation of hawk moths (*Manduca sexta*) during the night (Hoballah et al., 2005). In contrast, *P. integrifolia* has broad-based, purple flowers, which do not produce floral volatiles, and are visited throughout the day primarily by bees. Meanwhile, they grow together in nature yet generally do not produce hybrids even though they are fully cross-compatible (Ando et al., 2001).

In contrast to the simple example above, pollinator attraction by floral fragrance can be a complex associative process. Numerous variables underlie the association between a signal and a reward, to reference a few: distance, temporal factors, competitors, perception of the signal, quantity of signal produced, quality of signal, impact of reward, and availability of reward. Therefore, until basic science can empirically test all attributes of pollinator attraction individually, additively, and across numerous genetic backgrounds the general focus will remain identifying a single feature of pollinator attraction.

However, floral fragrance is not only important to biological organisms in a natural environment, but flowers themselves are treasured by humans for the beautiful colors, structures, and fragrances. In fact for 2005, wholesale value of floriculture crops topped 5.4 billion US dollars in 36 states surveyed (USDA-NASS, 2006: www.nass.usda.gov). Floriculture crops comprise cut flowers, cut cultivated greens, foliage plants, bedding and garden plants, flowering plants, and propagative materials. Societal examples of the demand for flowering plants and their VOCs are perfumes (e.g. Coco Chanel, Bvlgari, and Versace) and the many psychological

effects of receiving bouquet of flowers as a present (e.g. a dozen cut red roses for Valentine's Day or a mix of carnations, lilies, and daisies for an anniversary).

As solitary compounds the phenylpropanoids, eugenol and isoeugenol significantly limit colony forming abilities of a number of bacteria including *Campylobacter jejuni*, *Escherichia coli*, *Listeria monocytogenes*, *Salmonella enteric*, *Salmonella typhimurium* (Friedman et al., 2002). At relatively low concentrations, eugenol added to medium reduced fungal growth of *Botrytis fabae* by approximately 73 % (Oxenham et al., 2005). Multiple floral VOCs have been implicated in plant defense; however, the biological importance of these compounds with respect to plant defense is still unclear since a direct relationship has yet to be established between a volatile compound emitted from floral tissue and a reduction of microorganismal growth on floral tissue. For a short review refer to Pichersky and Gershenzon, 2002.

Chemical Composition of Floral Fragrance

Fragrance is defined as the quality of having a sweet and pleasant scent (www.dictionary.com). The classic example is that of a rose. By typing "scent AND rose" into the Google™ search engine, over five million results are available. Conceptualizing fragrance may be relatively easy, but when each aspect of fragrance is investigated further, a very complex and dynamic association is revealed. Fragrant angiosperm species may emit from one to 100 individual VOCs (Knudsen and Gershenzon, 2006). To begin, floral fragrance is composed of VOCs, which are generally lipophilic liquids with high vapor pressures and low molecular weights (Pichersky and Dudareva, 2000). When no barriers to diffusion exist, non-conjugated forms of VOCs can cross biological membranes freely (Dudareva et al., 2004). The floral VOCs are commonly separated into three main categories: benzenoids/phenylpropanoids, fatty-acid derivatives, and terpenoids. Additionally, carotenoid derivative, nitrogen containing and sulfur containing floral VOCs have been identified (Knudsen et al., 1993; Simkin et al., 2004).

Phenylpropanoids represent the largest pool of secondary metabolites (Peters, 2007), and more than 7000 phenylpropanoid compounds have been documented in plants (Wink, 2003). For obvious reasons, FVBP compounds define a large class of structurally diverse VOCs (ex. methyl benzoate and isoeugenol). FVBP compounds are putatively derived from the aromatic amino acid L-phenylalanine (Phe) [Boatright et al., 2004], which is synthesized in the plastid from metabolites originating in the shikimate pathway (Rippert et al., 2009). The characteristic benzene ring (derived from Phe) can be modified and adorned with multiple and varying side-groups. Specifically, benzenoids and phenylpropanoids have carbon side chains consisting of one to three carbon molecules (C_6-C_1, C_6-C_2, and C_6-C_3).

Fatty-acid derived VOCs are saturated and unsaturated hydrocarbons. Volatile fatty-acid derivatives are produced from the breakdown of C_{18} unsaturated fatty acids, primarily linolenic and linoleic acids, and include an assorted group of volatiles including green leaf volatiles and methyl jasmonate (Wasternack et al., 2002; Matsui, 2006). Fatty-acid derived VOCs appear to be synthesized in membranous structures of plant cells (Hudak and Thompson, 1997).

Terpenoids are derived from isopentyl diphosphate and dimethylallyl diphosphate. Terpenoids are produced through two alternative pathways, the cytosolic mevalonic acid pathway and the plastidic methyl-erythritol pathway (Newman and Chappell, 1999; Rohmer et al., 1999). Terpenoids are subdivided into five classes based on structure: hemiterpenes (C_5), monoterpenes (C_{10}), sesquiterpenes (C_{15}), homoterpenes (C_{11}-C_{16}), and diterpenes (C_{20}).

Petunia x hybrida cv "Mitchell Diploid"

Petunia is a Solanaceae family member and the genus consists of approximately 30 species. Petunia has been used as a model system for a number of varying topics, like flavonoid synthesis, floral development, transposons, epigenetics, VOCs, and senescence (Gerats and Vandenbussche, 2005). Within the last decade, *P. x hybrida* cv "Mitchell Diploid" (MD) has

become an indispensable model system for floral volatile studies. MD was identified from an individual haploid plant with high regeneration potential derived from a plant selected among the progeny of a *P. axillaris* x (*P. axillaris* x *P. hybrida* "Rose du Ciel") backcross (Mitchell et al., 1980). When this haploid plant was grown in tissue culture, doubling of the chromosomes was observed and resulted in a fertile, homozygous diploid line with no variation observed between the two sets of chromosomes (Griesbach and Kamo, 1996). MD was used in many of the fundamental experiments in plant transformation (Fraley et al., 1983; Horsch et al., 1985; Deroles and Gardner, 1988a, b) and subsequently, a well established transformation protocol exists (Jorgenson et al., 1996). Additionally, MD has a relatively short lifecycle, produces large quantities of floral VOCs, develops numerous large flowers per plant, has a vigorous growth habit, participates in ethylene-induced floral senescence, and an ethylene-insensitive transgenic petunia line 44568 (*CaMV* 35S*:etr1-1*) is available (Wilkinson et al., 1997).

MD FVBPs

Benzenoids and phenylpropanoids constitute the majority of the VOCs emitted by the MD flower (Kolosova et al., 2001a; Verdonk et al., 2003; Boatright et al., 2004; Underwood et al., 2005; Verdonk et al., 2005; Koeduka et al., 2006). In MD the FVBP compounds are putatively synthesized *de novo* (Pare and Tumlinson, 1997; Verdonk et al., 2003; Pichersky et al., 2006), and subsequent to synthesis, these compounds are emitted from epidermal cells of the corolla limb (Kolosova et al., 2001b; Underwood et al., 2005; Verdonk et al., 2005). MD flowers predominantly emit 13 FVBPs: benzaldehyde (Bald), benzyl acetate (BeAc), benzyl alcohol (BOH), benzyl benzoate (BeBA), methyl benzoate (MeBA), methyl salicylate (MeSA), phenylacetaldehyde (PAA), 2-phenylethyl acetate (2-PhAc), phenylethyl alcohol (2-POH), phenylethyl benzoate (PhBA), eugenol (EG), isoeugenol (IE), and vanillin (Figure 1-1) [Kolosova et al., 2001a; Verdonk et al., 2003; Boatright et al., 2004; Verdonk et al., 2005;

Koeduka et al., 2006]. Minor components of MD total floral VOCs include two sesquiterpenes (germacene D and cadina-3,9-diene), two aliphatic aldehydes (decanal and dodecanal), an apocarotenoid (β-ionone), and two fatty-acid derivatives (*cis*-3-hexenal and *trans*-2-hexanal) [Verdonk et al., 2003; Boatright et al., 2004; Simkin et al., 2004].

Regulation of FVBP Emission in MD

The production of floral VOCs could be a metabolically expensive enterprise for angiosperm species. The biosynthesis of FVBP compounds requires proteins, metabolites, energy, and multiple cofactors. Therefore, a complex regulation imparted upon FVBP production, to possibly optimize the ratio between physical cost and reproductive benefit, is evolutionarily straightforward. Substantial emission of MD FVBPs is confined to the corolla limb tissue during open flower stages of development, which coincides with the presentation of the reproductive organs (Verdonk et al., 2003; Underwood et al., 2005). MD FVBP internal metabolite pool accumulation and emission is nocturnal with the highest level detected between 22:00 and 1:00 h (Kolosova et al., 2001a; Verdonk et al., 2003; Underwood et al., 2005; Verdonk et al., 2005; Orlova et al., 2006). FVBP emission is greatly reduced following a successful pollination/fertilization event or exogenous treatment with ethylene (Hoekstra and Weges, 1986; Negre et al., 2003; Underwood et al., 2005). In short, four dimensions of regulation have been identified: tissue type, floral development, daily time-course, and hormone action.

Ethylene Signaling Pathway

Of the classic phytohormones, ethylene has been empirically shown to have a regulatory role in the production of floral VOCs in petunia (Negre et al., 2003; Underwood et al., 2005; Dexter et al., 2007; Dexter et al., 2008). For example, exposure to exogenous ethylene for 10 h results in a large reduction in FVBP emission, and a successful pollination and fertilization event, which generates endogenous ethylene, results in a severe reduction in FVBPs after 36 to

48 h, all in MD (Negre et al., 2003; Underwood et al., 2005). Subsequent to fertilization, the biological function of the petunia floral organ shifts from pollinator attractant to seed development. Therefore, a reduction in pollinator attractions such as floral fragrance is biologically efficient.

The gaseous phytohormone ethylene regulates an assortment of developmental processes and stress responses such as: germination, cell elongation, sex determination, flower & leaf senescence, and fruit ripening. Endogenous ethylene synthesis and the ethylene signal transduction pathway has been investigated extensively with a significant proportion identified in *Arabidopsis thaliana* through mutant analysis (reviewed in Chen et al., 2005). Ethylene is an unsaturated hydrocarbon with the chemical formula C_2H_4 and is the simplest alkene. The biosynthesis of ethylene begins with conversion of the amino acid methionine to S-adenosyl-L-methionine (SAM) by the enzyme SAM SYNTHETASE (Bleeker and Kende, 2000). SAM is then converted to 1-aminocyclopropane-1-carboxylic-acid (ACC) by the enzyme ACC SYNTHASE (ACS). The activity of ACS is the rate-limiting step in ethylene production, and therefore, regulation of ACS is crucial for ethylene biosynthesis. Oxygen is required for the last step, which involves the action of the enzyme ACC OXIDASE (ACO) [Wang et al., 2002]. Subsequent to synthesis, ethylene is distributed by way of a gaseous state and perceived through the ethylene signaling pathway. Additionally, ethylene biosynthesis can be induced by endogenous or exogenous ethylene and is therefore autocatalytic (Guo and Ecker, 2004).

The ethylene signaling pathway can involve a transmembrane protein dimer complex (receptor), a kinase cascade (signal transduction), membrane bound intermediate proteins (mediator), and transcriptional regulators (response factors). The first gene encoding an ethylene receptor was cloned from *Arabidopsis thaliana* (*AtETR1*) [Chang et al., 1993], followed by a

cloned gene in *Solanum lycopersicum*, *NEVER-RIPE* (Wilkinson et al., 1995). In Arabidopsis the ethylene signal is perceived by a small family of five proteins, comprised of AtETR1, AtETR2, AtEIN4, AtERS1 and AtERS2 (Schaller and Bleecker, 1995; Hua and Meyerowitz, 1998; Hua et al., 1998; Sakai et al., 1998; Hall et al., 2000), while the tomato ethylene receptor family of proteins consists of at least six individuals. AtETR1 can form a dimer complex through a disulfide linkage between the respective monomers (Schaller et al., 1995). AtETR1 has an ethylene-binding domain in the three N-terminal hydrophobic *trans*-membrane domains (Schaller and Bleecker, 1995). The chemical element, copper can act as a cofactor to enhance AtETR1 and ethylene binding activity (Rodriguez et al., 1999).

The C-terminus of AtETR1 displays high similarity to bacterial two-component regulators, which contain a histidine kinase domain and a receiver domain (Chang et al., 1993). The histidine kinase domain putatively interacts with the N-terminus of a Raf1-like kinase, AtCTR1 (Clark et al., 1998). Without ethylene bound to the AtETR1 receptor, AtCTR1 is in an activated form and suppresses ethylene signaling transduction. However, when ethylene is bound to the AtETR1 receptor, AtCTR1 is in an inactive form and suppression on downstream signaling components is relieved (reviewed in Zhu and Guo, 2008).

AtEIN3 is a plant-specific transcriptional regulator that functions downstream of the signaling pathway leading from AtCTR1 (Chao et al., 1997; Alonso et al., 1999). AtEIN3 binds to the promoter and induces transcription of *AtERF1* (Solano et al., 1998). AtERF1 is part of a large protein family called ethylene responsive element-binding proteins (EREBPs). EREBPs bind to a conserved promoter element, a GCC box (Solano et al., 1998).

In planta, ethylene synthesis is promoted by numerous environmental stimuli including pollination and fertilization. Pollination followed by increased ethylene production precede floral

senescence as the flower transitions from being a pollinator attractor to supporting seed development in petunia (Hoekstra and Weges, 1986; Negre et al., 2003; Underwood et al., 2005). Upon pollination of the MD flower, ethylene is rapidly produced in the stigma and style resulting in an increased ethylene production around 12 hours after pollination and peaking after approximately 24 hours in the ovary (Tang and Woodson, 1996). Subsequently, ethylene production is induced in the corolla tissue between 24 and 36 hours after pollination (Jones et al., 2003).The ethylene production in the corolla tissue is presumed to induce corolla senescence (Hoekstra and Weges, 1986).

The creation of the ethylene-insensitive (*CaMV* 35S::*etr1-1*) transgenic petunia line, 44568 (Wilkinson et al., 1997) has been indispensible for comparative ethylene studies such as adventitious root formation (Clark et al., 1999) and floral VOC production (Negre et al., 2003; Underwood et al., 2005; Dexter et al., 2007; Dexter et al., 2008). In short, the Arabidopsis *etr1-1* mutant is a missense mutation in the ethylene-binding domain of the protein. The missense mutation generates a protein that is unable to perceive ethylene that results in a constitutively suppressed ethylene signal transduction (Schaller and Bleeker, 1995). Heterologous expression of *Atetr1-1* under a constitutive promoter in the MD genetic background resulted in a single homozygous transgenic line (44568) with severely reduced ethylene perception (Wilkinson et al., 1997; Shibuya et al., 2004).

FVBP Genetics and Biochemistry

FVBP compounds are derived from the aromatic amino acid L-phenylalanine (Phe). Phe is derived from metabolites originating from primary metabolism (shikimate pathway). The plastid localized shikimate pathway begins with the condensation of erythrose-4-phosphate and phosphoenolpyruvate, and ends in the formation of chorismic acid (CA) through a total of seven enzymatic reactions (reviewed in Herrmann and Weaver, 1999). CA can be enzymatically

rearranged to prephenic acid by a protein called CHORISMATE MUTASE. Prephenic acid can then be dehydrated to pheylpyruvic acid by an enzyme called PREPHENATE DEHYDRATASE. Phenylpyruvic acid is transaminated to produce Phe. Phe is presumed to be exported from the plastid into the cytosol where the phenylpropanoid pathway is localized (Achnine et al., 2004). As the gateway to secondary metabolism, the phenylpropanoid pathway begins with the deamination of Phe by PHENYLALANINE AMMONIA-LYASE (PAL) to form *trans*-cinnamic acid (reviewed in Boudet, 2007). Next, *trans*-cinnamic acid is converted to *para*-coumaric acid through hydroxylation by an endomembrane bound enzyme, CINNAMATE-4-HYDROXYLASE (C4H) [Achnine et al., 2004]. A series of reactions can convert *para*-coumaric acid to ferulic acid through multiple enzymatic steps (reviewed in Yu and Jez, 2008). Metabolites for FVBP synthesis branch from the phenylpropanoid pathway at Phe, *trans*-cinnamic acid, and ferulic acid (Figure 1-1).

To date, seven genes involved in the direct biosynthesis of FVBP compounds or intermediate metabolites have been emperically identified in petunia: *S-ADENOSYL-L-METHIONINE:BENZOIC ACID/SALICYLIC ACID CARBOXYL METHYLTRANSFERASE 1* and *2* (*PhBSMT1* and *PhBSMT2*) [AY233465 and AY233466], *BENZOYL-COA:BENZYL ALCOHOL/PHENYLETHANOL BENZOYLTRANSFERASE* (*PhBPBT*) [AY611496], *PHENYLACETALDEHYDE SYNTHASE* (*PhPAAS*) [DQ243784], *CONIFERYL ALCOHOL ACYLTRANSFERASE* (*PhCFAT*) [DQ767969], *EUGENOL SYNTHASE 1* (*PhEGS1*) [EF467241], and *ISOEUGENOL SYNTHASE 1* (*PhIGS1*) [DQ372813]; Figure 1-1. *PhBSMT1* and *PhBSMT2* encode enzymes that catalyze the synthesis of MeBA and MeSA from benzoic acid and salicylic acid respectively (Negre et al., 2003; Underwood et al., 2005). *PhBPBT* encodes an enzyme that catalyzes synthesis of BeBA and PhBA from benzoyl-CoA and BOH or

2-POH respectively (Boatright et al., 2004; Orlova et al., 2006; Dexter et al., 2008). *PhIGS1* encodes an enzyme that catalyzes the formation of IE from coniferyl acetate (Koeduka et al., 2006), while *PhEGS1* encodes an enzyme responsible for the conversion of coniferyl acetate to eugenol (Koeduka et al., 2008). *PhPAAS* encodes a bifunctional decarboxylase/amine oxidase that catalyzes synthesis of PAA from phenylalanine (Kaminaga et al., 2006). *PhCFAT* encodes an enzyme that catalyzes the formation of coniferyl acetate (substrate for PhIGS1*)* from coniferyl alcohol and acetyl CoA (Dexter et al., 2007).

The seven petunia genes mentioned above have all been characterized in different ways, but a common transcript accumulation profile seems to be emerging. *PhBSMT1* and *PhBSMT2* mRNA transcripts accumulate to high levels in petunia corolla limb tissue, peak transcript accumulation is detected at mid-day, and transcript accumulation is greatly reduced after a successful pollination/fertilization event and/or exogenous ethylene exposure (Negre et al., 2003; Underwood et al., 2005). *PhBPBT* transcripts accumulate to high levels in petunia corolla limb tissue, peak transcript accumulation is detected at mid-day, and *PhBPBT* transcript accumulation is reduced after a successful pollination/fertilization event and/or exposure to exogenous ethylene (Boatright et al., 2004; Dexter et al., 2008). *PhIGS1* transcripts accumulate to high levels in both corolla tube and limb tissues of petunia (Koeduka et al., 2006). *PhEGS1* transcript accumulation is relatively high in corolla limb tissue, but *PhEGS1* transcripts accumulate to approximately 33 % of *PhIGS1* transcript accumulation in petunia corolla limb tissue (Koeduka et al., 2008). *PhPAAS* transcript accumulation is relatively high in corolla limb and ovary tissue of the petunia flower. *PhPAAS* transcript accumulation is only observed post-anthesis and peak transcript accumulation is detected at mid-day (Orlova et al., 2006). *PhCFAT* transcript accumulation is relatively high in the corolla limb tissue post-anthesis and peak transcript

abundance appears in the evening. Additionally, *PhCFAT* transcript accumulation is greatly reduced after a successful pollination/fertilization event and/or exogenous ethylene exposure (Dexter et al., 2007). To summarize, none of the previously reported MD FVBP genes have been transcriptionally profiled alike, however, high levels of all these gene transcripts seem to be confined to the petunia corolla limb tissue, which corresponds to the spatial location of FVBP emission.

A single transcriptional regulator involved in the production of FVBPs has been identified from petunia. *ODORANT 1* (*PhODO1*) [AY705977] is a R2R3-MYB transcriptional regulator that functions to regulate gene expression in the shikimate pathway (Verdonk et al., 2005). The accumulation of the shikimate pathway gene transcripts upon anthesis elevates levels of precursors, as deduced from benzoic acid levels, available for the FVBP biosynthesis pathways. *PhODO1* transcript accumulation is relatively high in the corolla limb tissue from anthesis to senescence, and peak transcript abundance is observed in the evening (Verdonk et al., 2005).

CHORISMATE MUTASE

CA is the last primary metabolite shared for production of the phenylpropanoid secondary metabolites. CM is the initial committed step in Phe biosynthesis in plants. Specifically, CM catalyzes an intramolecular, [3,3]-sigmatropic rearrangement of chorismic acid to prephenic acid, formerly a Claisen rearrangement (Haslem, 1993). Three CM genes have been identified in *Arabidopsis thaliana*, and each gene encodes a different isoform of the CM protein. All *AtCM*s have been cloned, transcriptionally profiled, and biochemically characterized in selected Arabidopsis tissue, but all the conclusions regarding subcellular localization are putative concepts based upon predicted amino acid sequence features (chloroplast transit peptide, cTP) and have not been tested directly. AtCM1 and AtCM3 are predicted to be plastid localized

isoforms, respective transcripts accumulate differentially, and *AtCM1* is induced upon pathogen attack (Eberhard et al., 1993; Eberhard et al., 1996b; Mobley et al., 1999). In addition, both isoforms are allosterically up-regulated by tryptophan and down-regulated by Phe and tyrosine. Of the two putative plastidic CM isoforms, recombinant AtCM3 has the lowest apparent K_m value for CA when expressed in a eukaryotic system (Mobley et al., 1999). AtCM2 predicted localization is the cytosol due to a lack of a cTP, it has the lowest apparent K_m value for chorismic acid of all three isoforms, and is allosterically unaffected by the three aromatic amino acids (Eberhard et al., 1996b; Mobley et al., 1999).

The identification and characterization of all three CM isoforms in Arabidopsis consisted of multiple manuscripts culminating in the authors of the final manuscript to speculate that the differential properties of AtCMs suggested each isoform fulfilled distinct physiological roles. Additionally, the authors point out that a loss-of-function mutation for each *CM* gene was required to clearly define any specific roles each isoform may have (Mobley et al., 1999). To date, loss-of-function mutations for any of the higher plant *CM* family members have not been reported. The majority of the upstream and downstream pathway proteins have been empirically tested for subcellular localization and all pathway proteins close to the CM step have been localized to the plastid in Arabidopsis leaf tissue (Herrmann and Weaver, 1999; Rippert et al., 2009). Therefore, the function of the Arabidopsis cytosolic isoform remains unclear, due to the separation from pathway proteins and substrate. Interestingly, a *Solanum lycopersicum* CM was cloned by one of the same labs that reported on the AtCMs, and it appears to be located in the cytosol because the predicted protein sequence lacks a cTP (Eberhard et al., 1996a). Additionally, activity of two CM isoforms from *Papaver somniferum* have been reported and differential centrifugation resulted in a plastidic and cytosolic isoform (Benesova and Bode,

1992). The question remains, why do multiple genetic backgrounds contain a *CM* sequence encoding for a protein that is unable to participate in a very specific enzymatic reaction? Has a new function evolved (broad substrate specificity), or maybe the biological separation between cytosol and plastid is dynamic and all variables have not been tested.

R2R3-MYB Transcriptional Regulators

Transcription is the biosynthesis of ribonucleic acid (RNA) chains under the direction of deoxyribonucleic acid (DNA) templates. Multiple factors are necessary for the process of transcription including DNA unwinding and/or remodeling, the RNA polymerase complex, and many other proteins involved in the pre-initiation complex. Additionally, other factors can control the transcription rate. Regulation of the transcription rate increases the versatility and adaptability of an organism by controlling when and where a protein is expressed. Proteins that recognize and bind DNA in a sequence specific manner in order to regulate the rate of initiation of transcription are called transcriptional regulators. These proteins can be activators, repressors, or both and have been classified into families based upon similarity of DNA binding domains (reviewed in Pabo and Sauer, 1992). Of these proteins, MYB transcriptional regulators comprise one of the largest families in the plant kingdom (Riechmann et al., 2000).

The oncogene *v-MYB* from the avian myeloblastosis virus was the first MYB transcriptional regulator identified (Klempnauer et al., 1982). *MYB* genes have since been identified from insects, plants, fungi, and slime molds (Lipsick, 1996). The MYB proteins are further classified into subfamilies based on the composition of the DNA binding domain, which is generally comprised of three imperfect repeats: R1, R2, and R3 (Ogata et al., 1992). In plants, R2R3-MYB transcriptional regulators contain two imperfect repeats and this subfamily consists of approximately 125 individual genes in *Arabidopsis thaliana*. Protein functions of these 125

genes vary from controlling cellular proliferation and differentiation to controlling phenylpropanoid metabolism (reviewed in Stracke et al., 2001).

Research Objectives

The object of this study was to investigate molecular, biochemical, and metabolic aspects of regulation committed to FVBP production in petunia. Therefore, MD genes previously identified as necessary for differential aspects of FVBP production were assayed for coordinate transcriptional regulation. Employing the transcript accumulation screen we focused further research on candidate genes whose transcript profiles were similar to known FVBP profiles. The identification of *PhCM1* and *PhMYB5d8* enabled an examination of metabolite control and flux through the phenylpropanoid pathway and ultimately to FVBP synthesis in petunia.

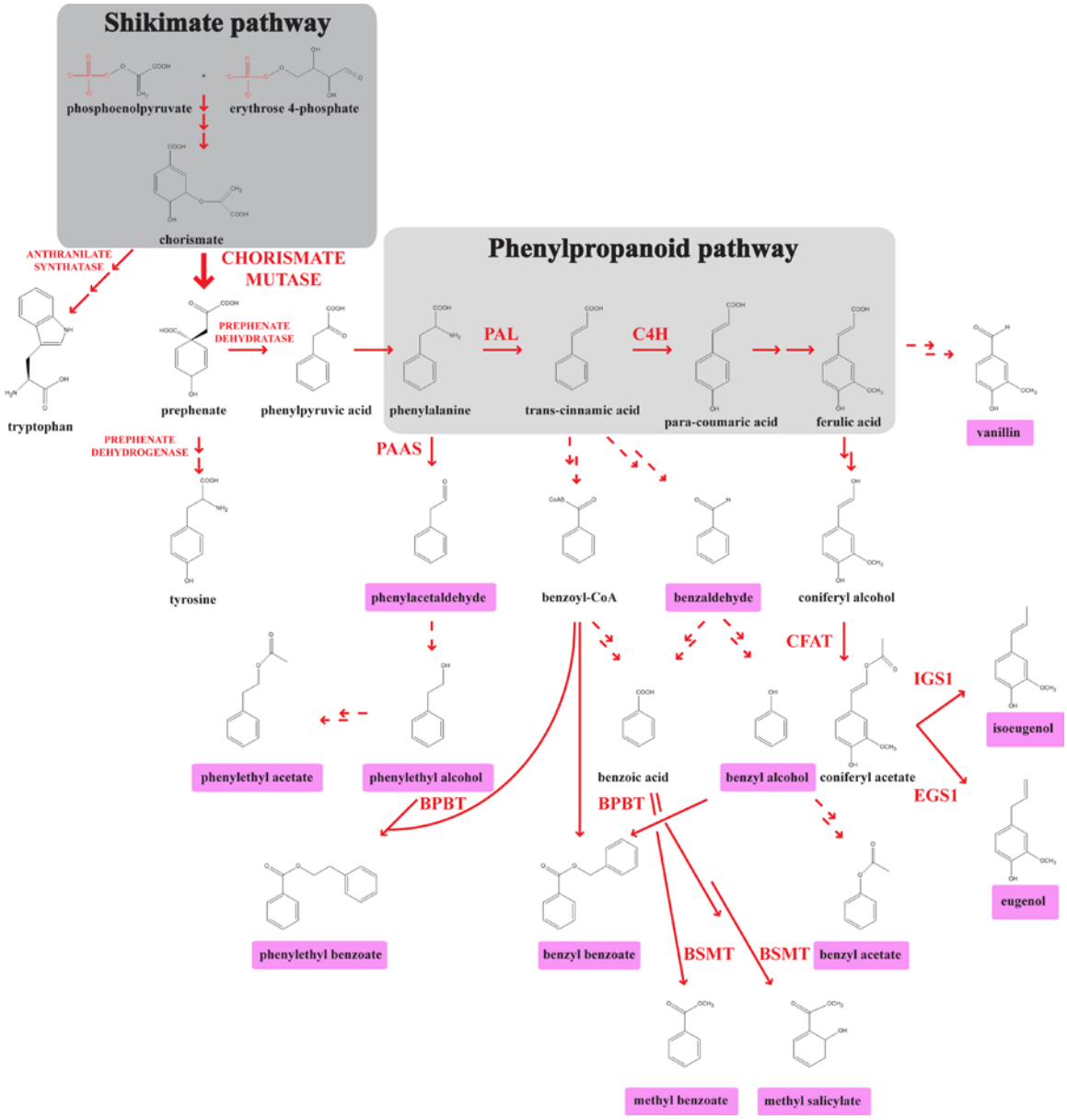

Figure 1-1. The floral volatile benzenoid/phenylpropanoid pathway. The shikimate pathway (dark grey) concludes with the formation of chorismate. CHORISMATE MUTASE catalyzes the rearrangement of chorismate to prephenate, directing the flux of metabolites to the production of phenylalanine and tyrosine. From the phenylpropanoid backbone (light grey), FVBP production consists of three main branch-points; phenylalanine, *trans*-cinnamic acid, and ferulic acid. Floral volatile compounds derived from each branch-point are highlighted in pink and known FVBP genes are abbreviated at the appropriate enzymatic positions. Enzymes are in red. Solid red arrows indicate established biochemical reactions. Multiple arrows indicate multiple biochemical steps. Dashed arrows indicate possible biochemical reactions.

CHAPTER 2
PETUNIA FLORAL VOLATILE BENZENOID/PHENYLPROPANOID GENES ARE REGULATED IN A SIMILAR MANNER

Preface

This work has been submitted to and accepted in modified form at the journal *Phytochemistry* for publication (Thomas A. Colquhoun, Julian C. Verdonk, Bernardus C.J. Schimmel, Denise M. Tieman, Beverly A. Underwood, and David G. Clark. [2009] Petunia Floral Volatile Benzenoid/Phenylpropanoid Genes are Regulated in a Similar Manner. *Phytochemistry*, [*In Press*])

Introduction

Floral volatile compounds serve multiple roles in the reproductive strategy of many angiosperms, functioning in antifeedant, antimicrobial, antifungal, and pollinator attractant roles (reviewed in Dudareva et al., 2006). The relatively large metabolic cost for scent production in many species underscores the importance of this enterprise. Many aspects regarding the regulation of the floral volatile system as a whole remain unclear; for example, are all the genes involved in the biosynthesis of floral volatiles a part of a transcriptionally regulated network?

Petunia x hybrida cv 'Mitchell Diploid' (MD) is an excellent model system for the study of floral volatiles. Benzenoids and phenylpropanoids constitute the majority of the volatile organic compounds emitted by the petunia flower (Kolosova et al., 2001a; Verdonk et al., 2003; Boatright et al., 2004; Underwood et al., 2005; Verdonk et al., 2005; Koeduka et al., 2006). These low molecular weight compounds have high vapor pressures and are putatively synthesized *de novo* (Pare and Tumlinson, 1997; Verdonk et al., 2003; Pichersky et al., 2006). Subsequent to synthesis, these compounds are emitted from epidermal cells of the corolla limb (Kolosova et al., 2001b; Underwood et al., 2005; Verdonk et al., 2005). MD flowers emit 13

benzenoids/phenylpropanoids; benzaldehyde (Bald), benzyl acetate (BeAc), benzyl alcohol (BOH), benzyl benzoate (BeBA), methyl benzoate (MeBA), methyl salicylate (MeSA), phenylacetaldehyde (PAA), 2-phenylethyl acetate (2-PhAc), phenylethyl alcohol (2-POH), phenylethyl benzoate (PhBA), eugenol (EG), isoeugenol (IE), and vanillin (Figure 1-1, Kolosova et al., 2001a; Verdonk et al., 2003; Boatright et al., 2004; Verdonk et al., 2005; Koeduka et al., 2006). Beginning at anthesis (flower opening) these volatile compounds are synthesized and emitted in a rhythmic pattern with a maximum emission at night (Kolosova et al., 2001a; Verdonk et al., 2003; Underwood et al., 2005; Verdonk et al., 2005).

In petunia, seven floral volatile benzenoid/phenylpropanoid (FVBP) biosynthetic genes have been identified: *S-ADENOSYL-L-METHIONINE:BENZOIC ACID/SALICYLIC ACID CARBOXYL METHYLTRANSFERASE 1* and *2* (*PhBSMT1* and *PhBSMT2*), *BENZOYL-COA:BENZYL ALCOHOL/PHENYLETHANOL BENZOYLTRANSFERASE* (*PhBPBT*), *PHENYLACETALDEHYDE SYNTHASE* (*PhPAAS*), *CONIFERYL ALCOHOL ACYLTRANSFERASE* (*PhCFAT*), *ISOEUGENOL SYNTHASE 1* (*PhIGS1*), and *EUGENOL SYNTHASE1* (*PhEGS1*) [Figure 1-1]. *PhBSMT1* and *PhBSMT2* encode enzymes that catalyze the synthesis of MeBA and MeSA from benzoic acid and salicylic acid respectively (Negre et al., 2003; Underwood et al., 2005). *PhBPBT* encodes an enzyme that catalyzes synthesis of BeBA and PhBA from benzoyl-CoA and BOH or 2-POH respectively (Boatright et al., 2004; Orlova et al., 2006; Dexter et al., 2008). *PhIGS1* encodes an enzyme that catalyzes the formation of IE from coniferyl acetate (Koeduka et al., 2006). *PhPAAS* encodes a bifunctional decarboxylase/amine oxidase that catalyzes synthesis of PAA from phenylalanine (Kaminaga et al., 2006). *PhCFAT* encodes an enzyme that catalyzes the formation of coniferyl acetate (substrate for PhIGS1*)* from coniferyl alcohol and acetyl CoA (Dexter et al., 2007). Most

recently PhEGS1 was shown to produce eugenol from coniferyl acetate (Koeduka et la., 2008; Koeduka et al., 2009a), but because the current work was started prior to these publications PhEGS1 was unfortunately not included.

To date, a single transcriptional regulator involved in the production of floral volatile benzenoids/phenylpropanoids has been identified from petunia. ODORANT 1 (PhODO1) is a R2R3-MYB transcriptional regulator that functions to regulate gene expression in the shikimate pathway (Verdonk et al., 2005). The shikimate pathway couples metabolism of carbohydrates to formation of aromatic amino acids (Figure 1-1) [Herrmann and Weaver, 1999]. The transcriptional up-regulation of the shikimate pathway genes upon anthesis elevates levels of precursors, as deduced from benzoic acid levels, available for the floral volatile benzenoid/phenylpropanoid biosynthesis pathways (Verdonk et al., 2005).

In petunia, pollination followed by increased ethylene production precede floral senescence as the flower transitions from being a pollinator attractor to supporting seed development (Hoekstra and Weges, 1986; Negre et al., 2003; Underwood et al., 2005). Upon pollination of the MD flower, ethylene is rapidly produced in the stigma and style resulting in increased ethylene production around 12 hours after pollination and peaking after approximately 24 hours in the ovary (Tang and Woodson, 1996). Subsequently, ethylene production is induced in the corolla tissue between 24 and 36 hours after pollination (Jones et al., 2003). Thirty-six hours after pollination, volatile benzenoid/phenylpropanoid emissions and transcript levels of *PhBSMT1* and *PhBSMT2* are significantly reduced when compared to unpollinated MD flowers or pollinated flowers of an ethylene-insensitive (*CaMV* 35S::*etr1-1*) transgenic petunia line, 44568 (Wilkinson et al., 1997; Negre et al., 2003; Underwood et al., 2005).

Since the petunia genes involved in the production of floral volatiles have been characterized in various ways and in large part one gene at a time, conceptualizing these genes into a specific group is difficult. Focusing at a molecular level, a spatial *PhIGS1* transcript accumulation profile has been reported (Koeduka et al., 2006), but a *PhPAAS* transcript accumulation profile for a spatial, floral development, and daily time-course has been reported (Orlova et al., 2006), while a spatial, daily time-course, and ethylene treated *PhCFAT* transcript accumulation profile has been reported (Dexter et al., 2007). Therefore, the statement that the genes involved in the production of floral volatiles share similar transcript accumulation profiles throughout a spatial, floral development, daily time-course, and ethylene treatment is a putative concept and requires further examination. We hypothesized the seven genes analyzed in this study would share similar transcript accumulation profiles because the corresponding floral volatile compounds share similar emission profiles. To test this hypothesis, we used four transcript accumulation criteria (spatial, flower development, ethylene regulated and rhythmic) and analyzed these seven FVBP gene transcript accumulation profiles in MD and 44568 plants. The results show similar transcript accumulation profiles of the FVBP genes in three out of four criteria examined. The FVBP gene group can be separated into two general rhythmic transcript accumulation patterns. Finally, ethylene studies suggest a reversible mechanism to the ethylene-dependent reduction of FVBP gene transcript levels.

Results

Spatial FVBP Gene Expression Analysis in MD Plants

The spatial transcript accumulation profiles for the floral volatile benzenoid/phenylpropanoid (FVBP) genes *PhBSMT1*, *PhBSMT2*, *PhBPBT*, *PhPAAS*, *PhIGS1*, *PhCFAT*, and *PhODO1*, were examined by semi-quantitative (sq)RT-PCR and quantitative (q)RT-PCR. Root, stem, stigma, anther, leaf, petal tube, petal limb, and sepal tissues of MD

plants were harvested at 16:00 h. Compared to the other plant tissues examined, the highest levels of FVBP gene transcripts were detected in the petal limbs of MD flowers (Figures 2-1 and 2-4A). *PhBSMT1* mRNA was detected in the petal tube and limb. *PhBSMT2* and *PhIGS1* transcripts were detected in the stigma, anther, petal tube, and petal limb. Only *PhBPBT* mRNA was detected in the petal limb and also weakly in leaf tissue. *PhPAAS* and *PhCFAT* transcripts were only detected in petal limb, and *PhODO1* mRNA was primarily detected in the petal limb with lower levels observed in the petal tube, stem, and stigma. Combined, these results not only corroborate the current literature (Negre et al., 2003; Boatright et al., 2004; Verdonk et al., 2005; Underwood et al., 2005; Koeduka et al., 2006; Kaminaga et al., 2006; Dexter et al., 2007; Dexter et al., 2008), but clearly illustrate coordinated transcription accumulation profiles for the seven FVBP genes in floral limb tissue.

Developmental FVBP Gene Expression Analysis in MD and 44568 Flowers

To identify FVBP transcript accumulation profiles during floral development, whole flowers were collected at eleven consecutive developmental stages of the MD and the ethylene-insensitive 44568 flower lifecycle (Figure 2-2) and transcript levels were analyzed by sqRT-PCR and qRT-PCR. This analysis revealed a common developmental transcript accumulation profile for all genes examined (Figures 2-3 and 2-4B). In both MD and 44568 flowers, FVBP gene transcripts were detected at relatively low levels throughout floral bud stages (1-5). In MD flowers, high levels of FVBP gene transcripts were detected at anthesis (stage 6) and remained high through the open flower stages (7-10), until transcript levels decreased upon senescence (stage 11) [Figures 2-3A and 2-4B]. In 44568 flowers, FVBP gene transcripts were detected in a similar developmental pattern through open flower stages as in MD flowers. However, FVBP gene transcripts were more abundant in observably senescing 44568 flowers (Figure 2-3B) than MD flowers at the same stage (11). The present analysis supports the existence of a concerted

system of transcriptional regulation with regard to these seven genes during the development of a petunia flower.

Volatile Emission throughout Development from MD and 44568 Flowers

In order to compare the developmental transcript accumulation analysis (Figures 2-3 and 2-4B) to developmental volatile benzenoid/phenylpropanoid emission in petunia flowers; excised whole buds and flowers from MD and 44568 plants at specific stages were analyzed for volatile benzenoid/phenylpropanoid emission (Figure 2-5). Benzyl alcohol (BOH), benzyl benzoate (BeBA), benzaldehyde (Bald), methyl benzoate (MeBA), methyl salicylate (MeSA), phenylethyl benzoate (PhBA), phenylacetaldehyde (PAA), phenylethylalcohol (2-POH), eugenol (EG) and isoeugenol (IE) emissions were measured at all floral developmental stages. All volatile compounds analyzed in MD and 44568 flowers were either at the detection limit or below detection in bud stages of floral development prior to stage 5. The initial detection of most volatiles was at anthesis (stage 6). High amounts of all volatiles were detected throughout open flower stages (stages 7-10) and markedly lower amounts of most volatiles were detected in senescing tissue (stage 11) of MD flowers but not 44568 flowers (Figure 2-5). These data coincide with the FVBP gene transcript results (Figures 2-3 and 2-4B). That is, FVBP gene transcripts and FVBP emissions are low or not detected in floral bud stages (1-5). The initial detection of substantial levels of both FVBP gene transcripts and emissions are at anthesis (stage 6) and high levels of both are detected throughout open flower stages (7-10). In addition, comparison of MD and 44568 FVBP transcript abundance and volatile emissions in senescing floral tissues (stage 11) supports the association further. Low levels of FVBP gene transcripts and emissions are found in MD flowers, but relatively higher amounts of FVBP gene transcripts and emissions are found in 44568 flowers (Figures 2-3 and 2-5).

Ethylene Dependent Down-Regulation of FVBP Gene Expression

Comparison between MD and 44568 FVBP gene transcript levels at developmental stage 11 (Figure 2-3) suggests transcription of all seven FVBP genes is affected by ethylene. To test this hypothesis, excised MD and 44568 flowers were treated with air or ethylene for 0, 1, 2, 4, and 8 hrs and gene transcript accumulation was analyzed by sqRT-PCR and qRT-PCR. All FVBP genes examined showed a reduction of transcript levels in MD flowers treated with ethylene compared to those treated with air (Figures 2-6 and 2-4C). In contrast, no reduction of expression was observed for any of the FVBP genes in 44568 flowers treated with ethylene or air.

PhBSMT1, *PhBSMT2*, and *PhCFAT* transcripts were reduced in MD flowers after two hours of ethylene exposure (Figure 2-6), which agreed with previously published data (Negre et al., 2003; Underwood et al., 2005; Dexter et al., 2007). *PhPAAS* and *PhODO1* transcript levels were also reduced after two hours of ethylene treatment in MD flowers. *PhBPBT* and *PhIGS1* transcript levels were reduced after four hours of ethylene treatment. These data show that two to four hours of exogenously applied ethylene is sufficient to reduce transcript levels of all seven FVBP genes examined in MD flowers.

Volatile Emission after Exogenous Ethylene Treatment

Ten hours of exogenous ethylene treatment has been shown to accelerate floral senescence and permanently reduce volatile emission in petunia flowers (Underwood et al., 2005). Two hours of ethylene treatment is sufficient to reduce transcript accumulation from many of the FVBP genes (Figure 2-6) without accelerating senescence (Figure 2-7). Therefore, MD and 44568 flowers were excised and treated with ethylene for 0, 2, and 10 h starting at 20:00 h of day 1 to determine if short term ethylene exposure that does not lead to senescence would lead to a permanent reduction in floral volatile benzenoid/phenylpropanoid synthesis. Individual

volatiles emitted from 44568 flowers the day after air and ethylene treatments were similar. Twenty four hours after the start of treatments, volatiles emitted from MD flowers treated with ethylene for 10 hours were greatly reduced. However, volatiles from MD flowers treated with ethylene for two hours were comparable to volatile levels of air treated MD flowers (Figure 2-8). Therefore, a relatively short exposure (two hours) to ethylene that did not accelerate senescence did not reduce volatile emissions, whereas a longer exposure (ten hours) to ethylene that did accelerate senescence (Figure 2-7) reduced volatile emissions. These results suggest a reversible component of ethylene in the regulation of floral volatile benzenoid/phenylpropanoid production in MD flowers, which is dependent on the exposure duration.

Rhythmic Regulation of FVBP Gene Expression in MD Flowers

Since emission of FVBPs is rhythmic and peaks around 1:00 h (Verdonk et al., 2005), FVBP gene transcript accumulation was analyzed by sqRT-PCR from stage 9 corollas every three hours over a 36 hour time period to achieve comparable, daily expression profiles in MD flowers. In general *PhBSMT1*, *PhBSMT2*, *PhBPBT*, *PhPAAS*, and *PhIGS1* (genes responsible for the direct formation of emitted volatile compounds) transcripts were detected at high levels during the light period (6:00 to 21:00 h), and lowest mRNA levels detected during the dark period, 24:00 to 6:00 h (Figure 2-9). *PhCFAT* and *PhODO1* (genes responsible for the availability of precursors and direct substrates for the above mentioned genes) transcripts were detected at high levels late in the light period and into the dark period (15:00 to 3:00 h). *PhODO1* and *PhCFAT* transcript accumulation profiles demonstrate an obvious shift towards the dark period as compared to the other FVBP transcript profiles examined These data indicate the presence of at least two transcriptional regulatory systems controlling rhythmicity of FVBP gene transcript accumulation in MD flowers.

PhPAAS Activity in MD Flowers

Transcript levels for the FVBP genes and volatile emission are rhythmic in petunia (Figure 8; Verdonk et al., 2005). To determine if protein activity contributes to rhythmic volatile emission, PhPAAS activity was examined in MD limb tissue from developmentally identical flowers (stage 8) at four time-points. Over the course of a 24 h experiment with time-points every six hours, PhPAAS activity was not significantly different from sample to sample (Figure 2-10). These data along with the data in figure 8 suggest that as is the case for PhBSMT activity (Kolosova et al., 2001a), rhythmic phenylacetaldehyde emission is not limited by enzyme activity levels, but rather the availability of substrate for PhPAAS.

Discussion

Through the efficient transcript accumulation analysis of the seven floral volatile benzenoid/phenylpropanoid (FVBP) genes investigated here, it is now clear the FVBP genes are spatially, developmentally, and ethylene regulated at the transcriptional level as a coordinated group. Compared to the other plant tissues examined, the highest levels of FVBP gene transcripts are in the petal limbs of MD flowers (Figure 2-1). This is in accordance with the specific floral tissue where the majority of volatile benzenoid/phenylpropanoid compounds are detected in the MD flower (Verdonk et al., 2003; Underwood et al., 2005; Dexter et al., 2007). Thus, an organ specific biological association between floral volatile benzenoid/phenylpropanoid production and gene regulation is apparent. These observations suggest a potential reproductive advantage for a fragrant flower with this level of spatial regulation by attracting a pollinator to the specific area where the best opportunity lies to come in contact with the receptacle for the male gametes and access the nectary (reward for the pollinator).

In order to better understand the regulation of floral volatile emission, we have examined a large set of FVBP genes in developmentally staged tissues. The resolution and standardization

of the petunia floral developmental stages (Figure 2-2) shows a tightly regulated subset of genes prior to and after anthesis in both MD and 44568 flowers. Transcripts from all FVBP genes examined are detected at the fully elongated bud stage (stage 5), followed by a substantial increase in transcript levels as the flower begins to open and becomes receptive to pollination (Figures 2-3 and 2-4B). Essentially, stages 1-5 of development can be termed “Box 1” of flower development in petunia. Box 1 is characterized with corolla tube elongation, pigment production in colored cultivars, a minimum level of FVBP gene transcripts (Figures 2-3 and 2-4B) and a minimum level of volatile emissions detected in MD (Figure 2-5) [Weiss et al., 1995; Ben-Nissan and Weiss, 1996; Moalem-Beno et al., 1997; Verdonk et al., 2003]. In short, Box 1 is a growth and maturation stage of development in a petunia flower. The next major developmental stage, anthesis (stage 6), is the transitionary stage (TS) between Box 1 and “Box 2” of flower development where the flower function shifts from growth and maturation to pollinator attraction and fertilization. The TS is characterized by slowed elongation of the corolla tube tissue, the incipient opening of the corolla limb, and up-regulation of the FVBP genes (Figures 2-3 and 2-4B). Box 2 encompasses the functional reproductive stage of flower development (open flowers) and is defined by volatile benzenoid/phenylpropanoid synthesis and emission (Figures 2-3, 2-4B, and 2-5). In a MD flower, anthers dehisce to disperse the male gametes (Wang and Kumar, 2007), and upon pollination and successful fertilization is followed by an ethylene mediated senescence of the corolla tissue (Negre et al., 2003; Underwood et al., 2005). This stage of flower development requires a large commitment of energy and resources in the synthesis of fragrance to facilitate reproduction. Therefore, the high level of FVBP gene transcription only when the flower is receptive to pollination is an excellent means to efficiently utilize metabolites.

We hypothesized that benzenoid/phenylpropanoid emission from developing MD and 44568 flowers would be similar from stage 1 to stage 10 of flower development, due to the similarity in FVBP gene expression between MD and 44568 flowers (Figure 2-3). In general, this is the case up to stage 11. The difference in volatile emission between MD and 44568 flowers at stage 11 can be explained by relatively higher levels of FVBP transcripts detected in observably senescing 44568 flowers when compared to transcript levels in MD flowers at the same stage (Figures 2-3 and 2-5). Stage 11 is accompanied by endogenous ethylene production mediating senescence in MD; however, in 44568 the ethylene is not perceived and results in a longer floral lifespan and presumably continued transcription of the FVBP genes with concomitant FVBP emission. Therefore, the developmental gene expression and emission observations suggest a developmentally direct relationship between FVBP gene transcript abundance and FVBP emissions.

We then tested all seven FVBP genes for any transcriptional effect subsequent to exogenously applied ethylene. Indeed, as indicated from the developmental FVBP gene expression comparison between MD and 44568 (Figure 2-3), where transcripts examined are still detected at substantial levels in observably senescing 44568 flowers when compared to MD flowers, ethylene treatment for two to four hours was sufficient to reduce transcript levels of the FVBP genes in MD flowers, but not in 44568 flowers (Figures 2-4C and 2-6). Thus, it is now evident that all seven of these FVBP genes are transcriptionally affected by ethylene exposure in a similar manner suggesting that there are transcriptional regulators common to all the FVBP genes examined here.

Since either pollination or 10 hours of exogenous ethylene treatment induces senescence in MD flowers (Wilkinson et al., 1997; Underwood et al., 2005) we postulated that the system-

wide repression of transcription for the FVBP genes by ethylene was due to an irreversible senescence program. While two hours of ethylene treatment is sufficient to reduce transcript levels of *PhBSMT1*, *PhBSMT2*, *PhPAAS*, *PhCFAT*, and *PhODO1* (Figure 2-6), this treatment does not accelerate floral senescence in MD flowers (Figure 2-7). Therefore we tested if two hours of ethylene treatment causes a long-term reduction of floral volatile emission in MD flowers. After two hours of ethylene treatment, flowers emitted levels of volatile benzenoids/phenylpropanoids equivalent to those of untreated flowers. In contrast, MD flowers treated with ethylene for 10 hours emitted greatly reduced levels of volatiles (Figure 2-8) and senesced earlier (Figure 2-7) than air treated flowers. These observations indicate MD flowers can tolerate a short burst of ethylene without entering into senescence and with no effect on floral volatile emission (reversible component), but a longer and sustained exposure to ethylene triggers a senescence program and long term reduction in volatile emission (irreversible component).

While a single molecular mechanism was not elucidated through the ethylene studies shown here, together these data along with previous findings (ethylene effect on PhBSMT activity (Negre et al., 2003)) clearly support a role for ethylene at the transcriptional and post-transcriptional levels in the regulation of floral volatile benzenoid/phenylpropanoid production in petunia flowers. Thus, the ethylene regulation imparted upon floral volatile production is multifaceted and may consist of more than one molecular action.

The rhythmic emission of floral volatile benzenoids/phenylpropanoids peaks around 1:00 h (Verdonk et al., 2005), which corresponds to when nocturnal moths, suspected petunia pollinators, are active (Hoballah et al., 2005). However, *PhBSMT1*, *PhBSMT2*, *PhBPBT*, *PhPAAS*, and *PhIGS1* transcript accumulation peaks around 15:00 h (Figure 2-9) [Negre et al.,

2003; Boatright et al., 2004; Underwood et al., 2005; Kaminaga et al., 2006; Koeduka et al., 2006; Orlova et al., 2006; Dexter et al., 2008], while *PhODO1* and *PhCFAT* transcript accumulation peaks around 21:00 h (Figure 2-9) [Verdonk et al., 2005; Dexter et al., 2007]. In addition, the internal substrate pools of benzoic acid and cinnamic acid are relatively low (around 4 and 0.04 µg gfw^{-1} respectively) at 10:00 h and are at high levels (around 24 and 0.4 µg gfw^{-1} respectively) at 22:00 h (Boatright et al., 2004; Underwood et al., 2005; Orlova et al., 2006). Therefore, *PhODO1* (regulating shikimate genes) and *PhCFAT* (responsible for the formation of the substrate for *PhIGS1*) transcript accumulation, internal substrate pool accumulation, and floral volatile benzenoid/phenylpropanoid emission demonstrate concurrent timing. In contrast, peak transcript levels of the genes responsible for the direct formation of emitted floral benzenoid/phenylpropanoid compounds (*PhBSMT1*, *PhBSMT2*, *PhBPBT*, *PhPAAS*, and *PhIGS1*) precedes volatile emission by approximately six hours, while PhBSMT and PhPAAS activity (Kolosova et al., 2001 and Figure 2-10, respectively) do not reflect a rhythmic nature required for control over the rhythmic emission of floral volatiles in flowers. Thus, the rhythmic transcript accumulation of at least the FVBP genes *PhBSMT1*, *PhBSMT2*, and *PhPAAS* are not the determining factor for rhythmic emission of the floral volatiles. In contrast, oscillations of precursor pools and the rhythmic transcript accumulation of *PhODO1* suggest the regulation controlling the rhythmic emission of floral fragrance is upstream in the floral volatile benzenoid/phenylpropanoid biosynthetic pathway, perhaps at the first committed step in phenylalanine biosynthesis.

The transcript accumulation analyses in this study illustrate four criteria with multiple categories therein, which can be used to standardize the characterization of any FVBP genes identified in the future. The seven FVBP genes examined here, are likely a part of a common

transcriptionally regulated network throughout three expression criteria (spatial, developmental, and ethylene regulated). Interestingly, two distinct rhythmic transcript accumulation profiles are clear, while the volatile emission profile has a single peak. Together, these observations suggest the rhythmic production and emission of volatile benzenoids/phenylpropanoids from the MD flower is controlled by the availability of substrates for the enzymes responsible (example: PhBSMT and PhPAAS) for the direct formation of the emitted volatile compounds. However, the regulatory mechanism depicting the level of corresponding transcripts to enzyme activity is not known. Furthermore, the regulatory role of ethylene may be more complex than merely a protagonist to floral senescence in the flower of *Petunia hybrida* cv. 'Mitchell Diploid'.

Experimental Procedures

Plant Materials

Inbred *Petunia x hybrida* cv 'Mitchell Diploid' (MD) plants were utilized as a 'wild-type' control in all experiments. The ethylene-insensitive *CaMV* 35S:*etr1-1* line 44568, generated in the MD genetic background (Wilkinson et al., 1997), was utilized as a negative control for ethylene sensitivity where applicable. MD and 44568 plants were grown as previously described (Underwood et al., 2005; Dexter et al., 2007). A growth chamber (Environmental Growth Cambers, model TC-1, Chagrin Falls, OH, USA) was utilized for experiments to determine rhythmic regulation of the FVBP genes. The chamber was programmed for 16 hrs light (approximately 400 µmol m^{-2} s^{-1}) and 8 hrs dark with a temperature of 24^{o}C. Four MD plants were acclimated in the growth chamber for two weeks prior to the start of the experimental collection. For exogenous application of ethylene experiments, excised MD and 44568 flowers from greenhouse grown plants were placed in 40 L glass tanks located in a climate controlled (23^{o}C) room with 10 µmol m^{-2} s^{-1} of fluorescent light. All exogenous ethylene treatments used two µL L^{-1} of ethylene with air treatments for controls.

Expression Series Construction

All expression experiments were conducted multiple times with equivalent results observed, and in all cases, total RNA was extracted as previously described (Verdonk et al., 2003). To determine the spatial regulation of all the FVBP genes in MD plants total RNA was isolated from root, stem stigma, anther, leaf, petal tube, petal limb, and sepal tissues of three individual plants at 16:00 h. To examine the developmental regulation of all FVBP genes, MD and 44568 floral tissue was collected at eleven different stages; floral bud < 0.5 cm, bud 0.5 < 1.5 cm, bud 1.5 < 3.0 cm, bud 3.0 < 5.0 cm, bud fully elongated 5.0 < 6.5 cm, flower opening 0 < 2 cm limb diameter (anthesis), flower fully open day 0, day 1, day 2, day 3, and observably senescing flower (flower opening day 7 for MD and flower opening day 13 for 44568 [due to the delayed senescence phenotype of 44568 flowers]). All tissues were collected at 16:00 h on the same day, and total RNA was isolated from all samples collected. To determine rhythmic regulation of the FVBP genes, on day 1 of tissue collection, five randomly selected corollas per stage were collected at 6:00 h and every three hours thereafter for a total of 36 hours. Samples were frozen in liquid N_2 and stored at -80°C. Total RNA was then isolated from all samples including multiple biological replicates. To investigate the effects of exogenous ethylene on the FVBP gene transcription, excised MD and 44568 fully open day 2 flowers (placed in tap water) from greenhouse grown plants were acclimated to treatment conditions for four hours prior to treatment. All excised flowers were placed into eight tanks, four for ethylene treatments and four for air treatments. Air and ethylene treatments were conducted for 0, 1, 2, 4, and 8 hours starting at 12:00 h. Individual samples consisted of three flowers. Immediately following treatment, each of the flower samples were collected, stored at -80^{o}C, and then total RNA was isolated from all corolla tissues once all samples had been collected.

Gene Expression Analysis

Semi-quantitative RT-PCR was performed using a Qiagen One-step RT-PCR kit (Qiagen Co., Valencia, CA, USA) with 50 ng total RNA. To visualize RNA loading concentrations, samples were amplified with *Ph18S* primers (forward primer 5'-TTAGCAGGCTGAGGTCTCGT-3' and reverse primer 5'-AGCGGATGTTGCTTTTAGGA-3') and analyzed on an agarose gel. The following primers were designed and utilized for the visualization of the mRNA levels corresponding to the floral volatile benzenoid/phenylpropanoid genes: *PhBSMT1* (accession number AY233465) and *PhBSMT2* (accession number AY233466) forward primer, 5'-AGAAGGAAGGATCATTCACCA-3'; *PhBSMT1* reverse primer, 5'-TATTCGGGTTTTTCGACCAC-3'; *PhBSMT2* reverse primer, 5'-GAGAGATCTGAAAGGACCCC-3'; *PhBPBT* (accession number AY611496) forward primer, 5'-TGGTGGACCAGCTAAAGGAG-3'; *PhBPBT* reverse primer, 5'-GGATTTGGCATTTCAAACAAA-3'; *PhPAAS* (accession number DQ243784) forward primer, 5'-TCCTTGTAGTTCTAGTACTGCTGGAA-3'; *PhPAAS* reverse primer, 5'-TCAACAGCAGTTGTTGAAGTAGTTC-3'; *PhCFAT* (accession number DQ767969) forward primer 5'-CCATATCTTCCACCCCTTGA-3'; *PhCFAT* reverse primer, 5'-CAAATGACTAAACCGGAGTTCA-3', *PhPhIGS1* (accession number DQ372813) forward primer, 5'-GCCTATGTCATGCCATTGAA-3'; *PhPhIGS1* reverse primer, 5'-TGCTTTAATTGTGTAGGCTGC-3', and *PhODO1* (accession number AY705977) forward primer, 5'-TTCAATTGGCTTTCGGGTTA-3'; *PhODO1* reverse primer, 5'-AGGCACCTTGGACTCTTCG-3'. In addition, quantitative (q)RT-PCR was used to validate the multiple biologically replicated sqRT-PCR results for three of the four transcript accumulation criteria using *PhPAAS* and *PhCFAT* as examples on a MyIQ real-time PCR detection system (Bio-Rad Laboratories Inc., Hercules, CA). qRT-PCR analysis with Power SYBR® Green RNA-

to-C_t™ 1-Step Kit (Applied Biosystems, Foster City, CA) was used to amplify and detect resulting products following the manufacturer's protocol. The following qRT-PCR primers were constructed in Primer Express® software v2.0 (Applied Biosystems, Foster City, CA) and demonstrated gene specificity during melt curve analysis and then optimized: *PhPAAS* forward primer, 5'-CCAACCCGAACCAATTGAGA-3'; *PhPAAS* reverse primer, 5'-CCTGGGAAAATATCGCTTCGA-3'; *PhCFAT* forward primer, 5'-AGGCAACTCGCAATGGAAGT-3'; *PhCFAT* reverse primer, 5'-AGGCGCTGAAACACTCCAAT-3'; *PhFBP1* (M91190) forward primer, 5'-TGCGCCAACTTGAGATAGCA-3'; *PhFBP1* reverse primer, 5'-TGCTGAAACACTTCGCCAATT-3'; Pa18S (AJ236020) forward primer, 5'-TGCAACAAACCCCGACTTCT-3'; Pa18S reverse primer, 5'-AGCCCGCGTCAACCTTTTAT-3'.

Floral Volatile Experiments and Emitted Volatile Quantification

For all volatile emission experiments, emitted floral volatiles from excised flowers were collected and quantified as previously described (Underwood et al., 2005; Dexter et al., 2007). For the developmental volatile emission experiment, flowers from MD and 44568 plants were analyzed for levels of emitted volatile compounds at each stage shown in figure 3. All flowers were tagged at stage 6 and allowed to reach the desired age as judged by days after this stage. Volatile collections were performed on three flowers for each developmental stage at 19:00 h, and each sample was replicated three times.

For volatile emission analysis from MD and 44568 flowers after ethylene treatment, open flowers at comparable stages of development were excised and used after a four hour acclimation period. Treatments started at 20:00 h of day 1 and lasted two and ten hours respectively with air treatments as controls. After all treatments, flowers were placed in ambient air conditions in the

same climate controlled room until 20:00 h of day 2. Therefore 24 hours after the start of all treatments floral volatiles were collected and quantified. All treatments consisted of three flowers per sample and six replicates for each sample.

Determination of PAAS Activity in Limb Crude Protein Extract

Limb tissue from developmentally identical flowers (beginning at flower open day 1, stage 8) were collected at 18:00 h, 0:00 h, 6:00 h, and 12:00 h from MD plants grown as previously described (Underwood et al., 2005; Dexter et al., 2007). Frozen limb tissue from nine flowers per sample was disrupted with liquid nitrogen in mortar and pestles. Chilled extraction buffer (50 mM Tris pH 8.5, 10 mM β-mercaptoethanol, 5 mM $Na_2S_2O_5$, 0.2 mM pyridoxal 5′-phosphate, 1% polyvinylpyrrolidone MW 360,000, 1mM phenylmethanesulphonylfluoride, and 10% glycerol) was added to the ground tissue and further disrupted until the material was liquid. Samples were centrifuged at 12,000 x *g* for 15 minutes. The supernatant was desalted and concentrated with centrifugal filters (Millipore) designed to eliminate compounds < 30,000 daltons. Phenylacetaldehyde synthase (PhPAAS) activity was measured through the production of ^{14}C-CO_2 in reactions containing 30 μM L-[U-^{14}C] phenylalanine (Amersham), 50 mM Tris pH 8.5, 0.2 mM pyridoxal 5′-phosphate, 0.1 mM EDTA, and 20 μL protein extract. ^{14}C-CO_2 was collected on filter paper infused with 2N KOH as described by Tieman et al., 2006. Reactions were incubated at room temperature for 30 minutes. Captured ^{14}C-CO_2 was quantified by scintillation counting. Activity in the extracts was determined against background activity in assays with boiled protein and reactions without protein. Results were averaged from three replicate assays per sample and two sets of duplicate tissues per time-point. Production of phenylacetaldehyde was verified by GC-MS from separate reactions containing ^{12}C-phenylalanine and otherwise identical reaction conditions.

Floral Longevity Subsequent to Ethylene Application in MD and 44568 Flowers

Excised MD and 44568 flowers were placed in water and treated with ethylene for 0, 2, and 10 hours (Fig S1). After all treatments the flowers were allowed ambient air conditions and monitored for signs of senescence for an experimental total of 32 h. Four flowers per genetic background were used for each time-point and the experiment was replicated three times.

Acknowledgements

The authors wish to thank Becky Hamilton and Joshua Bodenweiser for their excellent care of the petunia plants. This work was supported by grants from the USDA Nursery and Floral Crops Initiative, the Fred C. Gloeckner Foundation, and the Florida Agricultural Experiment Station.

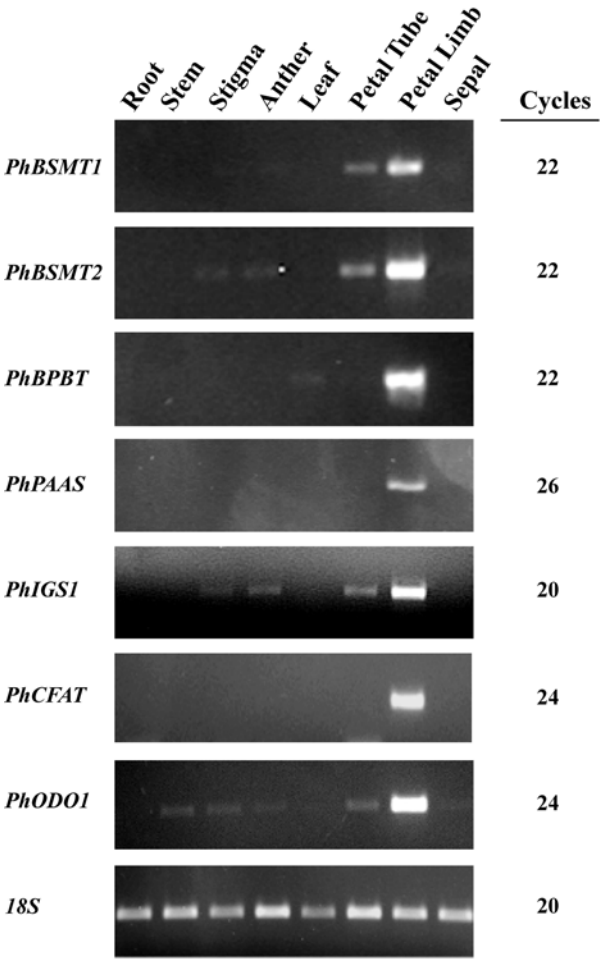

Figure 2-1. Tissue specific transcript accumulation analysis of seven FVBP genes in MD. Root, stem, stigma, anther, leaf, petal tube, petal limb, and sepal tissues were collected and total RNA was isolated from three MD plants at 16:00 h. Primers specific for *PhBSMT1*, *PhBSMT2*, *PhBPBT*, *PhPAAS*, *PhIGS1*, *PhCFAT*, and *PhODO1* with *Ph18S* as a loading control were used for semi-quantitative RT-PCR. The number of cycles used for amplification of each gene is shown on the right.

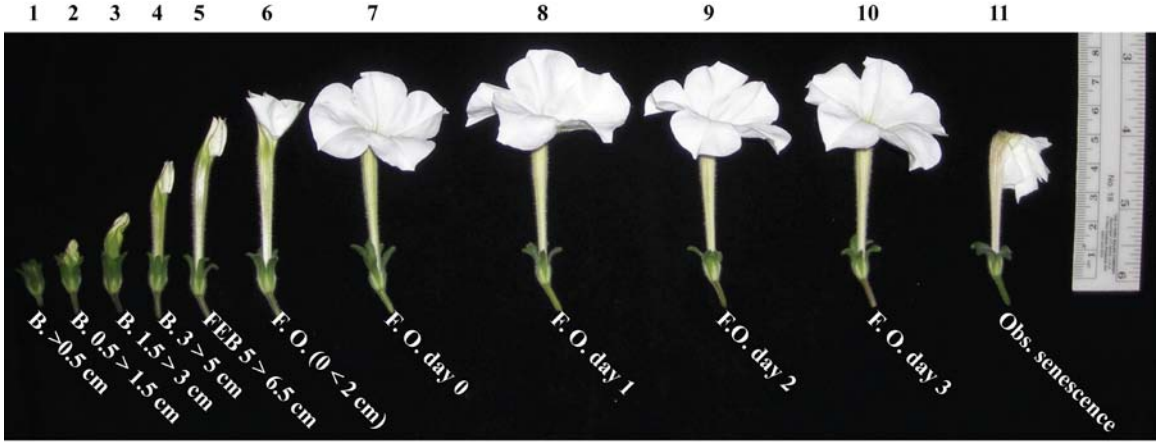

Figure 2-2. Picture of floral stages used for the developmental studies in MD and 44568. Floral tissues were collected at 11 different developmental stages; bud < 0.5 cm (1), bud 0.5 <1.5 cm (2), bud 1.5 < 3 cm (3), bud 3 < 5 cm (4), fully elongated bud 5 < 6.5 cm (5), flower opening [limb diameter 0 < 2 cm] (6), flower open day 0 (7), flower open day 1 (8), flower open day 2 (9), flower open day 3 (10), and observably senescing flower [flower open day 7 for MD and flower open day 13 for 44568] (11).

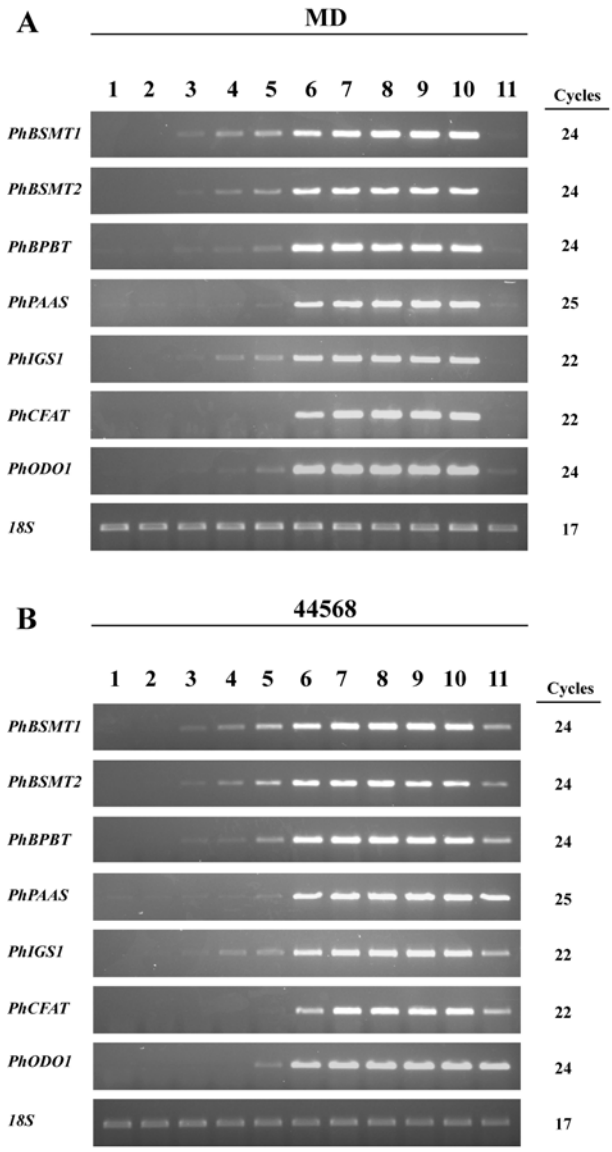

Figure 2-3. Developmental transcript accumulation analysis of seven FVBP genes in MD (A) and 44568 (B). Floral tissues were collected at 11 different developmental stages as shown in figure 3. Primers specific for *PhBSMT1*, *PhBSMT2*, *PhBPBT*, *PhPAAS*, *PhIGS1*, *PhCFAT*, and *PhODO1* with *Ph18S* as a loading control were used for semi-quantitative RT-PCR. The number of cycles used for amplification of each gene is shown on the right.

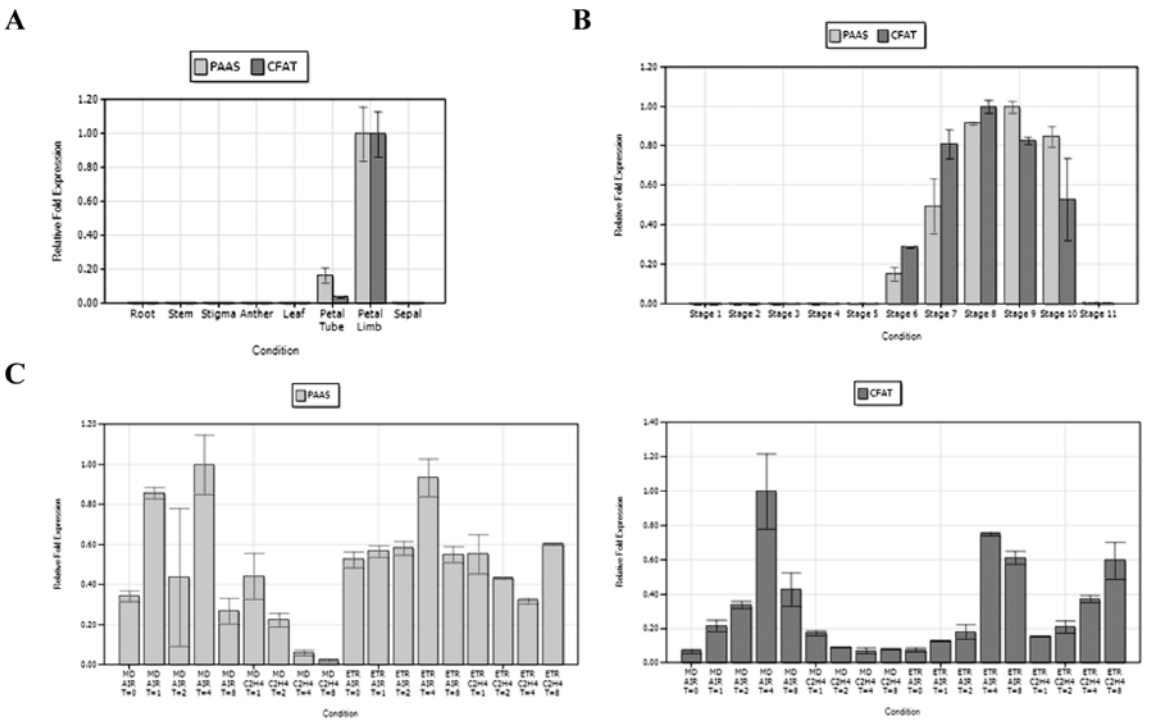

Figure 2-4. qRT-PCR transcript accumulation analysis of *PhPAAS* and *PhCFAT* in petunia. Spatial analysis used root, stem, stigma, anther, leaf, petal tube, petal limb, and sepal tissues of MD harvested at 16:00 h (A) The spatial experiment consisted of one biological replicate used for sqRT-PCR and one separate biological replicate with two technical replicates per biological replicate. Floral developmental analysis used MD flowers from 11 sequential stages at 16:00 h (B) The MD developmental analysis consisted of one biological replicate separate from the biological replicates used for the sqRT-PCR with three technical replicates. Ethylene treatment (two µL L^{-1}) analysis used excised MD and 44568 whole flowers treated for 0, 1, 2, 4, and 8 hours (C) The ethylene treated series consisted of one biological replicate used in the sqRT-PCR with two technical replicates. *PhFBP1* and *Ph18S* were used as references throughout these experiments.

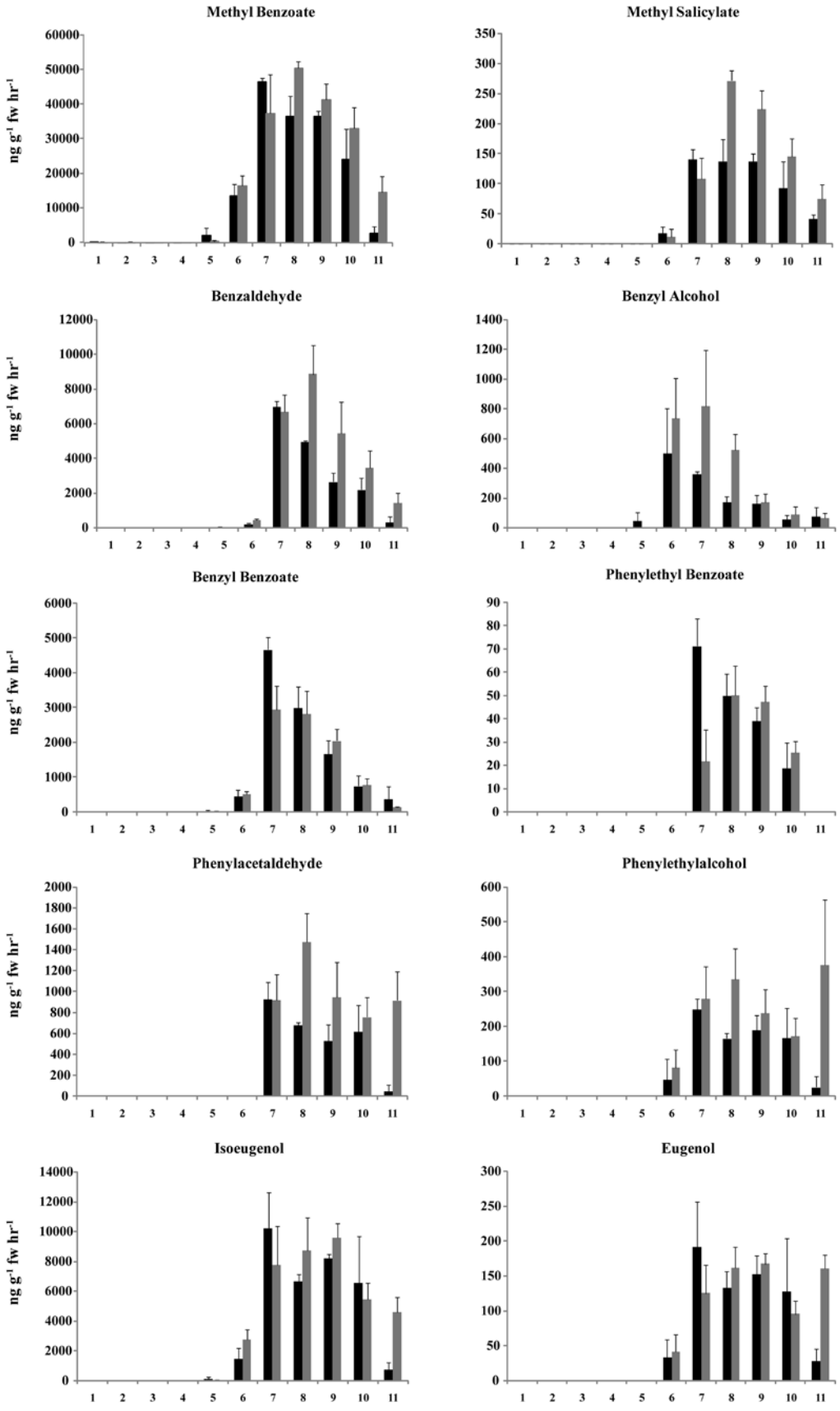
Methyl Benzoate
Methyl Salicylate
Benzaldehyde
Benzyl Alcohol
Benzyl Benzoate
Phenylethyl Benzoate
Phenylacetaldehyde
Phenylethylalcohol
Isoeugenol
Eugenol
ng g-1 fw hr-1

Figure 2-5. Developmental floral emission analysis of major volatile compounds from MD and 44568 flowers (mean ± se; n = 3). Each graph shows the concentration (ng g^{-1} fw hr^{-1}) of individual volatile compounds emitted from excised MD (black bars) and 44568 (gray bars) flowers over the course of eleven floral developmental stages as depicted in figure 3. Volatile collection was performed on whole flowers at 19:00 h.

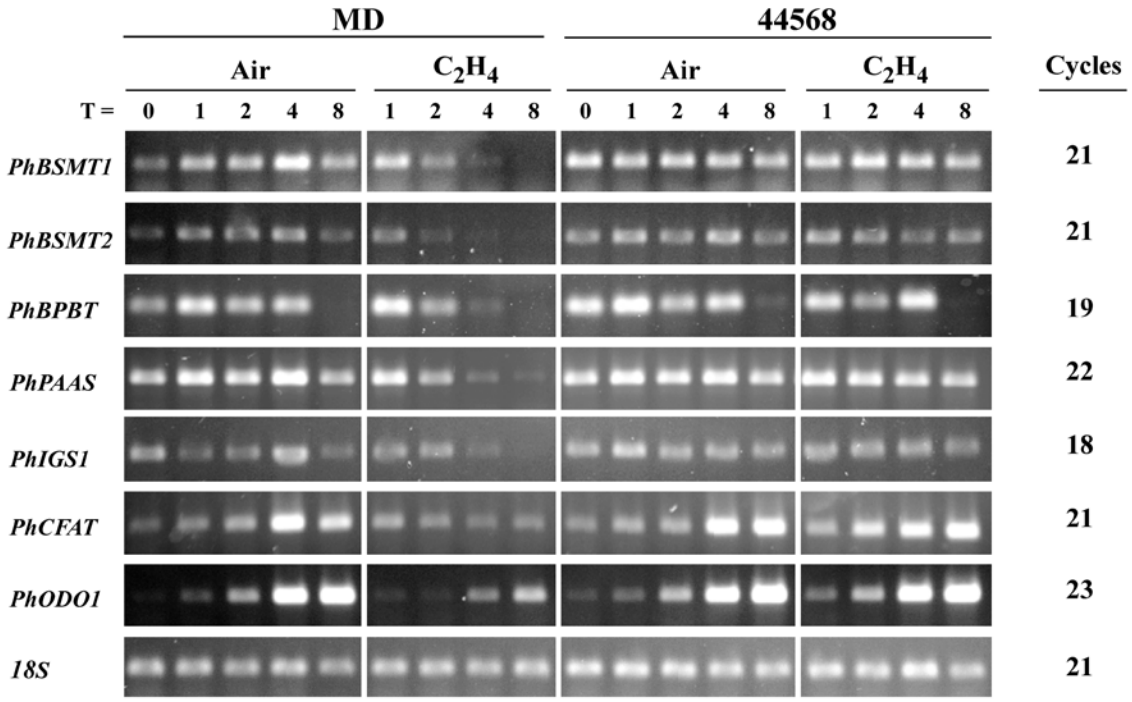

Figure 2-6. Transcript accumulation analysis of seven FVBP genes in MD flowers and 44568 flowers. MD and 44568 flowers were treated with ethylene (two µL L^{-1}) and air for 0, 1, 2, 4, and 8 hours. Corolla limbs were collected immediately after each time-point and total RNA was isolated. Primers specific for the floral volatile genes *PhBSMT1*, *PhBSMT2*, *PhBPBT*, *PhPAAS*, *PhIGS1*, *PhCFAT*, and *PhODO1* with *Ph18S* as a loading control were used for semi-quantitative RT-PCR. The number of cycles used for amplification of each gene is shown on the right.

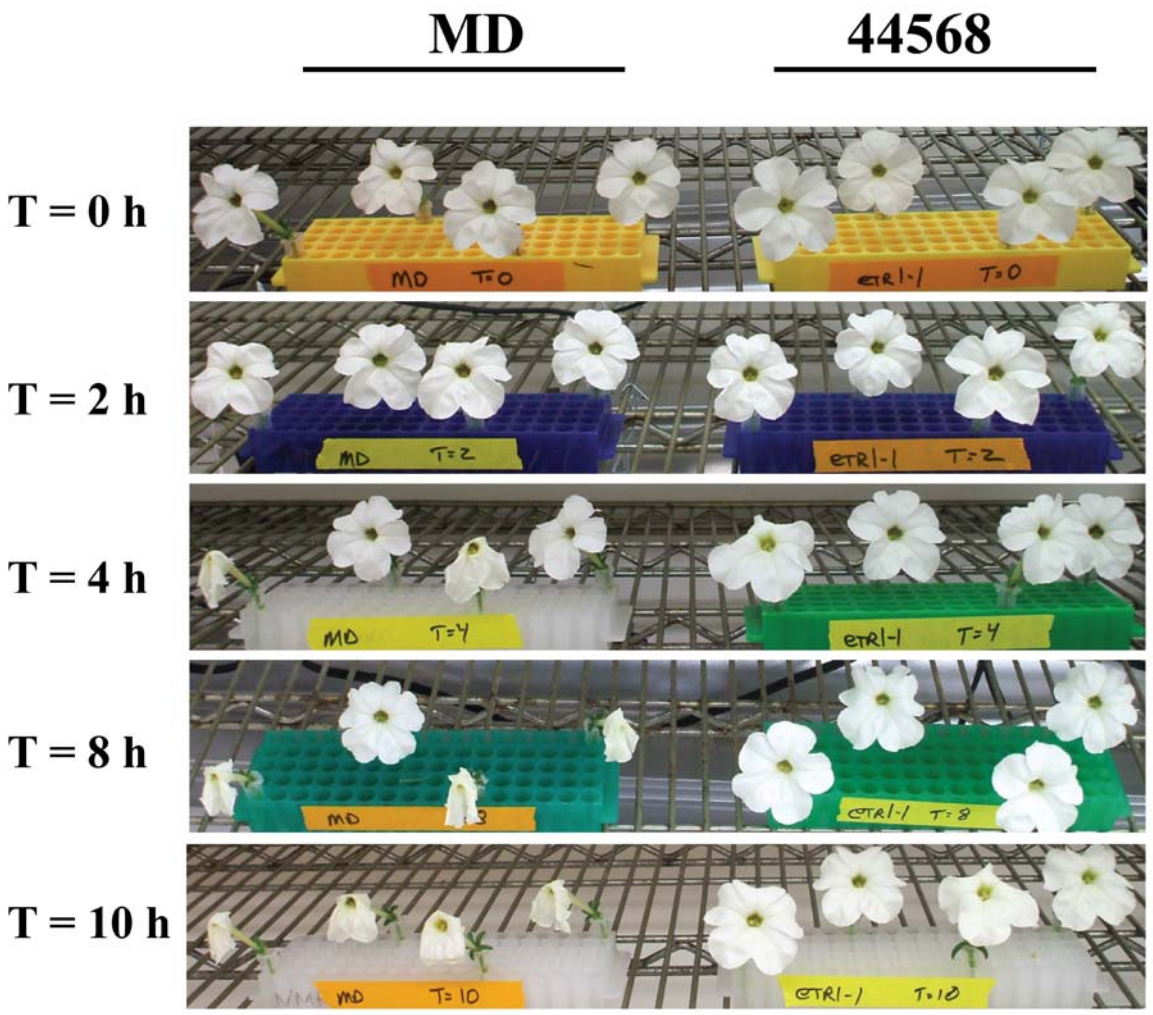

Figure 2-7. Picture of MD and 44568 flowers 32 hours after the initial treatments of ethylene for 0, 2, 4, 8, and 10 hours. MD is the left column and 44568 is the right column.

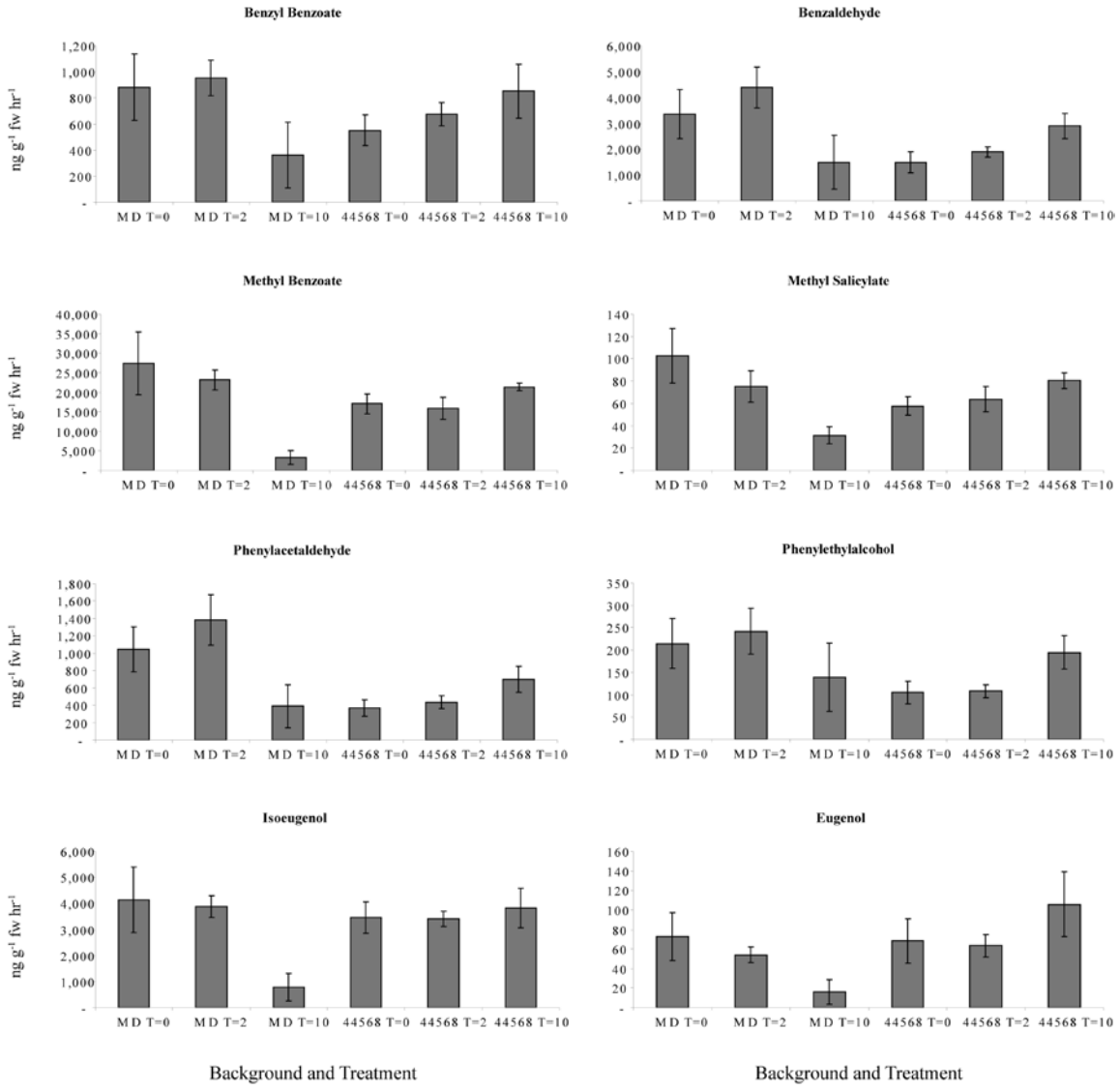

Figure 2-8. Emission analysis of major volatile compounds from MD and 44568 flowers subsequent to differential durations of ethylene exposure (mean ± se; n = 6). Excised MD and 44568 flowers were treated with ethylene (two µL L^{-1}) for 0, 2, and 10 hours beginning at 20:00 h on day 1. Upon completion of treatments, flowers were allowed ambient air conditions until 20:00 h on day 2 when volatile emissions were collected and quantified. Each graph shows the concentration (ng g^{-1} fw hr^{-1}) of individual volatile compounds emitted from MD and 44568 flowers.

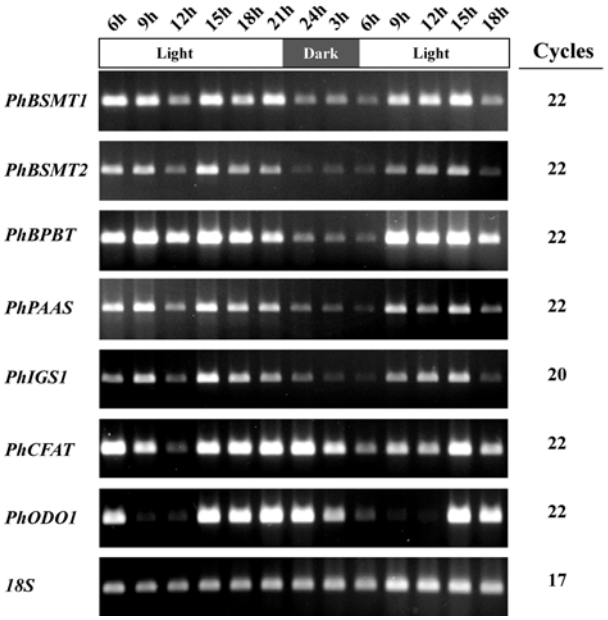

Figure 2-9. Rhythmic transcript accumulation analysis of seven FVBP genes in MD. Four plants were acclimated for two weeks in a large growth camber set at 24°C with a long-day photoperiod (16 hrs of light and 8 hrs of dark). Corolla tissue was collected every three hours beginning at 6:00 h of day 1 for 36 hrs. Primers specific for *PhBSMT1*, *PhBSMT2*, *PhBPBT*, *PhPAAS*, *PhIGS1*, *PhCFAT*, and *PhODO1* with *Ph18S* as a loading control were used for semi-quantitative RT-PCR. The number of cycles used for amplification of each gene is shown on the right.

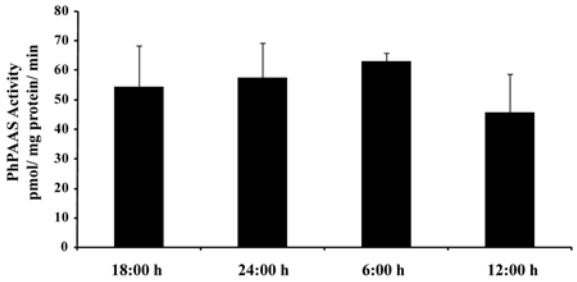

Figure 2-10. Rhythmic analysis of PhPAAS activity in corolla limb tissue of MD flowers. Corolla limb tissue was collected at six hour intervals for a total of 24 h, beginning with flowers from stage 8 (flower open day 1) at 18:00 h. Results were averaged from three replicate assays per sample and two sets of duplicate tissues per time-point.

CHAPTER 3
A SPECIALIZED CHORISMATE MUTASE IN THE FLOWER OF PETUNIA X HYBRIDA

Preface

This work has been submitted to and accepted in modified form at *The Plant Journal* for publication (Thomas A. Colquhoun, Bernardus C.J. Schimmel, Joo Young Kim, Didier Reinhardt, Kenneth Cline and David G. Clark. [2009] A petunia chorismate mutase specialized for the production of floral volatiles. *Plant J*. [In Press])

Introduction

Flowering plant species have developed several mechanisms for attracting pollinating organisms. Flower shape, color, and fragrance all contribute to an increased specialization of the floral phenotype aimed at the attraction of a pollinator (Fenster et al., 2004). Floral fragrance consists of an assortment of volatile organic molecules, which are commonly referred to as a scent bouquet. These volatile organic compounds are not only involved in plant reproductive processes, but also in plant-plant interactions, defense, and abiotic stress responses (Dudareva et al., 2006). The majority of volatile compounds are lipophilic liquids with high vapor pressures, which cross biological membranes freely in the epidermal cells of the petal (Pichersky et al., 2006). Floral volatiles are generally differentiated into three main groups; benzenoids/phenylpropanoids, terpenoids, and fatty acid derivatives.

Petunia (*Petunia x hybrida* cv ‘Mitchell Diploid’ [MD]) synthesizes and emits 13 known floral volatile benzenoid/phenylpropanoid (FVBP) compounds (Kolosova et al., 2001; Verdonk et al., 2003; Boatright et al., 2004; Verdonk et al., 2005; Koeduka et al., 2006) [Figure 1-1]. The majority of FVBP compounds are putatively derived from the aromatic amino acid phenylalanine (Boatright et al., 2004; Schuurink et al., 2006). Eight genes that are known to participate in FVBP synthesis have been isolated from petunia: *PhBSMT1*, *PhBSMT2*, *PhBPBT*, *PhPAAS*,

PhIGS1, *PhEGS1*, *PhCFAT*, and *PhODO1* (Negre et al., 2003; Boatright et al., 2004; Underwood et al., 2005; Verdonk et al., 2005; Kaminaga et al., 2006; Koeduka et al., 2006; Orlova et al., 2006; Dexter et al., 2007; Dexter et al., 2008; Koeduka et al., 2008) [Figure 1-1]. All of these gene products are involved in the direct formation of a FVBP compound except PhODO1 (Verdonk et al., 2005), which is a transcriptional regulator, and PhCFAT (Dexter et al., 2007), which produces substrate for PhIGS1 and PhEGS1.

Regulation of the petunia FVBP system is complex and very specific. Substantial emission of MD FVBPs is confined to the corolla limb tissue during open flower stages of development, which coincides with the presentation of the reproductive organs (Verdonk et al., 2003). MD FVBP internal substrate pool accumulation and emission is diurnal with the highest level detected during the dark period (Kolosova et al., 2001; Verdonk et al., 2003; Underwood et al., 2005; Verdonk et al., 2005). FVBP synthesis and emission, FVBP gene transcript accumulation, and PhBSMT activity are greatly reduced following a successful pollination/fertilization event or exogenous treatment with ethylene (Hoekstra and Weges, 1986; Negre et al., 2003; Underwood et al., 2005). Subsequent to a successful fertilization event, the corolla tissue senesces as the petunia flower shifts from pollinator attraction to supporting seed set.

The shikimate pathway couples metabolism of carbohydrates to the formation of aromatic amino acids (Figure 3-1) [Herrmann and Weaver, 1999]. CHORISMATE MUTASE (CM) catalyzes an intramolecular, [3,3]-sigmatropic rearrangement of chorismic acid to prephenic acid, the initial committed step in phenylalanine and tyrosine biosynthesis (Haslem, 1993). In *Arabidopsis thaliana*, three *CM* genes have been identified and characterized: *AtCM1*, *AtCM2*, and *AtCM3* (Eberhard et al., 1996b; Mobley et al., 1999). *AtCM1* and *AtCM3* encode

putatively plastid localized CM isoforms, which are allosterically down-regulated by phenylalanine and tyrosine, but up-regulated by tryptophan. *AtCM2* encodes a CM isoform not regulated by aromatic amino acids and appears to be located in the cytosol.

The majority of floral volatile studies in petunia have focused on identification of gene products involved in the formation of individual, emitted FVBP compounds (i.e. genes at the end of the FVBP pathway). Since the FVBPs are putatively derived from phenylalanine and CM is the first committed step in phenylalanine biosynthesis, we identified and characterized two petunia *CM* cDNAs (*PhCM1* and *PhCM2*). Additionally, we identify the principal CM responsible for the production of FVBP compounds in petunia.

Results

Identification of Two Distinct *CM* cDNAs

To identify putative *CM* genes, we searched a publicly available petunia EST database (http://www.sgn.cornell.edu) and a petunia root EST collection (courtesy of Dr. Didier Reinhardt at the University of Fribourg) for sequences with homology to any of the three *CM* genes from *Arabidopsis thaliana*. The *in silico* analysis identified two partial ESTs whose full-length sequences were recovered by 5' and 3' RACE technology. These two sequences exhibited high similarity to *AtCMs* and were subsequently renamed *CHORISMATE MUTASE1* (*PhCM1*) and *CHORISMATE MUTASE2* (*PhCM2*), which were deposited in GenBank under accession numbers, EU751616 and EU751617, respectively (Figure 3-2).

The predicted PhCM1 and PhCM2 proteins were 324 and 263 amino acids in length, respectively. PhCM1 contains a predicted N-terminal chloroplast transit peptide (cTP) of 56 amino acids (ChloroP 1.1) and is therefore predicted to be plastid localized (Predator v. 1.03), while PhCM2 is likely located in the cytosol (Benesova and Bode, 1992). The predicted mature PhCM1 and PhCM2 share 46.7 % amino acid identity. When aligned with CM amino acid

sequences from *Arabidopsis thaliana*, *Fagus sylvatica, Solanum lycopersicum, Nicotiana tabacum, Oryza sativa, Vitis vinifera, Zea mays,* and *Saccharomyces cerevisiae* common sequence features including a CM_2 superfamily domain in the N-terminal half of the predicted proteins and a conserved C-terminal domain of 19 amino acids were observed (Figure 3-3A). Additionally, an allosteric regulatory site (GS marked by red box) was present in PhCM1, but not PhCM2, which would be consistent with aromatic amino acid regulation of the putative plastidic PhCM1. Phylogenetic analysis demonstrated that the three solanaceous cytosolic CMs closely associate in an unrooted neighbor-joining tree (Figure 3-3B). PhCM1 associates with CMs from multiple species containing both a predicted cTP and the allosteric regulatory site. PhCM1 shares 62.2 % identity with AtCM1.

Chloroplast Import Assay

To test the predicted subcellular localization of PhCM1 and PhCM2, both full length coding sequences were cloned into a pGEM®-T Easy vector, *in vitro* transcribed and translated. The radiolabeled translation product was incubated with isolated chloroplasts (*Pisum sativum*) in a protein import assay (Figure 3-4). The radiolabeled PhCM2 translation product associated with the chloroplast fraction was equal in size to the original translation product and unprotected from the thermolysin protease treatment, indicating that PhCM2 did not enter the plastid. However, the PhCM1 translation product associated with the chloroplast fraction was processed to a smaller size and was protected from the thermolysin treatment, indicating PhCM1 is imported into the plastid and processed to a mature size. Furthermore, the radiolabeled PhCM1 was associated with the stromal fraction of separated chloroplasts. Together with primary amino acid sequence features, these results demonstrate PhCM1 is localized to the chloroplast stroma, while PhCM2 is most likely not located in the chloroplast.

PhCM1 and *PhCM2* Transcript Abundance Analysis

Because of the large drain on the free phenylalanine pool by the FVBP synthesis pathway, we hypothesized that a *CM* gene would be transcriptionally co-regulated with known FVBP genes. Three criteria of transcript accumulation spatial, flower development, and ethylene treated were chosen for analysis by semi-quantitative reverse transcriptase polymerase chain reaction (sqRT-PCR) and validated by quantitative (q)RT-PCR (Figures 3-5 and 3-6). The spatial analysis consisted of root, stem, stigma, anther, leaf, petal tube, petal limb, and sepal tissues (Figures 3-5A and 3-6A). *PhCM1* transcripts were detected at high levels in the petal limb and tube, and to a much lesser extent in the sexual organs, stem, and root. *PhCM2* transcripts were detected in all tissues examined with relatively high levels in the petal tube and stem tissues. The MD flower development series consisted of whole flowers collected at 11 consecutive stages beginning from a small bud to floral senescence (Figures 3-5B and 3-6B). *PhCM1* transcripts were detected at relatively low levels throughout the closed bud stages of development (stages 1-5). Relatively high levels of *PhCM1* transcripts were detected at anthesis (stage 6) and throughout all open flower stages of development examined (stage 7-10). *PhCM1* transcripts were detected at the lowest level in observably senescing flower tissue (stage 11). *PhCM2* transcripts were detected at similar levels throughout all stages examined except for stage 11 (Figures 3-5B and 3-6B). The ethylene study used excised whole flowers from MD and an ethylene-insensitive (*CaMV* 35S::*etr1-1*) transgenic petunia line, 44568 (Wilkinson et al., 1997). All flowers were treated with air or ethylene (2 µL L^{-1}) for 0, 1, 2, 4, and 8 hours beginning at 12:00 h with an experimental end time of 20:00 h (Figures 3-5C and 3-6C). *PhCM1* transcripts were reduced in MD flowers after four hours of ethylene treatment compared to air treatments, while no change in *PhCM1* transcript level was observed in experiments using 44568. In contrast, *PhCM2* transcript levels were unchanged throughout the treatment conditions in both

genetic backgrounds. Together, these results indicate the transcript accumulation profile for *PhCM1* is similar to that of known FVBP genes and is therefore sufficient for FVBP production.

Total CM Activity in Petunia Flowers

To investigate whether CM activity contributes to daily substrate pool oscillations (Underwood et al., 2005; Orlova et al., 2006) and concomitant rhythmic emission of FVBPs in MD (Verdonk et al., 2005), we developmentally staged MD flowers and collected whole corollas at three time points over the course of 24 h. Desalted crude protein extracts were obtained, and total CM activity was assayed for each time-point with close attention paid to non-enzymatic chorismic acid breakdown (Figure 3-7). Throughout the three daily time-points, total CM activity was unchanged with an approximate specific activity average of 0.07 nkat mg^{-1}. Not discounting the presence of a regulatory molecule *in vivo*, which may be lost through the extraction process, total CM activity in crude protein extracts from stage 9 and 10 MD corollas, did not parallel that of FVBP emission profiles.

Functional Complementation and Recombinant Enzyme Activity of PhCM1 and PhCM2

In spite of the high homology to other CMs at the amino acid level, it was necessary to test the biochemical function of both PhCM1 and PhCM2. The mature coding sequences for both genes were cloned into a pET-32 vector and transformed into the CM-deficient *E. coli* transformant KA12/pKIMP-UAUC, which was provided by Dr. Peter Kast at the Swiss Federal Institute of Technology Zurich. The KA12/pKIMP-UAUC system requires the complementation of both phenylalanine and tyrosine auxotrophies while under a double antibiotic selection and has been well characterized (Kast et al., 1996; Kast et al., 2000). Both pET-32-*PhCM1* and pET-32-*PhCM2* complemented KA12/pKIMP-UAUC when grown on minimal media without the addition of phenylalanine and tyrosine as compared to all controls (Table 3-1). This result

indicates both *PhCM1* and *PhCM2* encode proteins that are sufficient for the enzymatic, intramolecular conversion of chorismic acid to prephenic acid.

We then utilized the pET-32-CM vectors to transform *E. coli* strain BL21(DE3)pLysS with the aim of generating recombinant proteins for PhCM1 and PhCM2. PhCM1 and PhCM2 proteins were purified by Ni^{2+} affinity chromatography and assayed for CM activity with and without the addition of the aromatic amino acids (Figure 3-8). PhCM2 had a specific activity of approximately 5.0 nkat mg^{-1} and was not affected by the presence of aromatic amino acids. However, PhCM1 specific activity was close to 2.2 nkat mg^{-1} and increased approximately three-fold in the presence of tryptophan. As is the case in Arabidopsis, opium poppy, and tomato (Benesova and Bode, 1992; Eberhard et al., 1996a; Eberhard et al., 1996b; Mobley et al., 1999), the cytosolic PhCM2 is not allosterically regulated by the aromatic amino acids. In contrast to allosteric regulation patterns found for plastidic CMs in Arabidopsis and poppy, phenylalanine and tyrosine had no effect on PhCM1 enzymatic activity, but tryptophan regulation is similar in magnitude to AtCM1 (Eberhard et al., 1996b).

Suppression of *PhCM1* by RNAi

Because the transcript accumulation profile for *PhCM1* is similar to known FVBP genes (Figures 3-5 and 3-6) and the subcellular location for PhCM1 is in the plastidial stroma (Figures 3-3A and 3-4), *PhCM1* was chosen for RNAi mediated gene silencing. A 213 bp fragment at the 3' end of the *PhCM1* coding sequence was used for the RNAi inducing fragment (Figure 3-9). Since the *PhCM1* RNAi fragment was less than 60 % homologous to the corresponding region of *PhCM2*, we hypothesized *PhCM2* expression and possibly any other gene family members would be unaffected by the *PhCM1* silencing construct driven by a constitutive promoter (pFMV).

Fifty independent *PhCM1* RNAi (CM1R) plants were generated by leaf disc transformation, and analyzed for reduced levels of *PhCM1* transcripts when compared to MD by sqRT-PCR. Eight plants were chosen for further analysis and self-pollinated to produce T_1 seeds. Five transgenic T_1 CM1R lines segregated in an expected 3:1 manner for the transgene, and these lines were more extensively studied for gene transcript accumulation and FVBP emission differences compared to MD. Representative individuals from three independent T_1 CM1R lines (2-4, 24-9, and 33-9) showed reduced *PhCM1* transcript levels, but *PhCM2* transcript levels were unchanged (Figure 3-10). Additionally, when transcript levels of multiple other genes in the shikimate, phenylpropanoid, and FVBP pathways were analyzed, no differences were observed.

All three selected T_1 CM1R lines showed similar FVBP emission profiles. Using MD FVBP emission levels as a reference, phenylacetaldehyde was reduced 85 to 89 % in the CM1R lines (Figure 3-11). The emissions of three volatile compounds derived from *trans*-cinnamic acid (benzaldehyde, benzyl benzoate, and methyl benzoate) were reduced by 73 to 84 %, 62 to 75 %, and 50 to 68 %; respectively. Isoeugenol emission was modestly lower in the CM1R lines when compared to MD (14 to 28 %), but was not reduced as much as the rest of the major FVBPs analyzed here. Total FVBP emissions were abated by 33.5 to 40.9 % in the T_1 CM1R lines as compared to MD (Figure 3-11). Taken together, these data suggest the lower level of *PhCM1* transcripts in the CM1R lines resulted in lower levels of prephenic acid available for phenylalanine synthesis, and thus, concomitant FVBP emission.

All T_1 CM1R lines were self-pollinated and T_2 generation plants were screened for homozygosity. The screen resulted in two homozygous T_2 CM1R lines, termed 24-9 and 33-8 (Figure 3-12). Whole corollas from stage 9 MD, 24-9, and 33-8 plants were used for quantitative transcript accumulation and quantitative total CM activity assays (Figure 3-13). Compared to

MD, transcript accumulation for *PhCM1* was reduced in 24-9 and 33-8 by 80 to 85 %, while *PhCM2* transcript accumulation was unaffected (Figure 3-13A). Total CM specific activity from desalted crude extracts from 24-9 and 33-8 was reduced by 81 to 84 % compared to MD (Figure 3-13B). Together, these results indicate the reduction of *PhCM1* transcript and subsequent total CM activity are sufficient for the reduction in total FVBP emission in the CM1R lines compared to MD.

24-9 and 33-8 were grown side-by-side with MD numerous times and no observable phenotypic differences were observed. There were no significant differences between MD, 24-9, and 33-8 in seed germination, nor in fresh weight, number of true leaves, aerial height (of nine week old plants), or stem lignin content (Figures 3-14 and 3-15).

Discussion

CHORISMATE MUTASE (CM) has been extensively studied in prokaryotes and fungi, but comparatively less is known about CM in higher plants. The enzymatic reaction of CM is the initial committed step in synthesis of the aromatic amino acids phenylalanine and tyrosine (Haslem, 1993), and MD corollas synthesize and emit large quantities of volatile benzenoid/phenylpropanoid compounds, which are putatively derived from phenylalanine (Boatright et al., 2004). Therefore, we chose to investigate CM in petunia flowers through reverse genetic, molecular, biochemical, and metabolic approaches. The results indicate that *PhCM1* has a major role in the production of FVBPs in petunia flowers.

In petunia, two *CM* cDNAs have been isolated. PhCM1 is plastid localized based on a putative cTP sequence and a chloroplast import assay (ChloroP 1.1; Zybailov et al., 2008) [Figure 3-4]. Of the two putative plastidic Arabidopsis CMs, PhCM1 shares the highest identity to AtCM1 (Figure 3-3B). Transcript accumulation suggests that AtCM1 possesses a distinct role in the supply of phenylalanine and tyrosine under stressed conditions, while AtCM3 activity can

produce requisite levels of prephenic acid under non-stressed growing conditions (Eberhard et al., 1996b; Mobley et al., 1999). PhCM2 is likely to be located in the cytosol due to the lack of a signal peptide (Figure 3-3A), inability to be imported into a chloroplast (Figure 3-4), and the lack of allosteric amino acid regulation (Figures 3-3A and 3-8) similar to the cytosolic isoforms in Arabidopsis, tomato, and poppy (AtCM2, LeCM1, and CM2 from poppy) [Benesova and Bode, 1992; Eberhard et al., 1996a; and Eberhard et al., 1996b]. Recently, a subcellular localization study in Arabidopsis leaf tissue with all six arogenate dehydratases and two arogenate dehydrogenases showed these proteins, which are responsible for the ultimate production of phenylalanine and tyrosine (respectively), are plastidic proteins. Furthermore, pathway intermediates are confined to the plastid (Rippert et al., 2009). This indicates cytosolic isoforms of CM are separated from substrate and other pathway proteins under normal growing conditions. Therefore, PhCM2 most likely does not have a major role in the production of prephenic acid during non-stressed growing conditions, as proposed for AtCM3. We searched extensively for additional *CM* sequences in petunia, but did not isolate a potential *PhCM3*. That said, two lines of evidence support the existence of other plastidic CM family members in non floral tissues of petunia and at the same time illustrate the biological specificity of *PhCM1*. (1) The CM1R RNAi transgenic plants are not observably impaired in vegetative growth compared to MD plants (Figures 3-14 and 3-15), but show a specific FVBP phenotype (Figures 3-11). (2) Relative transcript accumulation for *PhCM1* is extremely low in all tissues examined except the corolla (Figures 3-5A and 3-6A). However, production of the aromatic amino acids phenylalanine and tyrosine are essential for cellular processes throughout the plant.

The *PhCM1* transcript accumulation profile is congruent with several other known FVBP genes in petunia. High levels of transcripts are detected in corollas from anthesis to senescence,

and are reduced by ethylene exposure, which mimics the pollination event (Figure 3-5 and 3-6). *PhCM2* transcript accumulation follows a more constitutive profile with a noticeable exception in senescing floral tissue of MD (stage 11) where transcript accumulates to relatively high levels (Figures 3-5B and 3-6B). However, *PhCM2* transcript accumulation does not appear to be affected by exogenous ethylene exposure (Figures 3-5C and 3-6C). This result implies that an increase in *PhCM2* transcript abundance during senescence is not a direct effect of ethylene perceived at that developmental stage, and may provide a favorable situation to examine the biological function of cytosolic CM isoforms *in planta*.

Since FVBP emission is rhythmic, transcript accumulation from FVBP biosynthetic genes are rhythmic, and intermediate substrate pools in the FVBP pathway oscillate from low to high in the evening (Underwood et al., 2005; Verdonk et al., 2005; Orlova et al., 2006), it is reasonable to hypothesize enzyme activity of one or more proteins in the FVBP pathway oscillate on a daily cycle. However, like PhBSMT activity (Kolosova et al., 2001) total CM activity is not significantly changed from morning to night in desalted crude extracts (Figure 3-7). Recombinant PhCM1 activity is increased in the presence of tryptophan (Figure 3-8), and so oscillations in the free tryptophan pool *in vivo* cannot be discounted as a regulatory mechanism affecting rhythmic FVBP emission.

AtCM1 and AtCM3 activities are allosterically down-regulated by phenylalanine and tyrosine (Eberhard et al., 1996b; Mobley et al., 1999), but recombinant PhCM1 is unaffected by these aromatic amino acids (Figure 3-8). Petunia corolla limb tissue accumulates a large free phenylalanine pool in the evening with a calculated concentration of 5.5 mM (Kaminaga et al., 2006). Therefore, PhCM1 is sufficient to direct the flux of chorismic acid to the production of phenylalanine without feedback inhibition in the petunia flower. However, it must be noted that

the phenylalanine concentration reported in petunia flowers is a whole tissue measurement, and compartmentalization of the free phenylalanine pool and PhCM1 at a subcellular level remains a plausible mechanism allowing for the large phenylalanine pool. That said, *Arabidopsis thaliana* tissues may not have a biological need for such a large phenylalanine pool, and it would be of interest to assay allosteric regulation of CMs from *Arabidopsis lyrata* ssp. *Petraea*, an outcrossing perennial, which emits relatively high levels of benzaldehyde and phenylacetaldehyde from floral tissues (Abel et al., 2009).

RNAi mediated gene silencing produced transgenic petunia plants (CM1R) reduced in *PhCM1* transcript, but not *PhCM2* (Figure 3-10 and 3-13A), and total CM enzyme activity (Figure 3-13B) with a concomitant reduction of FVBP emission (Figure 3-11). Therefore, PhCM1 has a central role in the production of FVBPs in a petunia flower. Interestingly, total FVPB emission is reduced in CM1R lines to about 40 % compared to MD and recombinant PhCM1 activity is increased over two fold in the presence of tryptophan (Figure 3-8). Therefore it is plausible the 20 % total CM activity would be increased *in vivo* by a presumably higher level of tryptophan in the flowers of the RNAi lines.

Metabolic analysis of the *PhCM1* RNAi lines (Figure 3-11) may illustrate the "demand" for substrate at each branch of the FVBP pathway. FVBPs derived directly from phenylalanine are the most affected by limiting substrate conditions, while the benzenoids formed from *trans*-cinnamic acid are affected significantly but to a lesser extent (Figure 3-11). In contrast, the phenylpropanoids derived from coniferyl acetate are the FVBPs least affected in the CM1R lines. However, too many variables may exist in the regulation at each branch point of the pathway, and therefore we can only speculate. *PhCM1* RNAi lines in conjugation with metabolite labeling experiments may aid in delineating the flux through the FVBP pathway in the future.

Experimental Procedures

Plant Materials

Inbred *Petunia x hybrida* cv 'Mitchell Diploid' (MD) plants were utilized as a 'wild-type' control in all experiments. The ethylene-insensitive *CaMV* 35S:*etr1-1* line 44568, generated in the MD genetic background (Wilkinson et al., 1997), was utilized as a negative control for ethylene sensitivity where applicable. MD, 44568, and *PhCM1* RNAi plants were grown as previously described (Dexter et al., 2007). Ethylene treatments used two μL L^{-1} of ethylene with air treatments for controls.

cDNA Isolation

Partial sequences from the SGN (http://www.sgn.cornell.edu) petunia EST database (Unigene: SGN-U208050) and from a petunia root EST collection (EST ID: dr001P0018N07_F.ab1), courtesy of Didier Reinhardt at the University of Fribourg, were used as references to obtain full-length cDNAs by 5' and 3' race with the SMART™ RACE cDNA Amplification Kit (Clontech Laboratories, Inc., Mountain View, CA) as per manufacturer's protocol. A resulting 1257 bp cDNA had a 975 bp coding sequence (GenBank accession number: EU751616) for a predicted 324 amino acid protein and was termed *PhCM1*, while another 913 bp cDNA had a 792 bp coding sequence (EU751617) for a predicted 263 amino acid protein termed *PhCM2*. Both *PhCM1* and *PhCM2* coding sequences were amplified by Phusion™ Hot Start High-Fidelity DNA Polymerase (New England Biolabs, Inc., Ipswich, MA) and were cloned into a pGEM®T-EASY vector (Promega Corp., Madison, WI), which were extensively sequenced and checked for errors. These constructs were used as template to clone the predicted mature *PhCM1* and *PhCM2* coding sequences into a pET-32 EK/LIC vector (Novagen, Gibbstown, NJ).

Transcript accumulation analysis

All experiments were conducted with at least two biological replicates with equivalent results observed. In all cases, total RNA was extracted as previously described (Verdonk et al., 2003) and subjected to TURBO™ DNase treatment (Ambion Inc., Austin, TX) followed by total RNA purification with RNeasy® Mini protocol for RNA cleanup (Qiagen, Valencia, CA). Total RNA was then quantified on a NanoDrop™ 1000 spectrophotometer (Thermo Scientific, Wilmington, DE) and 50 ng/µl dilutions were prepared and stored at -20^{o}C.

Semi-quantitative (sq)RT-PCR was performed on a Veriti™ 96-well thermal cycler (Applied Biosystems, Foster City, CA). All sqRT-PCR reactions used a Qiagen One-step RT-PCR kit with 50 ng total RNA template. To visualize RNA loading concentrations, samples were amplified with *Ph18S* primers and analyzed on an agarose gel. Gene specific primers were designed and utilized for the visualization of the relative transcript accumulation levels (Table 3-2).

The spatial transcript accumulation series consisted of total RNA isolated from root, stem stigma, anther, leaf, petal tube, petal limb, and sepal tissues of three individual MD plants at 16:00 h on multiple occasions over the course of a year. The developmental transcript accumulation series consisted of MD floral tissue collected at eleven different stages; floral bud < 0.5 cm (stage 1), bud 0.5 < 1.5 cm (2), bud 1.5 < 3.0 cm (3), bud 3.0 < 5.0 cm (4), bud fully elongated 5.0 < 6.5 cm (5), flower opening 0 < 2 cm limb diameter (anthesis) [6], flower fully open day 0 (7), day 1 (8), day 2 (9), day 3 (10), and observably senescing flower (flower open day 7 for MD), stage 11. All tissues were collected at 16:00 h on the same day, and total RNA was isolated from all samples collected. The developmental tissue collections were conducted multiple times over the course of a year. The exogenous ethylene series consisted of excised MD and 44568 stage 9 flowers (placed in tap water) placed into eight tanks, four for ethylene

treatments and four for air treatments. Air and ethylene treatments were conducted for 0, 1, 2, 4, and 8 hours starting at 12:00 h. Immediately following treatment, each of the flower samples were collected, stored at -80^{o}C, and total RNA was isolated from all corolla tissues once all samples had been collected. The ethylene treatment experiment consisted of two biological replicates and was conducted twice. For all tissue collections individual samples consisted of three flowers.

Quantitative (q)RT-PCR was performed and analyzed on a MyIQ real-time PCR detection system (Bio-Rad Laboratories Inc., Hercules, CA). Stage 9, whole corolla tissue was collected from MD and two independent homozygous T_2 *PhCM1* RNAi lines at 16:00 h. Total RNA was isolated from all samples as described earlier and transcript accumulation was initially analyzed by sqRT-PCR. For subsequent qRT-PCR analysis the Power SYBR® Green RNA-to-C_t™ 1-Step Kit (Applied Biosystems, Foster City, CA) was used to amplify and detect resulting products following the manufacturer's protocol. qRT-PCR primers (Table S2) were constructed with Primer Express® software v2.0 (Applied Biosystems, Foster City, CA), demonstrated gene specificity during melt curve analysis, and then optimized.

Protein Extraction, Overproduction, and Purification

Desalted crude protein extracts were obtained from whole corolla tissue by grinding in a mortar and pestle with liquid Nitrogen until a fine powder, addition of chilled extraction buffer (50 mM Bis Tris HCl pH 6.9, 10 mM B-mercaptoethanol, 5 mM $Na_2S_2O_5$, 1 % PVP, 1:100 protease inhibitor cocktail [Sigma, P9599], and 10 % glycerol), centrifugation at 4^{o}C (Beckman Coulter™, Avanti™ J-25) to separate cellular debris, and further separation of low molecular weight substances with a PD-10 desalting column (GE Healthcare, Piscataway, NJ). Total crude protein concentration was determined by the Bradford method using BSA as a standard (Rio-Rad).

Biologically active pET-32-*PhCM1* and pET-32-*PhCM2* were expressed in *E. coli* BL21(DE3)/pLysS with an induction of 1 mM IPTG overnight at 37^{o}C. Induction was analyzed from crude cellular extracts on a 10 % polyacrylamide, Tris-HCl Ready Gel (Bio-Rad). Soluble protein was obtained from induced cells lysed with BugBuster® protein extract reagent and affinity purified with His-Band® resin chromatography (Novagen). The resulting recombinant proteins were then separated from any low molecular weight compounds and concentrated with 30,000 NMWL Amicon® Ultra-4 centrifugal filter devices (Millipore, Billerica, MA). Recombinant protein concentration was determined by the Bradford method using BSA as a standard.

CHORISMATE MUTASE Enzyme Activity Assays

Specific activities *in vitro* were resolved by carefully following the absorbance of chorismic acid spectrophotometrically (Bio-Rad, SmartSpec™ 3000) at 274 nm ($\varepsilon = 2630\ M^{-1}\ cm^{-1}$) (Gilchrist and Connelly, 1987; Kast et al., 1996). All assays were conducted at 30^{o}C with 0.5 mM chorismic acid (> 90 %, Sigma, C1761) in 50 mM KPO_4 buffer, pH 7.6. Where stated, 50 µM phenylalanine, tyrosine, and tryptophan (Sigma: P2126, T3754, and T0254; respectively) were used to assay for allosteric regulation of enzyme activity. Non-enzymatic chorismic acid breakdown along with inactive protein controls were used to normalize all data generated. Additionally, no activity was detected when purified tag fusion proteins from the empty pET-32 vector were used. Multiple biological replicates and corresponding technical replicates were used to generate all data shown.

Chloroplast Import Assay

Full-length coding sequences for *PhCM1* and *PhCM2* were cloned into a pGEM®-T Easy (Promega, Madison, WI) vector in the SP6 orientation. The chloroplast import assay was conducted as described previously (Martin et al., 2009). Briefly, *in vitro* transcription and

translation with wheat germ TNT (Promega, Madison, WI) resulted in radiolabeled PhCM1, PhCM2, and PsOE23, which were individually incubated with isolated pea chloroplasts for 15 min. After import, the isolated chloroplasts were treated with 100 µg ml^{-1} thermolysin for 40 min at 4^{o}C as depicted in the figure. Proteolysis was terminated by the addition of EDTA to a final concentration of 10 mM, and the intact chloroplasts were then repurified by centrifugation through 35 % Percoll. Chloroplasts were washed, lysed, and fractionated into total membranes and stromal extracts by centrifugation for 18 min at 15,000 x g. The translation products, chloroplasts, thermolysin treated chloroplasts, stromal extracts, and total membranes were analyzed with SDS-PAGE and fluorography. In figure 3-4, PhCM2 and PsOE23 are from a 20 hour exposure. PhCM1 is from a 4 day exposure. These are from two different gels of the same samples loaded the same. The panels have been cropped and contrast adjusted, but no other modifications.

Volatile Emission

For all volatile emission experiments, emitted floral volatiles from excised flowers were collected at 17:00 h and quantified as previously described (Underwood et al., 2005; Dexter et al., 2007).

Generation of *PhCM1* RNAi Transgenic Petunia

The generation of *PhCM1* RNAi transgenic plants was as describe earlier (Dexter et al., 2007), but with two fragments of the *PhCM1* cDNA (Figure S3) amplified and ligated end to end in a sense/antisense orientation with additional sequence information used for an inter-fragment intron (hairpin).

Acknowledgements

This work was supported by grants from the USDA Nursery and Floral Crops Initiative (grant #: 00058029), the Fred C. Gloeckner Foundation (grant #: 00070429), Florida Agricultural

Experiment Station (grant #: 00079097), and in part by National Institutes of Health (grant #: R01 GM46951 to KC). The authors wish to thank Dr. Harry Klee (Horticultural Sciences Department, University of Florida) for critically reviewing the manuscript and Dr. Peter Kast (Swiss Federal Institute of Technology Zurich, Switzerland) for providing the CM-deficient *E. coli* transformant KA12/pKIMP-UAUC.

Table 3-1. Functional complementation of CM-deficient *E. coli* KA12/pKIMP-UAUC. M9c minimal media was used for all experiments and supplemented with 20 µg/ml of L-phenylalanine and L-tyrosine where stated. Antibiotics used were chloramphenicol [Ch] (30 µg/ml) for selection of the pKIMP plasmid and carbenicillin [Ca] (100 µg/ml) for selection of the pET-32 plasmid. KA12/pKIMP-UAUC is not a λDE3 lysogenic *E. coli*, so bacteriophage CE6 (Novagen, cat# 69390) infection was used to induce transcription from the pET-32 T7 promoter where stated and no CE6 administered (NA) where stated. Transformants were incubated at 37^{o}C for two days, and growth was scored as a plus (+) or minus (-). A sample of positive colonies was picked and colony PCR was performed for confirmation of pET-32-*CM1* or pET-32-*CM2* plasmids.

Bacteria/Plasmid	Media	Antibiotic	Treatment	Growth
KA12/pKIMP-UAUC	M9c/Phenylalanine, Tyrosine	Ch	NA	+
KA12/pKIMP-UAUC	M9c	Ch	NA	-
KA12/pKIMP-UAUC	M9c/Phenylalanine, Tyrosine	Ch	CE6	+
KA12/pKIMP-UAUC	M9c	Ch	CE6	-
KA12/pKIMP-UAUC	M9c/Phenylalanine, Tyrosine	Ch/Ca	NA	-
KA12/pKIMP-UAUC	M9c	Ch/Ca	NA	-
KA12/pKIMP-UAUC	M9c/Phenylalanine, Tyrosine	Ch/Ca	CE6	-
KA12/pKIMP-UAUC	M9c	Ch/Ca	CE6	-
KA12/pKIMP-UAUC/pET-32-CM1	M9c/Phenylalanine, Tyrosine	Ch/Ca	NA	+
KA12/pKIMP-UAUC/pET-32-CM1	M9c	Ch/Ca	NA	-
KA12/pKIMP-UAUC/pET-32-CM1	M9c/Phenylalanine, Tyrosine	Ch/Ca	CE6	+
KA12/pKIMP-UAUC/pET-32-CM1	M9c	Ch/Ca	CE6	+
KA12/pKIMP-UAUC/pET-32-CM2	M9c/Phenylalanine, Tyrosine	Ch/Ca	NA	+
KA12/pKIMP-UAUC/pET-32-CM2	M9c	Ch/Ca	NA	-
KA12/pKIMP-UAUC/pET-32-CM2	M9c/Phenylalanine, Tyrosine	Ch/Ca	CE6	+
KA12/pKIMP-UAUC/pET-32-CM2	M9c	Ch/Ca	CE6	+

Table 3-2. Gene specific primers used for the transcript accumulation analyses throughout this study.

Reference Number	Target	Direction	Primer Sequence (5'→3')
sqRT-PCR			
AJ236020	*Ph18S*	Forward	TTAGCAGGCTGAGGTCTCGT
		Reverse	AGCGGATGTTGCTTTTAGGA
AY233465	*PhBSMT1*	Forward	AGAAGGAAGGATCATTCACCA
		Reverse	TATTCGGGTTTTTCGACCAC
EU751616	*PhCM1*	Forward	GCCATTGACAAAGGAAGTTCA
		Reverse	TGTTCCAAACTTGAAAATTACATCA
EU751617	*PhCM2*	Forward	CCATCTTCTTGGTTTCCTGA
		Reverse	TCACAGGCAGCAGTAGTTGC
M21084	*PhEPSPS*	Forward	CGATGATCACAGGATGGCCATGG
		Reverse	CCCATTGTGGTTCTGATACCAG
DQ372813	*PhIGS1*	Forward	GCCTATGTCATGCCATTGAA
		Reverse	TGCTTTAATTGTGTAGGCTGC
AY705977	*PhODO1*	Forward	TTCAATTGGCTTTCGGGTTA
		Reverse	AGGCACCTTGGACTCTTCG
DQ243784	*PhPAAS*	Forward	TCCTTGTAGTTCTAGTACTGCTGGAA
		Reverse	TCAACAGCAGTTGTTGAAGTAGTTC
AY705976	*PhPAL1*	Forward	GCTATGAATGAAGGAAAGTTGG
		Reverse	CACAATCTTTCATACAAACCC
CO805160	*PhPAL2*	Forward	CCGAGCTGTTGACAGGAGAAGG
		Reverse	TAACCAGACTACTAAAGTTCAGC
SGN-U207570	*PhPD1*	Forward	ACATCGCAGCCAATAACCTT
		Reverse	CCCACATTTGCATCATCAAC
qRT-PCR			
AJ236020	*Ph18S*	Forward	TGCAACAAACCCCGACTTCT
		Reverse	AGCCCGCGTCAACCTTTTAT
EU751616	*PhCM1*	Forward	CCCTGATGAGCACCCATTC
		Reverse	ACTGCATGGGTGGCAACAC
EU751617	*PhCM2*	Forward	AACTTGCCTGCCTCAATCGT
		Reverse	GGATGCAAAACTGGTGGACAT
M91190	PhFBP1	Forward	TGCGCCAACTTGAGATAGCA
		Reverse	TGCTGAAACACTTCGCCAATT

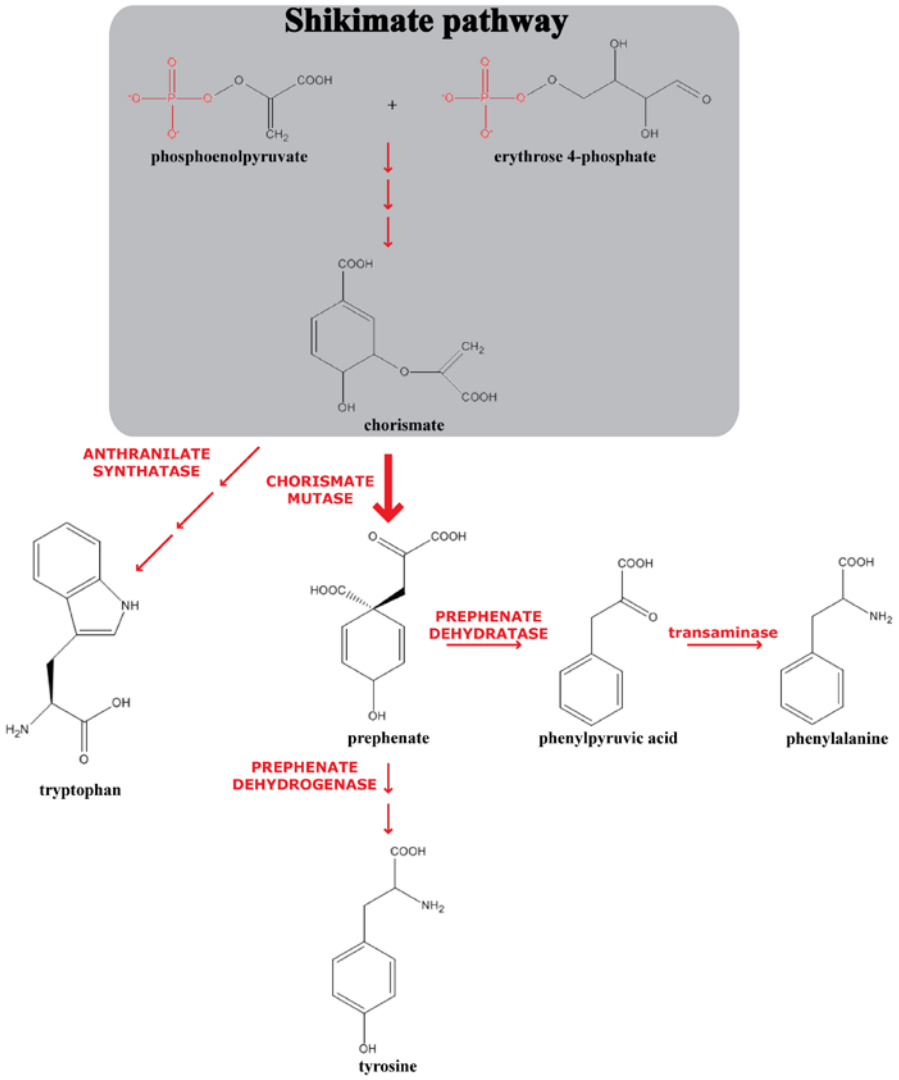

Figure 3-1. Aromatic amino acid biosynthesis pathway. CHORISMATE MUTASE directs the flux of metabolites from the shikimate pathway into the phenylpropanoid pathway by catalyzing a [3,3]-sigmatropic rearrangement of chorismate to prephenate. Phenylalanine is thought to be the precursor for the majority of the volatile benzenoids/phenylpropanoids emitted by a petunia flower.

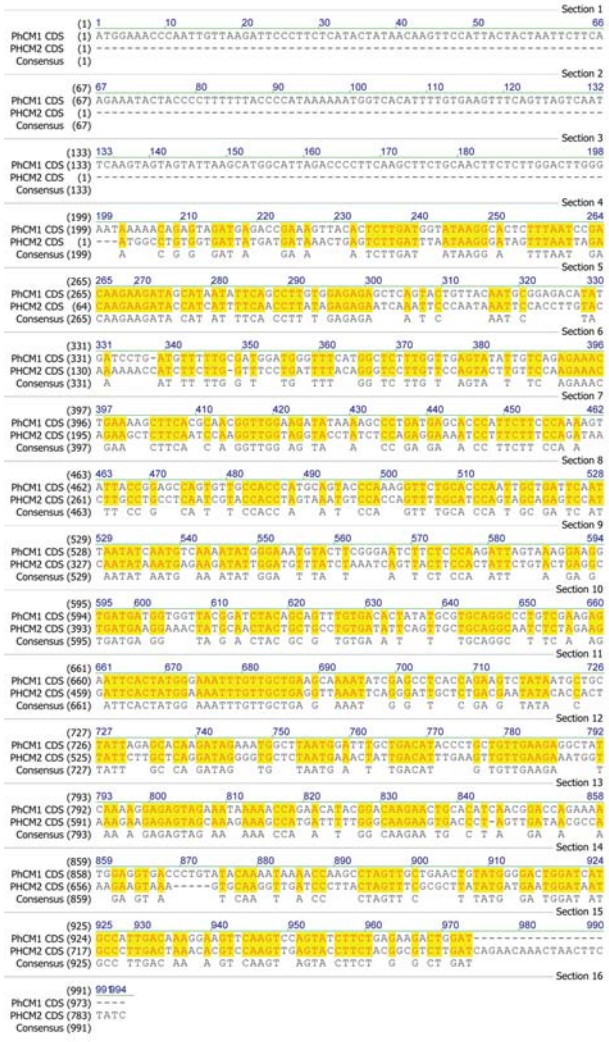

Figure 3-2. *PhCM1* and *PhCM2* CDS alignment using the Align X program in Vector NTI advance 10.3.0 software package (Invitrogen; Carlsbad, CA). *PhCM1* and *PhCM2* share 46.1 % identity at the nucleotide level.

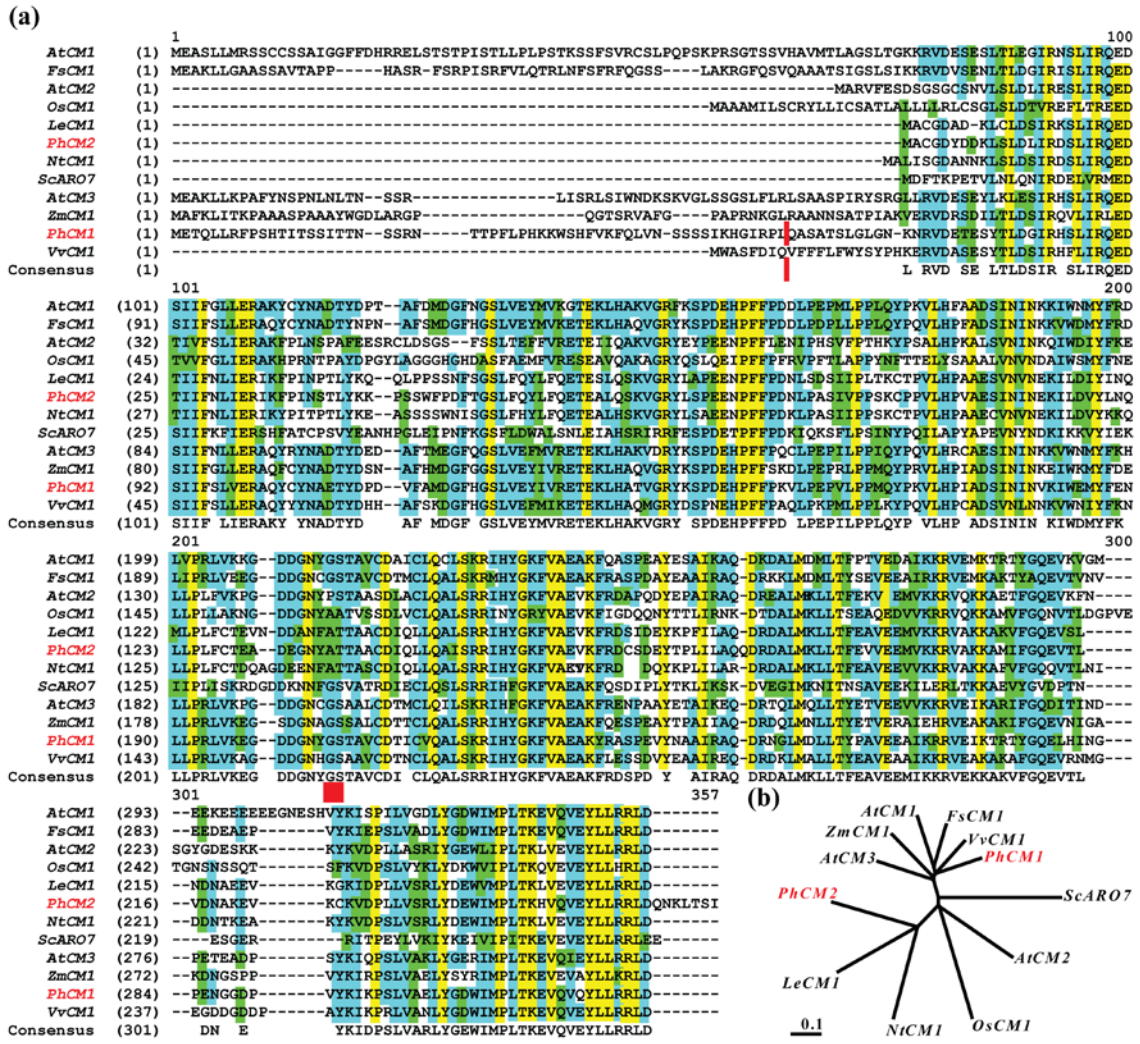

Figure 3-3. Predicted peptide sequence alignment and an unrooted neighbor-joining phylogenetic tree of CM proteins from various species. Sequences represented are from Arabidopsis thaliana (accession: NP_566846, NP_196648, and NP_177096), Fagus sylvatica (ABA54871), Solanum lycopersicum (AAD48923), Nicotiana tabacum (BAD26595), Oryza sativa (NP_001061910), Petunia x hybrida (EU751616, EU751617), Vitis vinifera (CAO15322), Zea mays (AY103806), and Saccharomyces cerevisiae (NP_015385). (a) Sequences were aligned using the AlignX program of the Vector NTI Advance 10.3.0 software (Invitrogen). Residues highlighted in: blue represent consensus residues derived from a block of similar residues at a given position, green represent consensus residues derived from the occurrence of greater than 50 % of a single residue at a given position, and yellow represent consensus residues derived from a completely conserved residue at a given position. Petunia sequences are highlighted in red to the left, a red vertical bar represents the beginning of the mature protein sequence used for PhCM1, and a red box indicates an allosteric regulatory site (GS). (b) TREEVIEW software with the nearest-joining method was used to create the resulting tree. Scale bar represents distance as the number of substitutions per site (i.e., 0.1 amino acid substitutions per site).

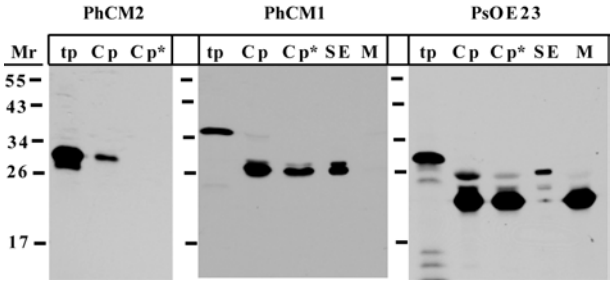

Figure 3-4. Plastid import assay. Radiolabeled PhCM1, PhCM2, and PsOE23 were individually incubated with isolated pea chloroplasts. After import, the isolated chloroplasts were treated with thermolysin as depicted in the figure. Proteolysis was terminated and the intact chloroplasts were then repurified, washed, lysed, and fractionated. PsOE23 is a thylakoid lumen protein with a stromal intermediate, which was used as a positive control. The translation products (tp), chloroplasts (Cp), thermolysin treated chloroplasts (Cp*), stromal extracts (SE), and total membranes (M) were analyzed with SDS-PAGE and fluorography. Positions of the molecular weight marker are depicted on the left.

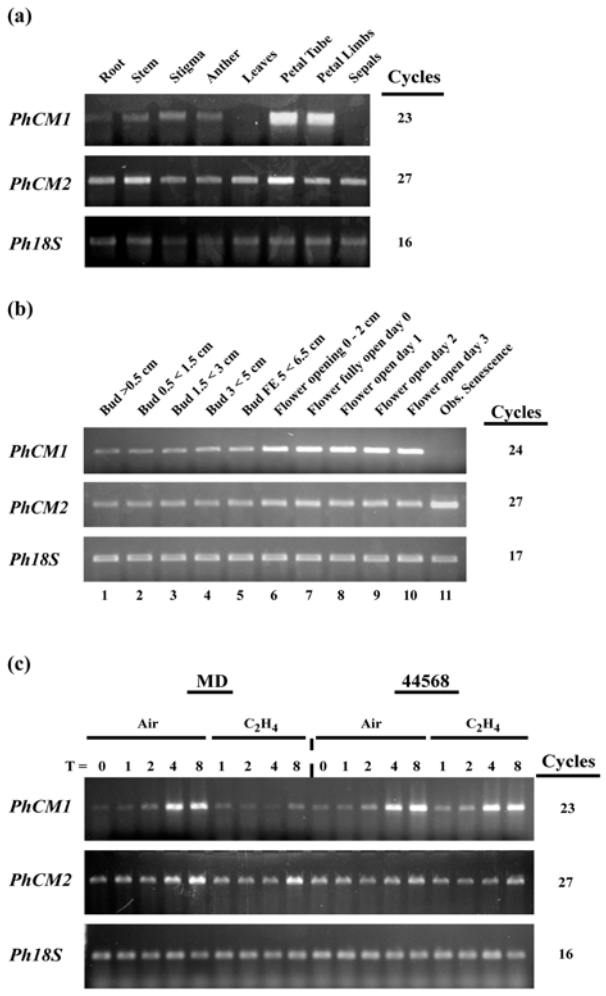

Figure 3-5. sqRT-PCR transcript accumulation analysis of *PhCM1* and *PhCM2* in petunia. Spatial analysis used root, stem, stigma, anther, leaf, petal tube, petal limb, and sepal tissues of MD harvested at 16:00 h (A). Floral developmental analysis used MD flowers from 11 sequential stages at 16:00 h (B). Ethylene treatment (two µL L^{-1}) analysis used excised MD and 44568 whole flowers treated for 0, 1, 2, 4, and 8 hours (C).The number of cycles used for amplification of each transcript is shown on the right. *Ph18S* was used as a loading control in all cases.

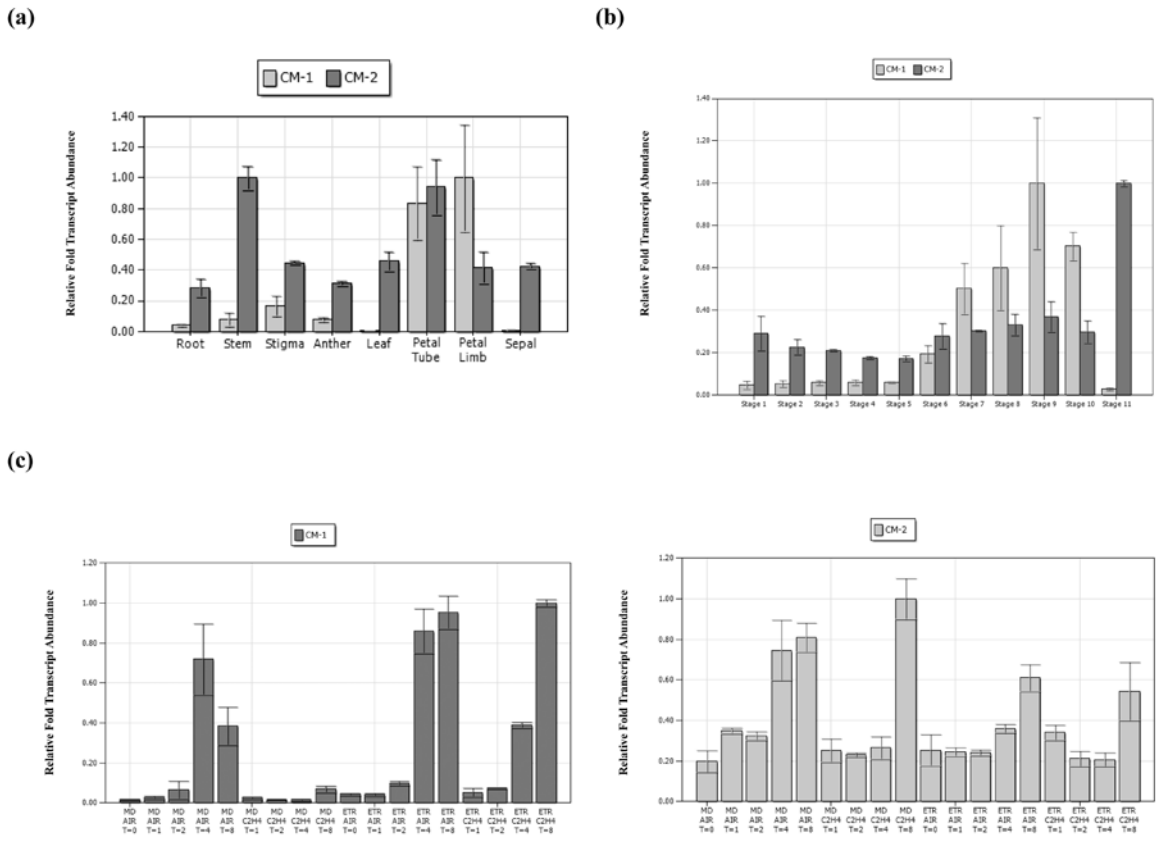

Figure 3-6. qRT-PCR transcript accumulation analysis of *PhCM1* and *PhCM2* in petunia. Spatial analysis used root, stem, stigma, anther, leaf, petal tube, petal limb, and sepal tissues of MD harvested at 16:00 h (A). The spatial experiment consisted of one biological replicate used for sqRT-PCR and one separate biological replicate with two technical replicates per biological replicate. Floral developmental analysis used MD flowers from 11 sequential stages at 16:00 h (B). The developmental analysis consisted of two biological replicates separate from the biological replicates used for the sqRT-PCR with three technical replicates. Ethylene treatment (two µL L^{-1}) analysis used excised MD and 44568 whole flowers treated for 0, 1, 2, 4, and 8 hours (C). The ethylene treated series consisted of one biological replicate used in the sqRT-PCR with two technical replicates per biological replicate. *PhFBP1* and *Ph18S* were used as references throughout these experiments.

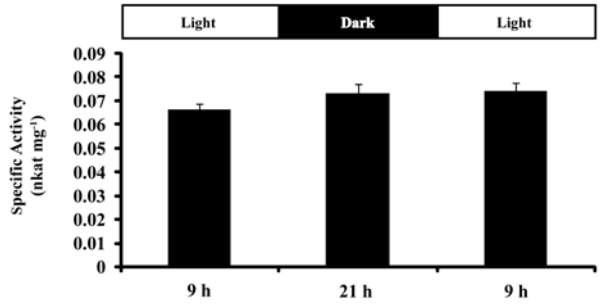

Figure 3-7. Total CM activity in desalted crude protein extracts from MD whole corollas starting at 9 h of stage 9 in flower development. (mean ± se; n = 6)

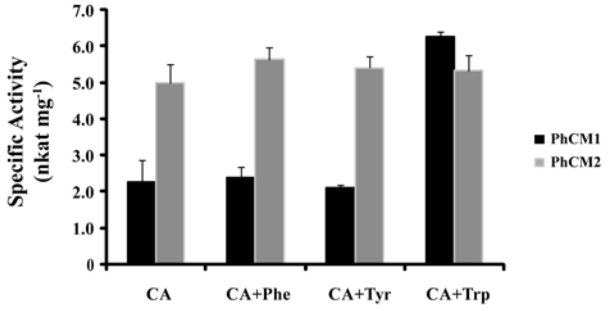

Figure 3-8. Enzyme activity of and effects of aromatic amino acids on petunia CMs. Recombinant protein was assayed for enzymatic activity in 50 mM KPO_4 buffer pH 7.6 with 0.5 mM chorismic acid (CA) as a substrate and 50 µM phenylalanine (Phe), tyrosine (Tyr), and tryptophan (Trp) as allosteric effectors. (mean ± se; n = 4)

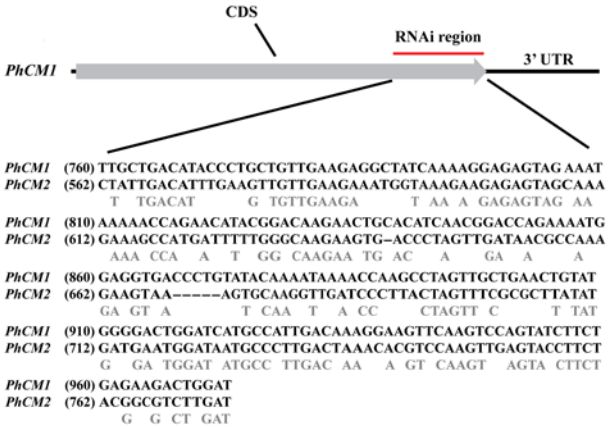

Figure 3-9. Schematic representation and nucleotide comparison of RNAi region used for the production of petunia *PhCM1* RNAi transgenic lines. 213 bases at the 3' end of the coding sequence of *PhCM1* were chosen for the RNAi construct. This region shared 58.2 % identity with the corresponding nucleotide region from *PhCM2*.

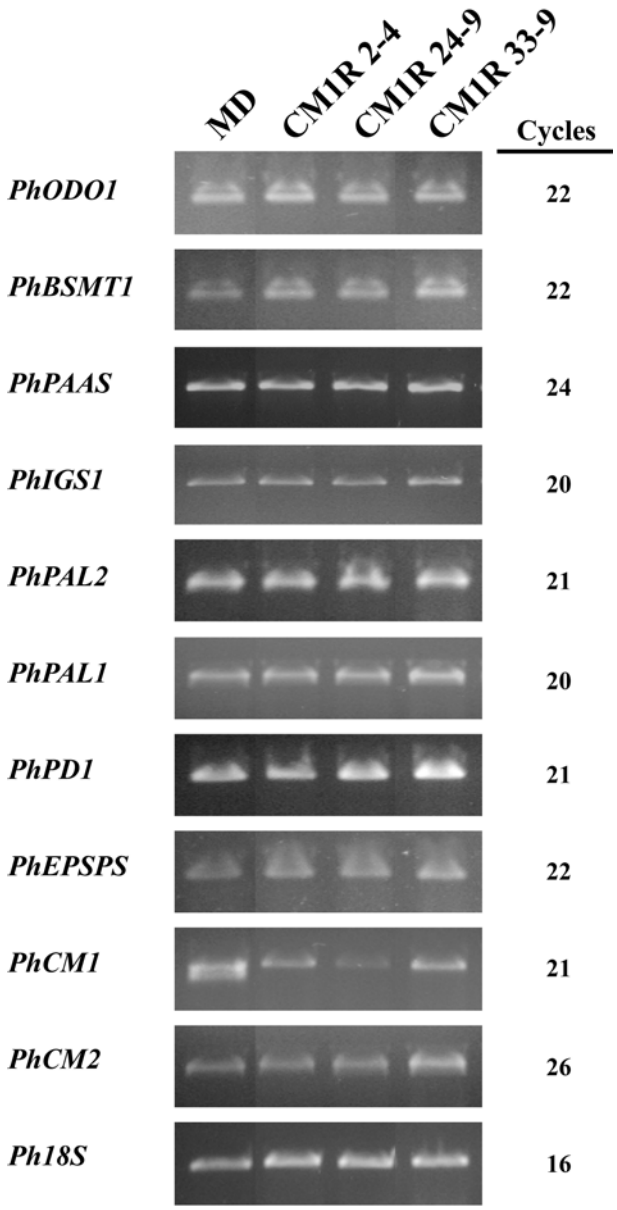

Figure 3-10. sqRT-PCR transcript accumulation analysis in floral tissues of three independent T_1 *PhCM1* RNAi lines. MD, CM1R 2-4, CM1R 24-9, CM1R 33-9 were used with primers specific for floral volatile benzenoid/phenylpropanoid, shikimate, and phenylpropanoid transcripts. The number of cycles used for amplification of each transcript is shown on the right. *Ph18S* was used as a loading control in all cases.

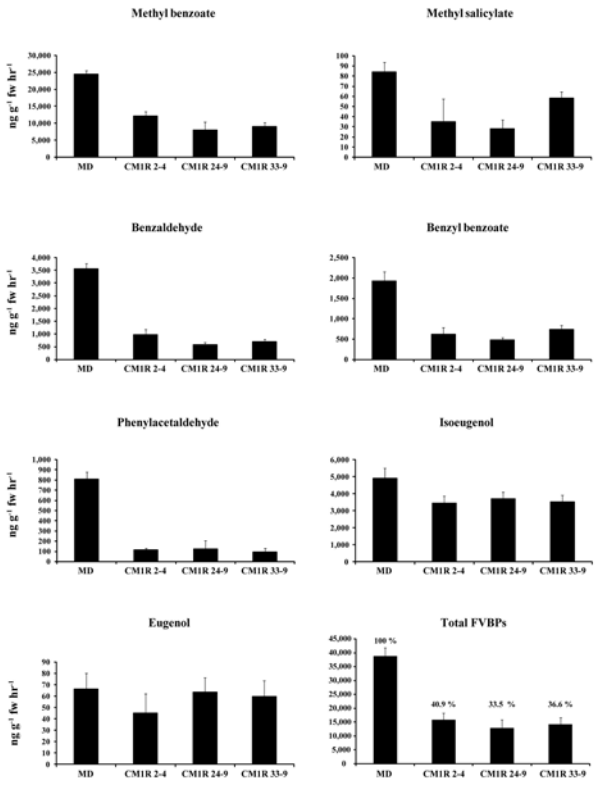

Figure 3-11. Floral volatile emission analysis from three independent T_1 *PhCM1* RNAi lines (mean ± se; n = 3). Major volatile compounds shown from MD, CM1R 2-4, CM1R 24-9, CM1R 33-9 flowers.

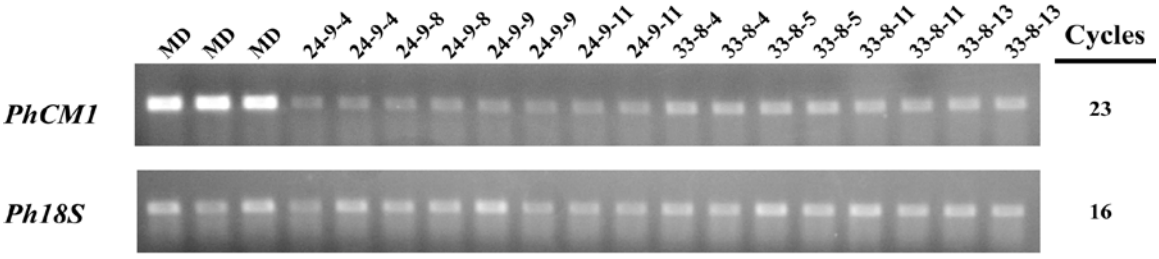

Figure 3-12. sqRT-PCR transcript accumulation analysis in floral tissues of two independent, homozygous T_2 *PhCM1* RNAi lines. Individuals and biological replicates from MD, 24-9, 33-8 were used with primers specific for *PhCM1*. The number of cycles used for amplification of each transcript is shown on the right. *Ph18S* was used as a loading control.

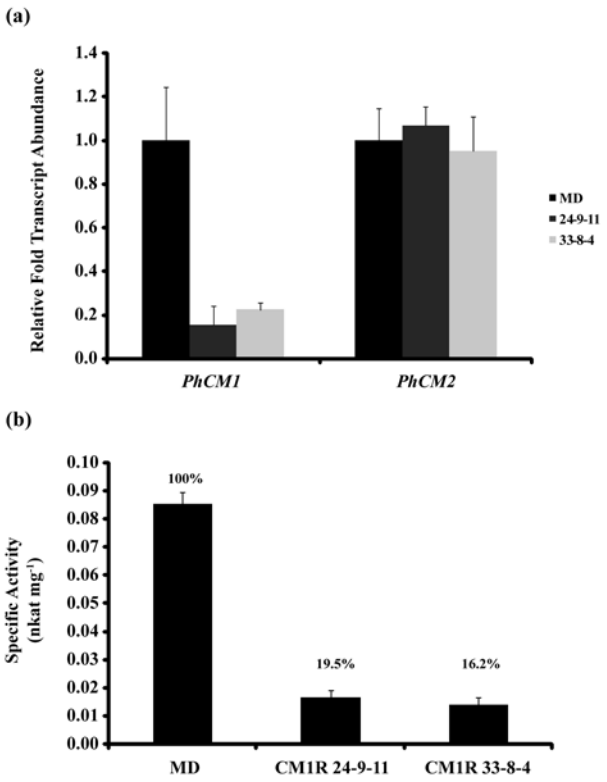

Figure 3-13. Comparative transcript analysis and total CM activity between MD and representative individuals from independent homozygous T_2 *PhCM1* RNAi lines. (A) qRT-PCR was carried out with two biological replicates and three technical replicates per biological replicate. The entire experiment was done in duplicate, and analyzed by ΔΔCt method with *PhFBP1* and *Ph18S* as the internal references. (B) Total CM activity in desalted crude protein extracts from whole corollas of MD and representative individuals from two independent homozygous T_2 *PhCM1* RNAi lines, 24-9 and 33-8.

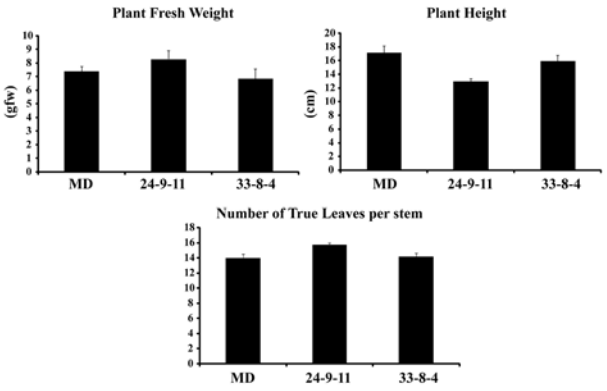

Figure 3-14. Physiological comparison between MD and representative independent T_2 *PhCM1* homozygous RNAi lines 24-9 and 33-8 in 9 week old petunia seedlings (mean ± se; n = 5).

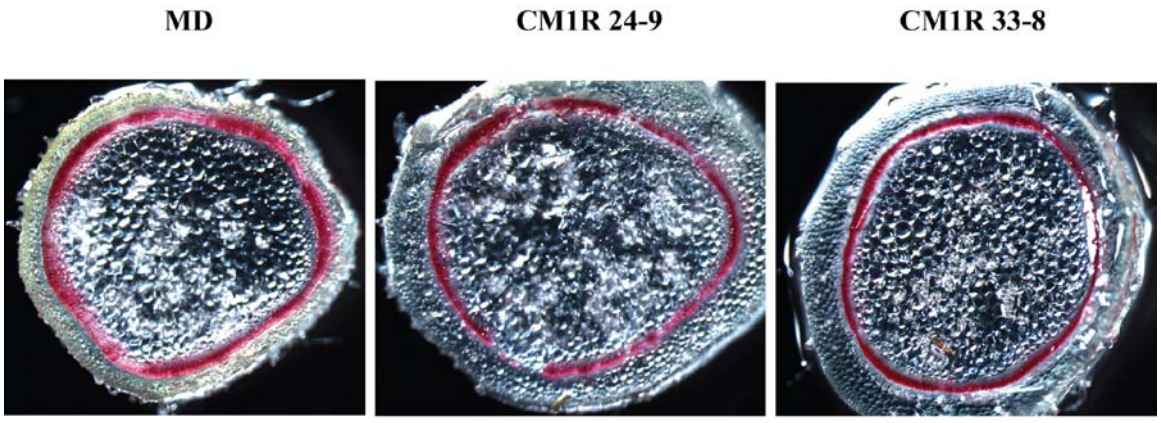

Figure 3-15. Stem cross-sections (between 7-8 node from apical meristem) from 9 week old petunias stained with Phloroglucinol. Shown are MD and representative individuals from two independent *PhCM1* homozygous T_2 RNAi lines, 24-9 and 33-8. Pictures are from light microscopy at 4X on a Leica MZ 16F and are representative of three biological replicates.

CHAPTER 4
PHMYB5D8 EFFECTS PHC4H TRANSCRIPTION IN THE PETUNIA COROLLA

Introduction

Floral fragrance consists of an array of volatile organic compounds. These volatile compounds are generally lipophilic liquids with high vapor pressures and putatively cross biological membranes by passive diffusion in the absence of a barrier (Pichersky et al., 2006). Many angiosperm species produce floral fragrance and each species produces a unique blend of volatile organic compounds, which facilitate environmental interaction (reviewed in Dudareva et al., 2006). The emission of floral volatiles can reach between 30 and 150 $\mu g\ h^{-1}$ for some species (Knudsen and Gershenzon, 2006; personal calculation). Therefore, the complexity and stringency of regulation imparted upon floral volatile production is not surprising.

Petunia x hybrida cv "Mitchell Diploid" (MD) has been used as a model system for floral volatile compound studies for nearly a decade. MD has relatively large, white flowers that produce large amounts of floral volatile compounds. Volatile benzenoid and phenylpropanoid compounds dominate the floral mixture of volatile compounds emitted by the MD flower (Schuurink et al., 2006) [Figure 1-1]. In MD, floral volatile benzenoid/phenylpropanoid (FVBP) production is confined to the corolla limb tissue subsequent to anthesis and until senescence, and high levels of emission peak during the dark period (Kolosova et al., 2001a; Verdonk et al., 2003; Underwood et al., 2005; Verdonk et al., 2005). Additionally, FVBP production and emission is severely reduced after a successful pollination and fertilization event or 10 h of exogenous ethylene exposure in petunia (Figures 2-6 and 2-8; Negre et al., 2003; Underwood et al., 2005; Dexter et al., 2007; Dexter et al., 2008).

In petunia, FVBPs are all putatively derived from the aromatic amino acid phenylalanine (Boatright et al., 2004) and the production of individual FVBP compounds stems from the

phenylpropanoid pathway at phenylalanine, *trans*-cinnamic acid, and ferulic acid (Figure 1-1). Numerous proteins must be involved in the production of FVBPs from the shikimate pathway to the end biochemical steps resulting in the direct formation of volatile compounds. To date, nine genes have been identified to encode proteins associated with the production of FVBPs in petunia: *PhBSMT1*, *PhBSMT2*, *PhBPBT*, *PhPAAS*, *PhIGS1*, *PhEGS1*, *PhCFAT*, *PhCM1*, and *PhODO1* (Negre et al., 2003; Boatright et al., 2004; Underwood et al., 2005; Verdonk et al., 2005; Kaminaga et al., 2006; Koeduka et al., 2006; Orlova et al., 2006; Dexter et al., 2007; Dexter et al., 2008; Koeduka et al., 2008; Chapter 3) [Figure 1-1]. The first six petunia genes listed are involved in the direct formation of FVBP compound, while *PhCFAT* and *PhCM1* are associated with the production of intermediate metabolites. *PhODO1* is an R2R3-MYB transcriptional regulator that is involved in the transcriptional control of shikimate and phenylpropanoid pathway genes, hence metabolite production.

All the FVBP genes are coordinately, transcriptionally regulated concomitant to FVBP emission (Chapters 2 and 3). That is, high levels of transcript accumulation from the FVBP genes is confined to the corolla limb, after anthesis and to senescence, each transcript has a peak accumulation through a daily cycle, and transcript accumulation is greatly reduced after a successful pollination/fertilization event or exposure to ethylene. The regulation of FVBP gene transcription is tightly controlled as appears to be a direct relationship with FVBP emission in a spatial, developmental, and hormone interaction context (Verdonk et al., 2003, Underwood et al., 2005; Verdonk et al., 2005; Chapter 2).

Since all the identified petunia genes involved in FVBP production display similar transcript accumulation profiles, we hypothesized that at least a subset of genes involved in the regulation of FVBP gene transcript accumulation would share similar transcript accumulation

profiles. Additionally, because a single R2R3-MYB transcriptional regulator has been previous identified as a FVBP metabolite regulator, and multiple R2R3-MYBs have been shown to function in a single pathway; we hypothesized that multiple R2R3-MYB transcriptional regulators are responsible for the overall level of regulation imparted upon the FVBP pathway. Therefore, we examined multiple sequences homologous to R2R3-MYBs through a transcript accumulation screen, which produced a candidate with a similar transcript accumulation profile as the FVBP genes, *PhMYB5d8*. A reverse genetic approach to test gene function generated transgenic petunia plants with elevated levels of isoeugenol and eugenol emission. The following results indicate multiple transcriptional regulators are responsible for the precise production and subsequent emission of FVBP in petunia.

Results

Identification of *PhMYB5d8*

We were interested in the regulation of the FVBP gene network; therefore, we searched a publicly available petunia EST database (http://www.sgn.cornell.edu) for sequences with high similarity to the conserved R2R3 domain of Arabidopsis R2R3-MYB proteins. This search produced multiple results, but one Unigene sequence was chosen for further investigation, SGN-U208628. Through a long standing collaboration with Dr. Robert Schuurink (University of Amsterdam), the full-length CDS sequence was obtained with the named *PhMYB5d8*. The predicted PhMYB5d8 amino acid sequence was 257 amino acids in length and predicted to be nuclear localized (WoLFPSORT). When aligned with highly similar amino acid sequences from varying species (Figure 4-1) three main features were observed: an N-terminal R2R3 domain, C1-motif (LLSRGIDPTTHXI), and a MYB subgroup 4 EAR-domain (PDLNLELKISPP). Phylogenetic analysis demonstrated that the two solanaceous MYB proteins (LeTH27 and PhMYB5d8) closely associate in an unrooted neighbor-joining tree (Figure 4-2). PhMYB5d8

shares 66.1 and 55.9 % identity with LeTH27 and AtMYB4, respectively. Of these two potential orthologs, AtMYB4 is best characterized in the literature with a supported function as a transcriptional repressor of *CINNAMATE-4-HYDROXYLASE* (*C4H*) [Jin et al., 2000].

PhMYB5d8 **transcript abundance analysis**

Four criteria of transcript accumulation spatial, flower development, daily time-course, and ethylene treated were chosen for analysis by semi-quantitative reverse transcriptase polymerase chain reaction (sqRT-PCR) [Figure 4-3]. The spatial analysis consisted of root, stem, stigma, anther, leaf, petal tube, petal limb, and sepal tissues (Figure 4-3A). *PhMYB5d8* transcripts were detected at relatively high levels in the petal limb, petal tube, anthers, stigma, and to a lesser extent in stem tissue. The MD and 44568 flower developmental series consisted of whole flowers collected at 11 consecutive stages beginning from a small bud to floral senescence (pictured in Figure 2-2). *PhMYB5d8* transcripts were detected at relatively low levels throughout the closed bud stages of development in both genetic backgrounds (Figure 4-3B). Relatively high levels of *PhMYB5d8* transcripts were detected at anthesis (stage 6) and throughout all open flower stages of development examined in both MD and 44568 (stage 7-10). *PhMYB5d8* transcripts were detected at the lowest level in observably senescing MD flower tissue (stage 11). In contrast, *PhMYB5d8* transcripts were detected at relatively high levels in observably senescing 44568 floral tissue, suggesting ethylene sensitivity is required to reduce transcript levels as observed in MD tissue at the same stage (Figure 4-3B). The daily time-course analysis used MD plants acclimated in a growth chamber with a long day photoperiod and samples collected every three hours for a total of 36 hours (Figure 4-3C). *PhMYB5d8* transcripts were detected at relatively high levels between 15:00 and 24:00 h, which is similar to *PhODO1* transcript accumulation pattern throughout a daily time-course analysis (Figure 2-9; Verdonk et al., 2005). The ethylene study used excised whole flowers from MD and an ethylene-insensitive

(*CaMV* 35S::*etr1-1*) transgenic petunia line, 44568 (Wilkinson et al., 1997). All flowers were treated with air or ethylene (2 μL L^{-1}) for 0, 1, 2, 4, and 8 hours beginning at 12:00 h with an experimental end time of 20:00 h (Figure 4-3D). *PhMYB5d8* transcripts were reduced in MD flowers after eight hours of ethylene treatment compared to air treatments, while no change in *PhMYB5d8* transcript level was observed in experiments using 44568. Together, these results indicate the transcript accumulation profile for *PhMYB5d8* is similar to that of known FVBP genes and suggests *PhMYB5d8* may be involved in FVBP production in petunia.

Suppression of *PhMYB5d8* by RNAi

The transcript accumulation profile for *PhMYB5d8* is similar to known FVBP genes (Figures 4-3, 2-1, 2-3, 2-9, and 3-5); therefore, *PhMYB5d8* was chosen for RNAi mediated gene silencing. A 200 bp fragment at the 3' end of the *PhMYB5d8* coding sequence was used for the RNAi inducing fragment (Figure 4-4). Fifty independent *PhMYB5d8* RNAi (*PhMYB5d8-R*) plants were generated by leaf disc transformation, and analyzed for reduced levels of *PhMYB5d8* transcripts by sqRT-PCR (Figure 4-5). *PhMYB5d8* transcript accumulation from at least nine individual T_0 *PhMYB5d8*-R plants was detected at relatively low levels compared to MD samples, while *PhMYB5d8* transcript accumulation from three representative *PhMYB5d8*-R plants was detected at similar levels as MD. Due to the previously reported function for *AtMYB4* (Jin et al., 2000), *PhC4H* transcript accumulation was also assayed (Figure 4-5). *PhC4H* transcript accumulation was detected at relatively higher levels in all 9 *PhMYB5d8*-R plants with reduced levels of *PhMYB5d8* transcripts. *PhC4H* transcript accumulation was detected at similar levels in MD and the representative *PhMYB5d8*-R plants with wildtype levels of *PhMYB5d8* transcripts. Additionally, when transcript levels of multiple other genes in the shikimate, phenylpropanoid, and FVBP pathways were analyzed, no differences were observed between

MD, *PhMYB5d8*-R with the expected reduced transcript levels of *PhMYB5d8*, and the transgenic control plants (data not shown).

Multiple, independent T_0 *PhMYB5d8*-R plants displayed a reduced level of *PhMYB5d8* transcripts, and an elevated level of *PhC4H* transcripts (Figure 4-5). The C6-C3 FVBP compounds, isoeugenol and eugenol, are downstream of C4H in the biosynthesis pathway (Figure 1-1). Therefore, we hypothesized elevated levels of *PhC4H* transcripts would increase C4H activity with a concomitant increase of metabolites directed to the production of isoeugenol and eugenol; thus, high levels of emission for these C6-C3 compounds in *PhMYB5d8*-R flowers compared to wildtype flowers. Six of the major FVBP compounds were analyzed from stage 9 (Figure 2-2) corollas of MD and *PhMYB5d8*-R plants (Figure 4-6). Benzaldehyde and benzyl benzoate were detected at similar levels throughout all samples. Methyl benzoate and phenylacetaldehyde were detected at lower levels in the *PhMYB5d8*-R corollas with reduced levels of *PhMYB5d8* transcript when compared to MD and *PhMYB5d8*-R 34 (wildtype levels of *PhMYB5d8* transcript). Isoeugenol and eugenol emission was detected at higher levels in the *PhMYB5d8*-R corollas with reduced levels of *PhMYB5d8* transcript, while MD and *PhMYB5d8*-R 34 corollas emitted comparable levels of isoeugenol and eugenol (Figure 4-6). These results suggest that a reduction of *PhMYB5d8* transcript elevates *PhC4H* transcript levels and emission of isoeugenol and eugenol.

Discussion

In petunia, floral volatile benzenoid/phenylpropanoid production and emission is both complex and controlled. Gene regulation is a key aspect of control, which appears coordinate through multiple categories that can be utilized to screen candidate genes possibly involved in the production of FVBPs (Chapter 2). Employing this similarity screen by sqRT-PCR provided a cost-effective and efficient method for the isolation of multiple genes involved in FVBP

production like *PhMYB5d8*. PhMYB5d8 predicted amino acid sequence is highly similar to a family of proteins called R2R3-MYB transcriptional regulators (Figure 4-1) [Stracke et al., 2001]. A small conserved domain (EAR-domain) in the C-terminal half of the protein, LNL(E/D)L, puts PhMYB5d8 into subgroup 4 and supports a repression function (Ohta et al., 2001). Additionally, the most similar Arabidopsis R2R3-MYB is AtMYB4 (Figure 4-2). AtMYB4 represses the transcription of the phenylpropanoid pathway gene, *CINNAMATE-4-HYDROXYLASE* (C4H) [Jin et al., 2000].

PhMYB5d8 transcripts accumulate to the highest levels in corolla tissue from anthesis to senescence (Figure 4-3A, B). *PhMYB5d8* transcript accumulation oscillates through a daily cycle similar to *PhODO1* (Figures 4-3C and 2-9), and transcript accumulation appears to be reduced after eight hours of ethylene exposure (Figure 4-3D). In short, *PhMYB5d8* transcripts are present in the tissue responsible for FVBP production, at the same developmental stages when FVBP are emitted, in a rhythmic pattern similar to the only other transcriptional regulator shown to be involved in FVBP production, and is affected by hormone exposure. The *PhMYB5d8* transcript analysis and function of AtMYB4 suggests PhMYB5d8 may be involved in the regulation of FVBP production in petunia.

To test the gene function of *PhMYB5d8* directly, we generated transgenic *PhMYB5d8*-RNAi petunia plants by using a 200 bp sequences at the 3' end of the coding sequence as an RNAi trigger (Figure 4-4). At least nine independent T_0 *PhMYB5d8*-RNAi plants had reduced levels of the desired *PhMYB5d8* transcripts (Figure 4-5). Similar to what was found in Arabidopsis with a dSpm insertion *Atmyb4* line (Jin et al., 2000), *PhC4H* transcripts accumulate to higher levels in the *PhMYB5d8*-RNAi plants compared to MD and transgenic controls (Figure 4-5). These results suggest that PhMYB5d8 negatively regulates *PhC4H* transcript accumulation.

However, it must be clear; we examined the transcript accumulation of specific genes and not a comprehensive set such as used in a microarray. In addition, we did not perform any direct assays to test for protein promoter interactions. Both microarray and protein-promoter assays will be conducted in the near future.

Because *PhC4H* transcript accumulation was increased in the *PhMYB5d8*-RNAi plants (Figure 4-5) and three FVBP compounds are "downstream" of C4H (Figure 1-1), we analyzed the emission of only major FVBP compounds (Figure 4-6). Four independent PhMYB5d8-RNAi plants emitted 3 to 4 fold higher levels of isoeugenol and eugenol compared to all controls. Emission of benzaldehyde, methyl benzoate, and phenylacetaldehyde were varied among the *PhMYB5d8*-RNAi plants compared to the controls, but the magnitude of difference was much smaller than observed for isoeugenol and eugenol (Figure 4-6). Together the transcript accumulation and FVBP emission analyses of the *PhMYB5d8*-RNAi plants indicate higher levels of *PhC4H* transcript results in higher levels of emitted FVBP compounds downstream of C4H.

FVBP production is highly regulated in petunia and likely consists of multiple interconnected factors. We found a cDNA that is highly similar to R2R3-MYB transcriptional regulators, and contains an EAR domain, which has a repression function. The transcript accumulation profile of the *PhMYB5d8* is highly similar to other known FVBP genes. A reduction of *PhMYB5d8* transcript accumulation results in an increase of *PhC4H* transcript accumulation, and an increase in emission of isoeugenol and eugenol. The data presented here suggests that PhMYB5d8 negatively regulates *PhC4H* transcript abundance (Figure 4-7) coinciding with the temporal, spatial, and developmental production of FVBP compounds in petunia. Further experimentation is required to confirm the above conclusion, however, the exact composition of the petunia floral volatile bouquet may be determined by an exact ratio of

specific proteins to substrates and PhMYB5d8 may be involved in the regulation of the exact ratio.

Experimental Procedures

Plant Materials

Inbred *Petunia x hybrida* cv 'Mitchell Diploid' (MD) plants were utilized as a 'wild-type' control in all experiments. The ethylene-insensitive *CaMV* 35S:*etr1-1* line 44568, generated in the MD genetic background (Wilkinson et al., 1997), was utilized as a negative control for ethylene sensitivity where applicable. MD, 44568, and *PhMYB5d8* RNAi plants were grown as previously described (Dexter et al., 2007). Ethylene treatments used two µL L^{-1} of ethylene with air treatments for controls.

Generation of *PhMYB5d8* RNAi Transgenic Petunia

The generation of *PhMYB5d8* RNAi transgenic plants was as describe earlier (Dexter et al., 2007), but with two fragments (3' of the R2R3 domain) of the *PhMYB5d8* cDNA amplified and ligated end to end in a sense/antisense orientation with additional sequence information used for an inter-fragment intron (hairpin).

Transcript accumulation analysis

All experiments were conducted with at least two biological replicates with equivalent results observed. In all cases, total RNA was extracted as previously described (Verdonk et al., 2003) and subjected to TURBO™ DNase treatment (Ambion Inc., Austin, TX) followed by total RNA purification with RNeasy® Mini protocol for RNA cleanup (Qiagen, Valencia, CA). Total RNA was then quantified on a NanoDrop™ 1000 spectrophotometer (Thermo Scientific, Wilmington, DE) and 50 ng/µl dilutions were prepared and stored at -20^{o}C.

Semi-quantitative (sq)RT-PCR was performed on a Veriti™ 96-well thermal cycler (Applied Biosystems, Foster City, CA). All sqRT-PCR reactions used a Qiagen One-step RT-

PCR kit with 50 ng total RNA template. To visualize RNA loading concentrations, samples were amplified with *Ph18S* primers (forward primer 5'-TTAGCAGGCTGAGGTCTCGT-3' and reverse primer 5'-AGCGGATGTTGCTTTTAGGA-3') and analyzed on an agarose gel. Gene specific primers were designed and utilized for the visualization of the relative transcript accumulation levels for *PhMYB5d8* (forward primer 5'-TTTTGCTGCTGGAATGAAGA-3' and reverse primer 5'-TTCCTGCTACAACTGCAACCT-3') and *PhC4H* [SGN-U210924] (forward primer 5'-CTTGGACCAGGAGTGCAAAT-3' and reverse primer 5'-GCTCCTCCTACCAACACCAA-3').

The spatial transcript accumulation series consisted of total RNA isolated from root, stem stigma, anther, leaf, petal tube, petal limb, and sepal tissues of three individual MD plants at 16:00 h on multiple occasions over the course of a year. The developmental transcript accumulation series consisted of MD floral tissue collected at eleven different stages; floral bud < 0.5 cm (stage 1), bud 0.5 < 1.5 cm (2), bud 1.5 < 3.0 cm (3), bud 3.0 < 5.0 cm (4), bud fully elongated 5.0 < 6.5 cm (5), flower opening 0 < 2 cm limb diameter (anthesis) [6], flower fully open day 0 (7), day 1 (8), day 2 (9), day 3 (10), and observably senescing flower (flower open day 7 for MD), stage 11. All tissues were collected at 16:00 h on the same day, and total RNA was isolated from all samples collected. The developmental tissue collections were conducted multiple times over the course of a year. The exogenous ethylene series consisted of excised MD and 44568 stage 9 flowers (placed in tap water) placed into eight tanks, four for ethylene treatments and four for air treatments. Air and ethylene treatments were conducted for 0, 1, 2, 4, and 8 hours starting at 12:00 h. Immediately following treatment, each of the flower samples were collected, stored at -80^{o}C, and total RNA was isolated from all corolla tissues once all samples had been collected. The ethylene treatment experiment consisted of two biological

replicates and was conducted twice. For all tissue collections individual samples consisted of three flowers.

Volatile Emission

For all volatile emission experiments, emitted floral volatiles from excised flowers were collected at 18:00 h and quantified as previously described (Underwood et al., 2005; Dexter et al., 2007).

Acknowledgements

Dr. Rob Schuurink is acknowledged for his contribution of the *PhMYB5d8* coding sequence.

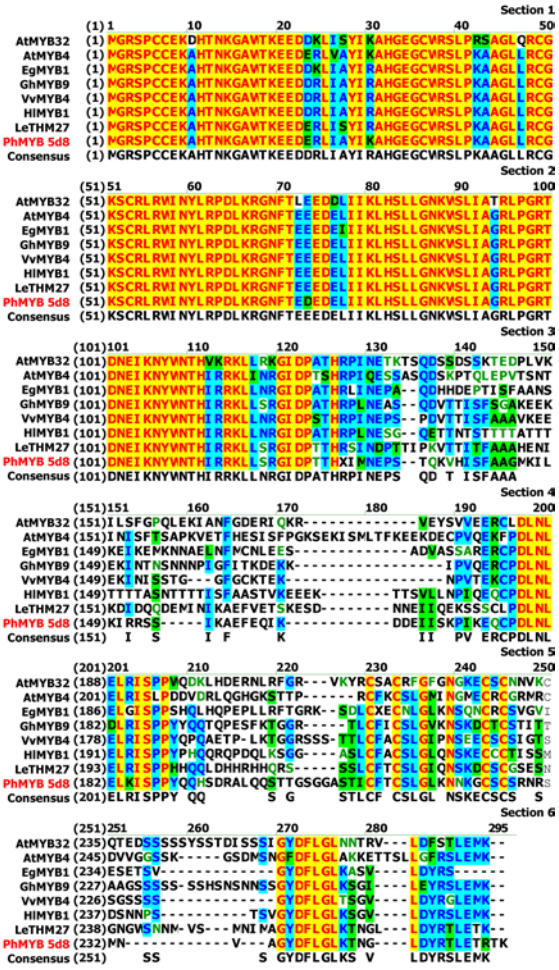

Figure 4-1. Predicted peptide sequence alignment of homologous R2R3-MYB proteins from various species. Sequences represented are from Arabidopsis thaliana (accession: NM_119665 [MYB32] and AY070100 [MYB4]), Eucalyptus gunnii (AJ576024), Gossypium hirsutum (AF336286), Vitis vinifera (EF113078), Humulus lupulus (AB292244), Solanum lycopersicum (X95296), and Petunia x hybrida (EB175095). Sequences were aligned using the AlignX program of the Vector NTI Advance 10.3.0 software (Invitrogen). Residues highlighted in: blue represent consensus residues derived from a block of similar residues at a given position, green represent consensus residues derived from the occurrence of greater than 50 % of a single residue at a given position, and yellow represent consensus residues derived from a completely conserved residue at a given position. Petunia sequences are highlighted in red to the left.

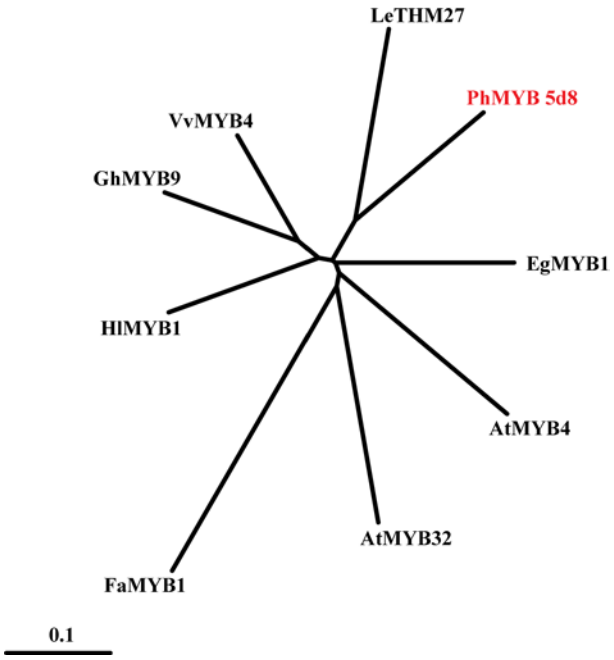

Figure 4-2. An unrooted neighbor-joining phylogenetic tree of homologous R2R3-MYB proteins from various species. TREEVIEW software with the nearest-joining method was used to create the resulting tree. Scale bar represents distance as the number of substitutions per site (i.e., 0.1 amino acid substitutions per site).

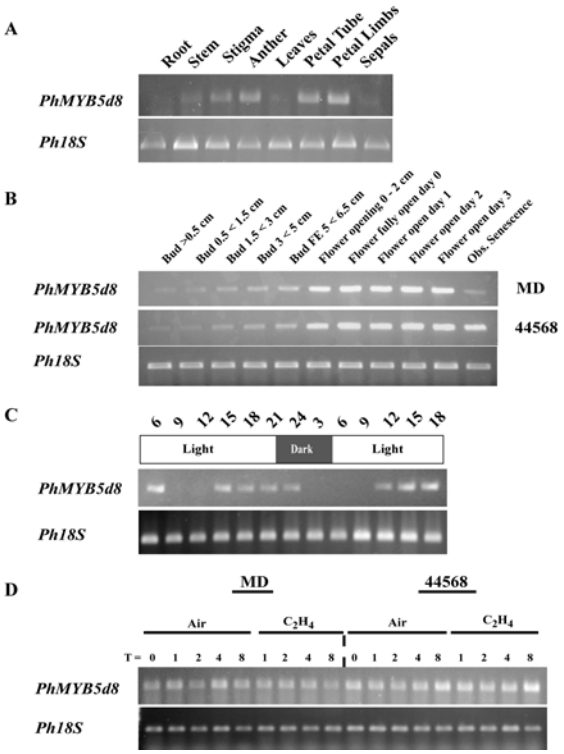

Figure 4-3. *PhMYB5d8* transcript accumulation analysis (sqRT-PCR). Spatial analysis used root, stem, stigma, anther, leaf, petal tube, petal limb, and sepal tissues of MD harvested at 16:00 h (A). Floral developmental analysis used MD flowers from 11 sequential stages at 16:00 h (B). Rhythmic analysis used MD plants acclimated in a growth chamber with a long day photoperiod and samples collected every three hours for a total of 36 hours (C). Ethylene treatment (two µL L^{-1}) analysis used excised MD and 44568 whole flowers treated for 0, 1, 2, 4, and 8 hours (D).The number of cycles used for amplification of each transcript is shown on the right. *Ph18S* was used as a loading control in all cases.

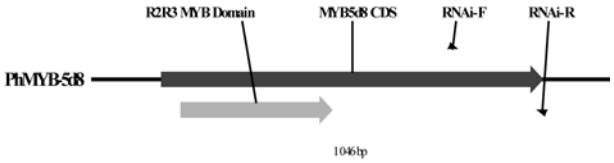

Figure 4-4. *PhMYB5d8* cDNA model with the RNAi region used for the production of petunia *PhMYB5d8* RNAi transgenic lines. 200 bases at the 3' end of the coding sequence of *PhMYB5d8* were chosen for the RNAi construct (between RNAi-F and RNAi-R primers).

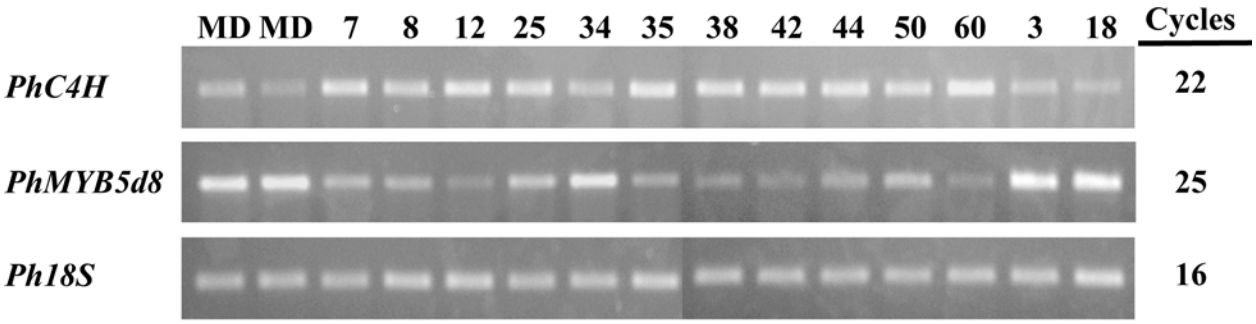

Figure 4-5. sqRT-PCR transcript accumulation analysis in floral tissues of independent T_0 *PhMYB5d8*-RNAi lines and MD plants. Gene specific primers for *PhMYB5d8* and *PhC4H* were used. The number of cycles used for amplification of each transcript is shown on the right. *Ph18S* was used as a loading control.

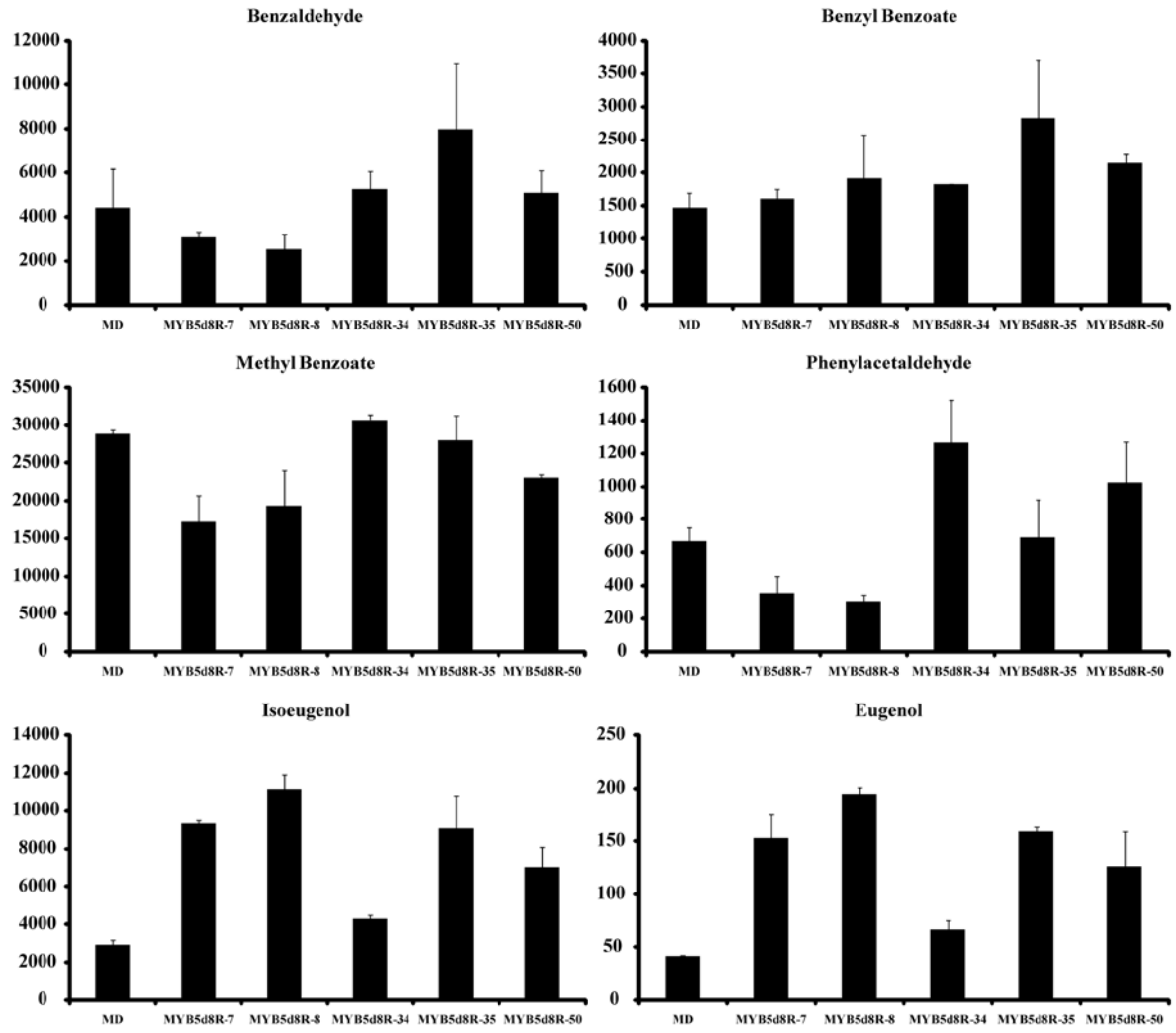

Figure 4-6. Floral volatile emission analysis from five independent T_0 *PhMYB5d8* RNAi lines (mean ± sd; n = 2). Only major volatile compounds are shown.

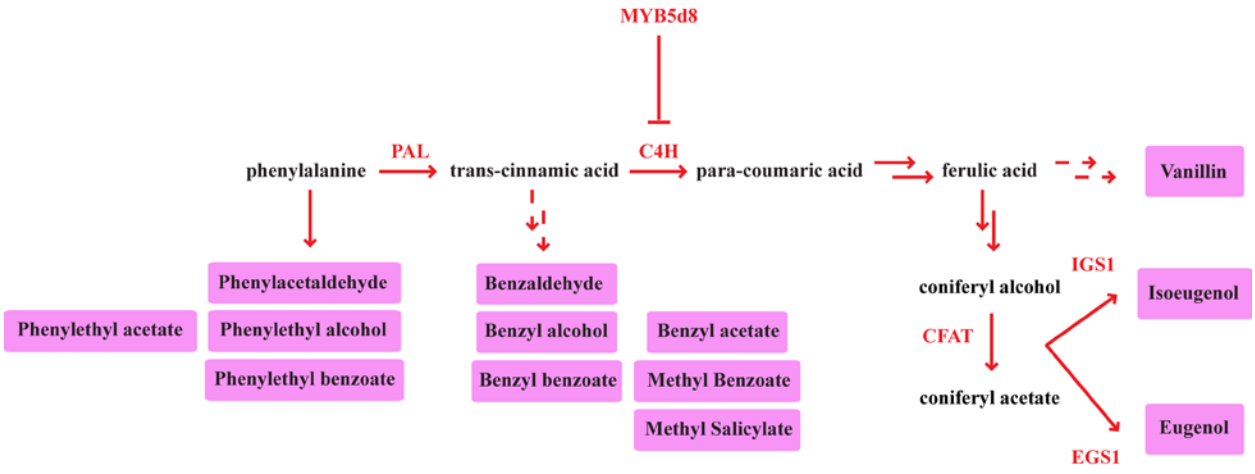

Figure 4-7. Schematic model of the FVBP pathway in petunia. FVBP production consists of three main branch-points; phenylalanine, *trans*-cinnamic acid, and ferulic acid. Floral volatile compounds derived from each branch-point are highlighted in pink and proteins are in red. Solid red arrows indicate established biochemical reactions. Multiple arrows indicate multiple biochemical steps. Dashed arrows indicate possible biochemical reactions.

LIST OF REFERENCES

Abel, C., Clauss, M., Schaub, A., Gershenzon, J., and Tholl, D. (2009). Floral and insect-induced volatile formation in *Arabidopsis lyrata* ssp. *petraea* , a perennial, outcrossing relative of *A. thaliana*. Planta 10, 921-927.

Achnine, L., Blancaflor, E.B., Rasmussen, S., and Dixon, R.A. (2004). Colocalization of L-PHENYLALANINE AMMONIA-LYASE and CINNAMATE 4-HYDROXYLASE for metabolic channeling in phenylpropanoid biosynthesis. Plant Cell 16, 3098-3109.

Alonso, J.M., Hirayama, T., Roman, G., Nourizadeh, S., and Ecker, J.R. (1999). EIN2, a bifunctional transducer of ethylene and stress responses in Arabidopsis. Science 284, 2148-2152.

Ando, T., Nomura, M., Tsukahara, J., Watanabe, H., Kokubun, H., Tsukamoto, T., Hashimoto, G., Marchesi, E., and Kitching, I.J. (2001). Reproductive isolation in a native population of *Petunia sensu* Jussieu (Solanaceae). Ann. Bot. 88, 403-413.

Benesova, M., and Bode, R. (1992). CHORISMATE MUTASE isoforms from seeds and seedlings of *Papaver somniferum*. Phytochemistry 31, 2983-2987.

Ben-Nissan, G., and Weiss, D. (1996). The petunia homologue of tomato *GAST1*: transcript accumulation coincides with gibberellin-induced corolla cell elongation. Plant Mol. Biol. 32, 1067-1074.

Bleecker, A.B., and Kende, H. (2000). Ethylene: a gaseous signal molecule in plants. Annu. Rev. Cell Dev. Biol. 16, 1-18.

Boudet, A.M. (2007). Evolution and current status of research in phenolic compounds. Phytochemistry 68, 2722-2735.

Boatright, J., Negre, F., Chen, X., Kish, C.M., Wood, B., Peel, G., Orlova, I., Gang, D., Rhodes, D., and Dudareva, N. (2004). Understanding *in vivo* benzenoid metabolism in petunia petal tissue. Plant Physiol. 135, 1993-2011.

Chang, C., Kwok, S.F., Bleecker, A.B., and Meyerowitz, E.M. (1993). Arabidopsis ethylene-response gene *ETR1* - similarity of product to 2-component regulators. Science 262, 539-544.

Chao, Q.M., Rothenberg, M., Solano, R., Roman, G., Terzaghi, W., and Ecker, J.R. (1997). Activation of the ethylene gas response pathway in Arabidopsis by the nuclear protein ETHYLENE-INSENSITIVE3 and related proteins. Cell 89, 1133-1144.

Chen, Y.F., Etheridge, N., and Schaller, G.E. (2005). Ethylene signal transduction. Ann. Bot. 95, 901-915.

Clark, D.G., Gubrium, E.K., Barrett, J.E., Nell, T.A., and Klee, H.J. (1999). Root formation in ethylene-insensitive plants. Plant Physiol. 121, 53-59.

Clark, K.L., Larsen, P.B., Wang, X.X., and Chang, C. (1998). Association of the Arabidopsis CTR1 Raf-like kinase with the ETR1 and ERS ethylene receptors. Proc. Natl. Acad. Sci. U. S. A. 95, 5401-5406.

Deroles, S.C., and Gardner, R.C. (1988a). Expression and inheritance of kanamycin resistance in a large number of transgenic petunias generated by Agrobacterium-mediated transformation. Plant Mol. Biol. 11, 355-364.

Deroles, S.C., and Gardner, R.C. (1988b). Analysis of the T-DNA structure in a large number of transgenic petunias generated by Agrobacterium-mediated transformation. Plant Mol. Biol. 11, 365-377.

Dexter, R., Qualley, A., Kish, C.M., Ma, C.J., Koeduka, T., Nagegowda, D.A., Dudareva, N., Pichersky, E., and Clark, D. (2007). Characterization of a petunia acetyltransferase involved in the biosynthesis of the floral volatile isoeugenol. Plant J. 49, 265-275.

Dexter, R.J., Verdonk, J.C., Underwood, B.A., Shibuya, K., Schmeltz, E.A., and Clark, D.G. (2008). Tissue-specific *PHBPBT* expression is differentially regulated in response to endogenous ethylene. J. Exp. Bot. 59, 609-618.

Dudareva, N., Negre, F., Nagegowda, D., and Orlova, I. (2006). Plant volatiles: recent advances and future perspectives. Crit. Rev. Plant Sci. 25, 417-440.

Dudareva, N., and Pichersky, E. (2000). Biochemical and molecular genetic aspects of floral scents. Plant Physiol. 122, 627-633.

Dudareva, N., Pichersky, E., and Gershenzon, J. (2004). Biochemistry of plant volatiles. Plant Physiol. 135, 1893-1902.

Eberhard, J., Raesecke, H.R., Schmid, J., and Amrhein, N. (1993). Cloning and expression in yeast of a higher plant CHORISMATE MUTASE. Molecular cloning, sequencing of the cDNA and characterization of the *Arabidopsis thaliana* enzyme expressed in yeast. FEBS Lett. 15, 233-236.

Eberhard, J., Bischoff, M., Raesecke, H.R., Amrhein, N., and Schmid, J. (1996a). Isolation of a cDNA from tomato coding for an unregulated, cytosolic CHORISMATE MUTASE. Plant Mol. Biol. 31, 917-922.

Eberhard, J., Ehrler, T.T., Epple, P., Felix, G., Raesecke, H.R., Amrhein, N., and Schmid, J. (1996b). Cytosolic and plastidic CHORISMATE MUTASE isozymes from *Arabidopsis thaliana*: molecular characterization and enzymatic properties. Plant J. 10, 815-821.

Fenster, C., Armbruster, W., Wilson, P., Dudash, M., and Thomson, J. (2004). Pollination syndromes and floral specialization. Annu. Rev. Ecol. Evol. S. 35, 375-403.

Fraley, R.T., Rogers, S.G., and Horsch, R.B. (1983). *In vitro* plant transformation by bacterial co-cultivation and expression of foreign genes in plant-cells. In Vitro Cell Dev. B. 19, 284-284.

Friedman, M., Henika, P.R., and Mandrell, R.E. (2002). Bactericidal activities of plant essential oils and some of their isolated constituents against *Campylobacter jejuni*, *Escherichia coli*, *Listeria monocytogenes*, and *Salmonella enterica*. J. Food Prot. 65, 1545-1560.

Gerats, T., and Vandenbussche, M. (2005). A model system for comparative research: petunia. Trends Plant Sci. 10, 251-256.

Gilchrist, D.G., and Connelly, J.A. (1987). CHORISMATE MUTASE from Mung Bean and Sorghum. Methods Enzymol. 142, 450-463.

Griesbach, R.J., and Kamo, K.K. (1996). The effect of induced polyploidy on the flavonols of petunia 'Mitchell'. Phytochemistry 42, 361-363.

Guo, H.W., and Ecker, J.R. (2004). The ethylene signaling pathway: new insights. Curr. Opin. Plant Biol. 7, 40-49.

Hall, A.E., Findell, J.L., Schaller, G.E., Sisler, E.C., and Bleecker, A.B. (2000). Ethylene perception by the ERS1 protein in Arabidopsis. Plant Physiol. 123, 1449-1457.

Haslam, E. (1993). Shikimic acid: metabolism and metabolites. Chichester, Wiley.

Herrmann, K.M., and Weaver, L.M. (1999). The shikimate pathway. Annu. Rev. Plant Physiol. Plant Mol. Biol. 50, 473-503.

Hoballah, M.E., Stuurman, J., Turlings, T.C., Guerin, P.M., Connetable, S., Kuhlemeier, C. (2005). The composition and timing of flower odour emission by wild *Petunia axillaris* coincide with the antennal perception and nocturnal activity of the pollinator *Manduca sexta*. Planta 222, 141-150.

Hoekstra, F., and Weges, R. (1986). Lack of control by early pistillate ethylene of the accelerated wilting of *Petunia hybrida* flowers. Plant Physiology 80, 403-408.

Horsch, R.B., Fry, J.E., Hoffmann, N.L., Eichholtz, D., Rogers, S.G., and Fraley, R.T. (1985). A simple and general method for transferring genes into plants. Science 227, 1229-1231.

Hua, J., and Meyerowitz, E.M. (1998). Ethylene responses are negatively regulated by a receptor gene family in *Arabidopsis thaliana*. Cell 94, 261-271.

Hua, J., Sakai, H., Nourizadeh, S., Chen, Q.H.G., Bleecker, A.B., Ecker, J.R., and Meyerowitz, E.M. (1998). EIN4 and ERS2 are members of the putative ethylene receptor gene family in Arabidopsis. Plant Cell 10, 1321-1332.

Hudak, K.A., and Thompson, J.E. (1997). Subcellular localization of secondary lipid metabolites including fragrance volatiles in carnation petals. Plant Physiol. 114, 705-713.

Jin, H., Cominelli, E., Bailey, P., Parr, A., Mehrtens, F., Jones, J., Tonelli, C., Weisshaar, B., and Martin, C. (2000). Transcriptional repression by AtMYB4 controls production of UV-protecting sunscreens in Arabidopsis. EMBO J. 19, 6150-6161.

Jones, M.L., Langston, B.J., and Johnson, F. (2003). Pollination-induced senescence of ethylene sensitive and insensitive petunias, in: Vendrell, M., Klee, H., Pech, J.C., Romotaro, F. (Eds.), Biology and Biotechnology of the Plant Hormone Ethylene III. IOS Press, Amsterdam, pp. 324-327.

Jorgensen, R.A., Cluster, P.D., English, J., Que, Q.D., and Napoli, C.A. (1996). CHALCONE SYNTHASE cosuppression phenotypes in petunia flowers: comparison of sense vs antisense constructs and single-copy vs complex T-DNA sequences. Plant Mol. Biol. 31, 957-973.

Kaminaga, Y., Schnepp, J., Peel, G., Kish, C.M., Ben-Nissan, G., Weiss, D., Orlova, I., Lavie, O., Rhodes, D., Wood, K., Porterfield, D.M., Cooper, A.J., Schloss, J.V., Pichersky, E., Vainstein, A., and Dudareva, N. (2006). Plant PHENYLACETALDEHYDE SYNTHASE is a bifunctional homotetrameric enzyme that catalyzes phenylalanine decarboxylation and oxidation. J. Biol. Chem. 281, 23357-23366.

Kast, P., Asif-Ullah, M., Jiang, N., and Hilvert, D. (1996). Exploring the active site of CHORISMATE MUTASE by combinatorial mutagenesis and selection: the importance of electrostatic catalysis. Proc. Natl. Acad. Sci. U. S. A. 93, 5043-5048.

Kast, P., Grisostomi, C., Chen, I.A., Li, S., Krengel, U., Xue, Y., and Hilvert, D. (2000). A strategically positioned cation is crucial for efficient catalysis by CHORISMATE MUTASE. J. Biol. Chem. 275, 36832-36838.

Klempnauer, K.H., Gonda, T.J., and Bishop, J.M. (1982). nucleotide-sequence of the retroviral leukemia gene *V-MYB* and its cellular progenitor *C-MYB* - the architecture of a transduced oncogene. Cell 31, 453-463.

Knudsen, J.T., Eriksson, R., Gershenzon, J., and Stahl, B. (2006). Diversity and distribution of floral scent. Bot. Rev. 72, 1-120.

Knudsen, J., Tollsten, L., and Berstrom, L. (1993). Floral scents - a checklist of volatile compounds isolated by headspace techniques. Phytochemistry 33, 253-280.

Koeduka, T., Fridman, E., Gang, D.R., Vassao, D.G., Jackson, B.L., Kish, C.M., Orlova, I., Spassova, S.M., Lewis, N.G., Noel, J.P., Baiga, T.J., Dudareva, N., and Pichersky, E. (2006). Eugenol and isoeugenol, characteristic aromatic constituents of spices, are biosynthesized via reduction of a coniferyl alcohol ester. Proc. Natl. Acad. Sci. U. S. A. 103, 10128-10133.

Koeduka, T., Louie, G.V., Orlova, I., Kish, C.M., Ibdah, M., Wilkerson, C.G., Bowman, M.E., Baiga, T.J., Noel, J.P., Dudareva, N., and Pichersky, E. (2008). The multiple PHENYLPROPENE SYNTHASES in both *Clarkia breweri* and *Petunia hybrida* represent two distinct protein lineages. Plant J. 54, 362-374.

Kolosova, N., Gorenstein, N., Kish, C.M., and Dudareva, N. (2001a). Regulation of circadian methyl benzoate emission in diurnally and nocturnally emitting plants. Plant Cell 13, 2333-2347.

Kolosova, N., Sherman, D., Karlson, D., and Dudareva, N. (2001b). Cellular and subcellular localization of S-ADENOSYL-L- METHIONINE:BENZOIC ACID CARBOXYL METHYLTRANSFERASE, the enzyme responsible for biosynthesis of the volatile ester methylbenzoate in snapdragon flowers. Plant Physiology 126, 956-964.

Lipsick, J.S. (1996). One billion years of MYB. Oncogene 13, 223-235.

Martin, J.R., Harwood, J.H., McCaffery, M., Fernandez, D, E., and Cline, K. (2009). Localization and integration of thylakoid protein translocase subunit cpTatC. Plant J. 58, 831-842.

Matsui, K. (2006). Green leaf volatiles: hydroperoxide lyase pathway of oxylipin metabolism. Curr. Opin. Plant Biol. 9, 274-280.

Mitchell, A.Z., Hanson, M.R., Skvirsky, R.C., and Ausubel, F.M. (1980). Anther culture of petunia - genotypes with high-frequency of callus, root, or plantlet formation. Z Pflanzenphysiol 100, 131-146.

Moalem-Beno, D., Tamari, G., Leitner-Dagan, Y., Borochov, A., and Weiss, D. (1997). Sugar-dependent gibberellin-induced *CHALCONE SYNTHASE* gene expression in petunia corollas. Plant Physiol. 113, 419-424.

Mobley, E.M., Kunkel, B.N., and Keith, B. (1999). Identification, characterization and comparative analysis of a novel *CHORISMATE MUTASE* gene in *Arabidopsis thaliana*. Gene 240, 115-123.

Negre, F., Kish, C.M., Boatright, J., Underwood, B., Shibuya, K., Wagner, C., Clark, D.G., and Dudareva, N. (2003). Regulation of methylbenzoate emission after pollination in snapdragon and petunia flowers. Plant Cell 15, 2992-3006.

Newman, J.D., and Chappell, J. (1999). Isoprenoid biosynthesis in plants: carbon partitioning within the cytoplasmic pathway. Crit. Rev. Biochem. Mol. Biol. 34, 95-106.

Ogata, K., Hojo, H., Aimoto, S., Nakai, T., Nakamura, H., Sarai, A., Ishii, S., and Nishimura, Y. (1992). Solution structure of a DNA-binding unit of MYB - a helix turn helix-related motif with conserved tryptophans forming a hydrophobic core. Proc. Natl. Acad. Sci. U. S. A. 89, 6428-6432.

Ohta, M., Matsui, K., Hiratsu, K., Shinshi, H., and Ohme-Takagi, M. (2001). Repression domains of class II ERF transcriptional repressors share an essential motif for active repression. Plant Cell 13, 1959-1968.

Orlova, I., Marshall-Colon, A., Schnepp, J., Wood, B., Varbanova, M., Fridman, E., Blakeslee, J.J., Peer, W.A., Murphy, A.S., Rhodes, D., Pichersky, E., and Dudareva, N. (2006). Reduction of benzenoid synthesis in petunia flowers reveals multiple pathways to benzoic acid and enhancement in auxin transport. Plant Cell 18, 3458-3475.

Oxenham, S.K., Svoboda, K.P., and Walters, D.R. (2005). Altered growth and polyamine catabolism following exposure of the chocolate spot pathogen *Botrytis fabae* to the essential oil of *Ocimum basilicum*. Mycologia 97, 576-579.

Pabo, C.O., and Sauer, R.T. (1992). Transcription factors - structural families and principles of DNA recognition. Annu. Rev. Biochem. 61, 1053-1095.

Pare, P.W., and Tumlinson, J.H. (1997). *De novo* biosynthesis of volatiles induced by insect herbivory in cotton plants. Plant Physiol. 114, 1161-1167.

Peters, D. (2007). Raw materials. Adv. Biochem. Eng. Biot. 105, 1-30.

Pichersky, E., Noel, J.P., and Dudarev,a N. (2006). Biosynthesis of plant volatiles: nature's diversity and ingenuity. Science 311, 808-811.

Pichersky, E., and Gang, D.R. (2000). Genetcs and biochemistry of secondary metabolites in plants: an evolutionary perspective. Trends Plant Sci. 5, 439-445.

Pichersky, E., and Gershenzon, J. (2002). The formation and function of plant volatiles: perfumes for pollinator attraction and defense. Curr. Opin. Plant Biol. 5, 237-243.

Riechmann, J.L., and Ratcliffe, O.J. (2000). A genomic perspective on plant transcription factors. Curr. Opin. Plant Biol. 3, 423-434.

Rippert, P., Puyaubert, J., Grisollet, D., Derrier, L., and Matringe, M. (2009). Tyrosine and phenylalanine are synthesized within the plastids in Arabidopsis. Plant Physiol. 149, 1251-1260.

Rodriguez, F.I., Esch, J.J., Hall, A.E., Binder, B.M., Schaller, G.E., and Bleecker, A.B. (1999). A copper cofactor for the ethylene receptor ETR1 from Arabidopsis. Science 283, 996-998.

Rohmer, M. (1999). The discovery of a mevalonate-independent pathway for isoprenoid biosynthesis in bacteria, algae and higher plants. Nat. Prod. Rep. 16, 565-574.

Sakai, H., Hua, J., Chen, Q.H.G., Chang, C.R., Medrano, L.J., Bleecker, A.B., and Meyerowitz, E.M. (1998). *ETR2* is an *ETR1*-like gene involved in ethylene signaling in Arabidopsis. Proc. Natl. Acad. Sci. U. S. A. 95, 5812-5817.

Schaller, G.E., and Bleecker, A.B. (1995). Ethylene-binding sites generated in yeast expressing the Arabidopsis *ETR1* gene. Science 270, 1809-1811.

Schaller, G.E., Ladd, A.N., Lanahan, M.B., Spanbauer, J.M., and Bleecker, A.B. (1995). The ethylene response mediator ETR1 from Arabidopsis forms a disulfide-linked dimer. J. Biol. Chem. 270, 12526-12530.

Schuurink, R.C., Haring, M.A., and Clark, D.G. (2006). Regulation of volatile benzenoid biosynthesis in petunia flowers. Trends Plant Sci. 11, 20-25.

Shibuya, K., Barry, K.G., Ciardi, J.A., Loucas, H.M., Underwood, B.A., Nourizadeh, S., Ecker, J.R., Klee, H.J., and Clark, D.G. (2004). The central role of PhEIN2 in ethylene responses throughout plant development in petunia. Plant Physiol. 136, 2900-2912.

Simkin, A.J., Underwood, B.A., Auldridge, M., Loucas, H.M., Shibuya, K., Schmelz, E., Clark, D.G., and Klee, H.J. (2004). Circadian regulation of the *PhCCD1* carotenoid cleavage dioxygenase controls emission of beta-ionone, a fragrance volatile of petunia flowers. Plant Physiol. 136, 3504-3514.

Solano, R., Stepanova, A., Chao, Q.M., and Ecker, J.R. (1998). Nuclear events in ethylene signaling: a transcriptional cascade mediated by *ETHYLENE-INSENSITIVE3* and *ETHYLENE-RESPONSE-FACTOR1*. Gene Dev. 12, 3703-3714.

Stracke, R., Werber, M., and Weisshaar, B. (2001). The *R2R3-MYB* gene family in *Arabidopsis thaliana*. Curr. Opin. Plant Biol. 4, 447-456.

Tang, X., and Woodson, W.R. (1996). Temporal and spatial expression of *1-AMINOCYCLOPROPANE-1-CARBOXYLATE OXIDASE* mRNA following pollination of immature and mature petunia flowers. Plant Physiol. 112, 503-511.

Tieman, D.M., Taylor, M., Schaurer, N., Fernie, A.R., Hanson, A.D., and Klee, H.J. (2006). Tomato aromatic amino acid decarboxylases participate in synthesis of the flavor volatiles 2-phenylethanol and 2-phenylacetaldehyde. Proc. Natl. Acad. Sci. U. S. A. 103, 8287-8292.

Underwood, B.A., Tieman, D.M., Shibuya, K., Dexter, R.J., Loucas, H.M., Simkin, A.J., Sims, C.A., Schmelz, E.A., Klee, H.J., and Clark, D.G. (2005). Ethylene-regulated floral volatile synthesis in petunia corollas. Plant Physiol. 138, 255-266.

Verdonk, J.C., Haring, M.A., Van Tunen, A.J., and Schuurink, R.C. (2005). *ODORANT1* regulates fragrance biosynthesis in petunia flowers. Plant Cell 17, 1612-1624.

Verdonk, J.C., Ric De Vos, C.H., Verhoeven, H.A., Haring, M.A., Van Tunen, A.J., and Schuurink, R.C. (2003). Regulation of floral scent production in petunia revealed by targeted metabolomics. Phytochemistry 62, 997-1008.

Wang, K.L.C., Li, H., and Ecker, J.R. (2002). Ethylene biosynthesis and signaling networks. Plant Cell 14, S131-S151.

Wang, Y., and Kumar, P.P. (2007). Characterization of two ethylene receptors PHERS1 and PHETR2 from petunia: PHETR2 regulates timing of anther dehiscence. J. Exp. Bot. 58, 533-544.

Weiss, D., Van Der Luit, A., Knegt, E., Vermeer, E., Mol, J., and Kooter, J.M. (1995). Identification of endogenous gibberellins in petunia flowers (induction of anthocyanin biosynthetic gene expression and the antagonistic effect of abscisic acid). Plant Physiol. 107, 695-702.

Wasternack, C., and Hause, B. (2002). Jasmonates and octadecanoids: signals in plant stress responses and development. Prog. Nucleic Acid Res. Mol. Biol. 72, 165-221.

Wasternack, C., Stenzel, I., Hause, B., Hause, G., Kutter, C., Maucher, H., Neumerkel, J., Feussner, I., and Miersch, O. (2006). The wound response in tomato--role of jasmonic acid. J. Plant Physiol. 163, 297-306.

Wilkinson, J.Q., Lanahan, M.B., Clark, D.G., Bleecker, A.B., Chang, C., Meyerowitz, E.M., and Klee, H.J. (1997). A dominant mutant receptor from Arabidopsis confers ethylene insensitivity in heterologous plants. Nat. Biotechnol. 15, 444-447.

Wilkinson, J.Q., Lanahan, M.B., Yen, H.C., Giovannoni, J.J., and Klee, H.J. (1995). An ethylene-inducible component of signal-transduction encoded by NEVER-RIPE. Science 270, 1807-1809.

Wink, M. (2003). Evolution of secondary metabolites from an ecological and molecular phylogenetic perspective. Phytochemistry 64, 3-19.

Yu, O., and Jez, J.M. (2008). Nature's assembly line: biosynthesis of simple phenylpropanoids and polyketides. Plant J. 54, 750-762.

Zhu, Z., and Guo, H. (2008). Genetic basis of ethylene perception and signal transduction in Arabidopsis. J. Integr. Plant Biol. 50, 808-815.

Zybailov, B., Rutschow, H., Friso, G., Rudella, A., Emanuelsson, O., Sun, Q., and van Wijk, K.J. (2008). Sorting signals, N-terminal modifications and abundance of the chloroplast proteome. PLoS ONE 3, e1994.

BIOGRAPHICAL SKETCH

Thomas Angus Colquhoun was born in Fargo, North Dakota. He was raised by Linda Lou Colquhoun and Thomas E. Colquhoun along with two older sisters, Tesa D. Larson and Christann Schmid. After graduating from Fargo South High School, Thomas attended Coastal Carolina University, South Carolina for his freshmen year, and then transferred to Minnesota State University of Moorhead (MSUM) for the remainder of his undergraduate career. During his undergraduate career, Thomas met and married the love of his life, Cynthia M. Colquhoun. Additionally, at MSUM Thomas worked in Dr. Chris Chastain's lab helping to characterize a pyruvate, orthophosphate dikinase in developing rice (Oryza sativa) seeds (Chastain et al., 2006). Dr. Chastain had a profound effect on Thomas and his education, for it was through Dr. Chastain's mentorship that Thomas found his interest in basic research and plants in general. University of Florida and the Plant Molecular and Cellular Biology Program was the next appointment for Thomas, and Dr. David G. Clark was his Ph.D. advisor. Dr. Clark was Thomas' second intellectual mentor and advisor, although Dr. Clark also actively participated in personal mentorship with Thomas. It was through Dr. Clark that Thomas gained a deeper understanding of biology and science as a whole, which led Thomas into a never ending form of question and answer with nature.